The Role of Krüppel-like Factor 11 in Vascular Homeostasis

by

Wenying Liang

A dissertation submitted in partial fulfillment
of the requirements for the degree of
Doctor of Philosophy
(Molecular and Integrative Physiology)
in the University of Michigan
2021

Doctoral Committee:

Professor Y. Eugene Chen, Chair
Professor Daniel T. Eitzman
Associate Professor Michael Holinstat
Professor Jiandie Lin
Professor Richard Mortensen

Wenying Liang

wenyingl@umich.edu

ORCID iD: 0000-0001-9985-6674

Dedication

To my dear mom, dad, and Da, who support me all the time with unconditional love.

To my mentor, Dr. Y. Eugene Chen, who guides me through this fantastic Ph.D. journey.

Acknowledgments

I would like to give my sincere gratitude to all the people who have supported me throughout my six years' Ph.D. journey.

First and foremost, I greatly appreciate my academic mentor, Professor Y. Eugene Chen, for his patient guidance, strong support, and insightful vision. It is a great honor to have him as both my academic advisor and life mentor. In his lab, I had the valuable chance to participate in much translational research and access collaborating labs to broaden my horizon. Specifically, I am very grateful for his understanding and support of my personal career development. Given my clinical interest, he guided me on improving the clinical relevance of my studies and helped me build new connections to the clinical side. In addition, he is a very supportive mentor, always willing for discussion, even out of the regular office hour. I consider Professor Chen my role model, who has a true love and works very hard to promote translational science.

Besides, the great privilege of studying in Professor Chen's lab comes from other excellent scientists, both including past and present faculty members and students. In particular, I would like to thank Dr. Yanbo Fan. Before joining Dr. Chen's lab, I did not have much in-depth laboratory experience in biomedical research. It was Dr. Fan who spent a great number of efforts to guide me patiently on how to design a study, conduct experiments and analyze data. He shared his valuable research experiences with me and helped me prepare for my first scientific presentation, grant, poster, and manuscript. I am very lucky and grateful to have his strong support. Without his invaluable encouragement and guidance, I could never achieve this. Dr.

Jifeng Zhang is another senior and experienced scientist in our lab. His office is always open to me, and I truly enjoy talking with him, both on research projects and life suggestions, for his insightfulness and kindness. Especially, I greatly appreciate his efforts in helping with my deep vein thrombosis manuscript. Dr. Haocheng Lu, a previous Ph.D. student and current postdoctoral fellow in Dr. Chen's lab, is a peer role model for me. He is very knowledgeable and generously gave me countless support on all of my research. Whenever I met any problems (both academic and personal), he is always there, willing to help. We worked in the same office and shared the same bench for nearly six years. I greatly appreciate the friendship and have learned a lot from him. Dr. Yanhong Guo kindly shared much of her valuable experience on lipid metabolism and kindly gave me many suggestions. Dr. Oren Rom generously shared his protocol and reagents for my lipid studies and always provided me with his constructive suggestions. Dr. Minerva T. Garcia-Barrio did a thorough revision for my first manuscript and taught me how to think/present scientifically. Dr. Lin Chang generously lent me his equipment and tools for my mice deep vein thrombosis surgery. Our lab manager Tianqing Zhu helped to handle all my order requests efficiently and ensured my experiments performed smoothly. I also want to thank all the past or present fellows and students, including Dr. Ziyi Chang, Dr. Jinjian Sun, Dr. Guizhen Zhao, Huilun Wang, Yuhao Liu, Yang Zhao, Yonghong Luo, Dr. Chao Xue, Dr. Yui Koike, Dr. Tomonari Koike, Dr. Wenting Hu, Dr. Wenhao Xiong, Dr. Die Hu, Dr. Yin Li, and Dr. Congzhen Qiao, for the constructive collaboration as well as insightful suggestions on my work.

I am honored to have the continuing support from my fantastic dissertation committee. Professor Daniel T. Eitzman spent time talking with me about my career development and gave me suggestions according to my clinical interest. He also generously allowed me to perform the key arterial thrombosis mouse model in his lab. Professor Michael Holinstat guided me on

designing the thrombosis research and let his lab members help on my platelet and laser-induced thrombosis experiments. Professor Richard Mortensen and Professor Jiandie Lin gave me many suggestions that helped me revise and improve my projects. The encouragement from all committee members motivated me to pursue better research.

I would like to thank the joint institute between the University of Michigan Health System and Peking University Health Science Center for giving me this "M.D.-Ph.D." training opportunity. In addition, I appreciate the support from the Global Reach Office, especially Dr. Amy Huang, for building the smooth connection between the two medical schools.

I am also very grateful for my financial support from Richard Rogel Fellowship and American Heart Association Predoctoral Fellowship. They provided me with the opportunity to pursue my interests in biomedical science and broaden my academic insights.

I greatly appreciate the supports from my Ph.D. program, the Department of Molecular and Integrative Physiology. I am very lucky to have supports from the past or current Ph.D. Graduate Program Chairs, Dr. Suzanne Moenter, Dr. Daniel E. Michele, and Dr. Susan V. Brooks. They took time discussing my training experiences and giving me suggestions for career development. I also want to thank Michele Boggs, our Ph.D. Program Administrator, who I bothered most and was always very helpful to tackle with issues I met during my graduate training. Dr. Lei Yin and Dr. Liangyou Rui were on my prelim committee, and I am grateful for their kind support and suggestions. Dr. Ormond MacDougald, Dr. Yatrik Shah, and Dr. Jun Wu led the seminars that broadened my horizon and developed my scientific thinking.

Last but not least, I would like to express my sincerest thanks to my family. Deepest appreciation goes to my dear mom and dad for their unconditional and tremendous support. They tried their best to give me a better education and always reminds me of the importance of being a

kind and honest person. Their love is the biggest motivation for me all the time. Finally, my beloved fiancé, Da, deserves the most credit for this dissertation. He is always there for me with his endless encouragement and love. He makes large sacrifices so that I can have time to pursue my dream. I have never known a love like this before. His intelligence, kindness, and love will always sustain me.

Table of Contents

List of Tables

List of Figures

Abstract

Krüppel-like factors (KLFs) are transcription factors containing three conserved zinc finger motifs in the carboxy-terminus and have shown associations with many diseases, including cancer, diabetes, and vascular disorders. Krüppel-like factor 11 (KLF11), originally identified as the causative gene for maturity-onset diabetes of the young type 7 (MODY7), has been reported to facilitate insulin transcription in pancreatic β cells. Previous studies have found that endothelial KLF11 has a protective effect in sepsis, ischemic stroke, and abdominal aortic aneurysm. Considering the common vascular complications in diabetes patients, in this project, we aim to study further the role of KLF11 in vascular homeostasis, especially thrombosis.

We applied a ferric chloride-induced thrombosis model to investigate the role of KLF11 in arterial thrombosis. We found that the occlusion time was significantly reduced in conventional *Klf11* knockout (*Klf11* KO) mice, while bone marrow transplantation could not rescue this phenotype. Given the increased expression of tissue factor (TF; encoded by the *F3* gene) in the tunica media of aorta in *Klf11* KO mice, we further applied the arterial thrombosis model in vascular smooth muscle cell (VSMC) specific *Klf11* knockout mice and found a significant reduction of occlusion time. In human aortic smooth muscle cells, siRNA-mediated knockdown of KLF11 increased TF expression. Consistent results were observed upon adenovirus-mediated overexpression of KLF11. Mechanistically, KLF11 downregulates *TF* gene expression at the transcriptional level as determined by reporter and chromatin immunoprecipitation assays. In sum, our data demonstrate that KLF11 is a novel transcriptional

suppressor of the *TF* gene in VSMCs, constituting a potential molecular target for inhibition of arterial thrombosis.

To study the role of KLF11 in venous thrombosis, we utilized a stasis-induced murine deep vein thrombosis (DVT) model and cultured endothelial cells (ECs). We identified an increase in KLF11 expression under prothrombotic conditions both *in vivo* and *in vitro*. The expression change of thrombosis-related genes was determined by utilizing gain- and loss-of-function approaches to alter KLF11 expression in ECs. Among these genes, KLF11 significantly downregulated tumor necrosis factor-alpha (TNF-α) induced TF expression. Using reporter gene assay, chromatin immunoprecipitation assay, and co-immunoprecipitation, we revealed that KLF11 could reduce TNF-α-induced binding of early growth response 1 (EGR1) to the *TF* gene promoter in ECs. In addition, we demonstrated that conventional *Klf11* KO mice were more susceptible to developing stasis-induced DVT. These results suggest that under prothrombotic conditions, KLF11 downregulates *TF* transcription *via* inhibition of EGR1 in ECs. In conclusion, KLF11 protects against DVT, constituting a potential molecular target for treating thrombosis.

In summary, KLF11 inhibits the basal *TF* expression in VSMCs and interrupts the induced EGR1 binding to the *TF* gene promoter under prothrombotic conditions. Thus KLF11 is important in maintaining vascular homeostasis and can be a promising therapeutic target for preventing or treating arterial thrombosis and DVT.

Chapter 1 Introduction

Krüppel-like factors (KLFs) overview

KLFs Overview

Krüppel-like factors (KLFs) are a group of transcription factors that bind at specific DNA regions to regulate the expression of various genes involved in either physiological or pathological processes. The name "Krüppel" means "cripple" in German and was originally derived from its homologous protein in Drosophila[1]. KLF1 (EKLF), the first member of KLFs, was identified in 1993 by binding with the β-globin promoter in erythroid cells[2]. Thus far, eighteen isoforms have been discovered in this family, with a common regulation mechanism while different tissue distribution and biology[3].

KLFs Structure

The carboxy-terminus (C-terminus) of KLFs contains DNA-binding region and nuclear localization signals. There are three conserved zinc finger motifs (two cysteine and two histidine residues, C_2H_2 type), which bind to the GC-rich region (also known as Sp1 binding region) widely distributed in promoters[4]. Contrary to the high similarity in C-terminus within this family or among different species, the amino-terminus (N-terminus) is unique, characterized by distinct motifs interacting with various proteins, which can be either transcription regulators or induce KLFs post-translational modification[4].

Based on the N-terminus structure and the downstream transcriptional regulation mechanism, KLFs can be divided into three groups. The first group (including KLF1, KLF2,

KLF4, KLF5, KLF6, and KLF7) primarily binds to co-regulators with acetyltransferase activity (*e.g.*, cyclic adenosine monophosphate-response element binding protein-binding protein and p300) and thus functions as a transcriptional activator. The second group (including KLF3, KLF8, and KLF12) is defined as capable of binding to transcriptional regulator C-terminal binding protein (CtBP), and the third group (including KLF9, KLF10, KLF11, KLF13, KLF14, and KLF16) binds to the transcriptional repressor Sin3A. As both CtBP and Sin3A can recruit histone methyltransferase and histone deacetylase (HDAC), these last two groups of KLFs primarily inhibit gene expression.

KLFs Biology

At the cellular level, KLFs control the transcription of proteins in cell cycle regulation (*e.g.*, cyclins D1, cyclin-dependent kinase inhibitors) and other proliferation-related transcription factors (*e.g.*, c-myc) to regulate proliferation[5-7]. Apart from cellular growth, KLFs can also regulate apoptosis and contributes to cancer[8, 9]. KLFs also play important roles in differentiation and therefore maintaining tissue homeostasis. These developmental processes include erythroid maturation (KLF1), intestinal epithelium differentiation (KLF4), adipogenesis (KLF2-7, KLF11, KLF15), vascular smooth muscle cell development (KLF2, KLF4, KLF5), *etc*[4, 10-14]. KLFs have distinct functions in various cell types and ensure important cellular functions on proliferation, apoptosis, and differentiation.

At the systemic level, animal models or human studies focusing on genetic KLFs variations further demonstrate their critical roles in tissue development, cancer, metabolic diseases, and cardiovascular diseases.

Krüppel-like factor 11 Biology

KLF11 Structure

Originally cloned from a human pancreatic epithelial cell line, KLF11 was identified as a new Sp1-like zinc finger protein with high homology with the transforming growth factor-beta (TGF-β) inducible immediate early gene (TIEG1 or KLF10), thus also known as TIEG2[15]. Further studies have defined TIEG2/KLF11 as the human isoform and Tg3/KLF11 as the isoform in mice[16].

In the C-terminus of KLF11, there is a basic tetra peptide within the second and the third highly homologous zinc finger motif that functions as the nuclear localization signal and is critical for its site-specific transcription activity. The DNA binding domain within the zinc finger motif can activate gene transcription[17]. In N-terminus, KLF11 contains three repression domains (*i.e.*, R1, R2, and R3), tethered to the target DNA region and inhibit gene transcription[18]. Among them, the R1 domain is recognized as an essential domain mediating transcription repression. As an alpha-helical repression motif, this R1 domain interacts with Sin3A, which recruits other transcriptional machinery (*e.g.*, HDAC) to inhibit gene transcription[18, 19]. Therefore, KLF11 functions as both a transcription activator and repressor, depending on the different cellular context (cell types and promoter condition)[15, 17].

Regulation of KLF11

The regulation of KLF11 is mostly studied in the cancer field. First known as TIEG2, KLF11 is a TGF-β-inducible gene and potentiates TGF-β-mediated anti-proliferation effects[15]. The binding of TGF-β ligand to its type 2 receptor and recruit and phosphorylate type 1 receptor, resulting in the formation of Smad complex (R-smad and Smad 4). This heterodimeric complex will translocate to the nucleus and induce KLF11 expression. One of the downstream target

genes of the KLF11-Sin3A-HDAC complex is Smad7, a negative feedback loop of TGF-β signaling. Therefore, the TGF-β-induced KLF11 can suppress the inhibitory Smad7 and thus increase TGF-β signaling[20].

Phosphorylation is a common post-translational mechanism that inhibits KLF11 activity. It has been reported that phosphorylation of the Sin3 interacting domain in KLF11 by oncogenic signaling ERK/MAPK disrupts the interaction between KLF11 and Smad3, reducing TGF-β-induced c-myc repression[21]. Similarly, KLF11 activity is suppressed after phosphorylation of the four serine or threonine sites adjacent to the Sin3 interacting domain by epidermal growth factor (EGF)-Ras-MEK1-ERK2 signaling[22].

Methylation of the KLF11 promoter has been documented to result in KLF11 downregulation and is involved in various cancers. Hypermethylation of KLF11 was observed in 15% of myelodysplastic syndromes and associated with a high International Prognostic Scoring System score[23]. In breast cancer, KLF11 hypermethylation is correlated with an increased risk of metastasis[24].

KLF11 and Diseases

KLF11 Variants from Human Genetics

KLF11 has been reported as the causative gene for maturity-onset diabetes of the young, type VII (MODY7, OMIM: 610508) in 2005. Genetic analysis in families of early-onset type II diabetes mellitus discovered the segregation of two rare KLF11 variants (Ala347Ser and Thr220Met)[25]. A more frequent polymorphic KLF11 variant Gln62Arg was found associated with type II diabetes in the North European population[25]. A novel KLF11 variant His418Gln was identified in a Japanese family with early childhood-onset type 1B diabetes[26]. Mechanistically,

KLF11 can activate insulin promoters in pancreatic β cells, while these variants alter the binding capability and thus reduce insulin transcription[25, 27].

KLF11 in Cardiovascular Diseases

Our lab was among the first to study the role of KLF11 in cardiovascular diseases. Utilizing conventional *Klf11* KO mice, we reported that KLF11 could interact with p65 to inhibit the nuclear factor-kappaB (NF-κB) signaling pathway. KLF11 prevented vascular inflammation and inhibited leukocyte recruitment to the endothelium after lipopolysaccharide administration in mice[28]. We have also demonstrated KLF11 as a new peroxisome proliferator-activated receptor gamma (PPARγ) co-regulator. KLF11 mediated the cerebral vascular endothelial protection in ischemic stroke by enhancing PPARγ repression of the microRNA-15, a pro-apoptotic gene[29].

Further studies in the cerebral vascular system found that KLF11 can directly bind to some major cerebral tight junction proteins (*e.g.*, occludin and ZO-1) and thus promote their activity to preserve the blood-brain barrier integrity[30]. Fenofibrate, a diabetes drug functioning as the peroxisome proliferator-activated receptor alpha (PPARα) ligand, can suppress endothelin-1 transcription via inducing KLF11 expression. Therefore, KLF11 mediates the beneficial effects of fenofibrate in diabetes-related microvascular complications[31]. Recently, our lab established that endothelial KLF11 protected against abdominal aortic aneurysm by inhibiting MMP9 activity and production of reactive oxygen species[32]. We also reported that KLF11 deficiency in endothelial cells could induce dedifferentiation and apoptosis of smooth muscle cells[32]. In sum, KLF11 plays a beneficial role in maintaining vascular homeostasis.

KLF11 in Metabolic Diseases

KLF11 in glucose metabolism

KLF11 is expressed ubiquitously but is highly enriched in the pancreas. The role of KLF11 in metabolism is also first identified in the pancreas, the key organ regulating glucose metabolism. Apart from the previously mentioned human genetic data indicating the association of KLF11 in the monogenic form of diabetes, following studies further found that KLF11 interacts with the coactivator p300 to activate pancreatic and duodenal homeobox 1 (PDX1), the causal gene for MODY4, and a master regulator for pancreatic β cell development[27, 33]. Conventional *Klf11* KO mice consistently revealed defects in insulin production but maintained normal blood glucose levels, which may due to the enhanced insulin sensitivity in peripheral tissues and interspecies differences[34].

Besides insulin secretion, KLF11 can also inhibit hepatic gluconeogenesis via directly suppressing the transcription of phosphoenolpyruvate carboxykinase (PEPCK) and PPARγ coactivator-1 alpha (PGC-1α). PEPCK is a critical rate-limiting enzyme in gluconeogenesis, and PGC-1α is an essential transcription factor regulating energy metabolism, including gluconeogenesis[35]. Adenovirus-mediated overexpression of hepatic KLF11 alleviated hyperglycemia and improved glucose intolerance in diabetic db/db mice[35].

KLF11 in Lipid Metabolism

KLF11 can regulate hepatic fatty acid and lipid metabolism. It was reported that hepatic KLF11 expression is reduced in the livers of diet-induced obesity and db/db mice[36]. Hepatic KLF11 overexpression activates PPARα and its downstream targets involved in lipid oxidation, alleviating lipid accumulation in a diet-induced obesity mice model[36]. PPARα loss-of-function abolishes the stimulatory effects of KLF11 in fatty acid oxidation and consequently aggravates triglyceride accumulation in the liver[36].

In a mouse study, global KLF11 deficiency protected against high fat diet-induced obesity and reduced cholesterol and triglyceride level. Genome-wide profiling and pathway-specific qPCR of liver tissue revealed that KLF11 deficiency altered several gene clusters involved in fatty acid metabolism (*e.g.*, fatty acid biosynthetic process), at least partially via disrupting PPARγ target genes[34].

In white adipose tissue, KLF11 was discovered as a direct transcription activator of uncoupling protein 1 (UCP1), an essential regulator of browning[37]. PPARγ can also induce KLF11, and KLF11 functions as a co-regulator of PPARγ to increase its activity[29]. PPARγ agonist such as rosiglitazone is one of the commonly prescribed diabetes drugs. It has been demonstrated that the interaction between KLF11 and PPARγ is required for the therapeutic effects of PPARγ agonist in improving oxidative capacity and adipose tissue browning[38].

KLF11 in Cancer

Due to its critical role in growth regulation, KLF11 has been reported in various tumors, including pancreatic cancer, small-cell lung cancer, breast cancer, ovarian cancer, gastric cancer, esophageal cancer, hepatocellular carcinoma, neuroblastoma, myelodysplastic syndrome, and leukemia[39]. Similar to TGF-β signaling, which has dual effects in carcinogenesis, KLF11 functions as either a tumor suppressor or an inducer. In breast cancer, microRNA-30d (miRNA-30d) aggravates tumor cell survival by inhibiting apoptosis, increasing migration/invasion, and mediating epithelial-mesenchymal transition. These tumor-promoting effects are mediated by the KLF11-STAT3 pathway[40]. KLF11 can be induced after hyperthermia treatment in non-small-cell lung cancer and elevated intracellular reactive oxygen species, resulting in increased apoptosis and reduced cell proliferation, subsequently improving treatment efficiency[41]. KLF11 was found upregulated in gastric cancer and promoted tumor cell migration and invasion by increasing

TWIST1 expression[42]. Apart from tumor-promoting effects, KLF11 was also identified as a tumor suppressor in pancreatic cancer. The complex of KLF11-Smad3 bound to the promoter of oncogenic gene c-myc and silenced c-myc expression[21].

Summary

The function of KLF11 in normal cell types or tissues is summarized in **Table 1.1**. Accumulating evidence indicates that KLF11 is a critical transcription regulator in multiple intracellular processes, including suppressing inflammation, inducing cell differentiation, and regulating cell survival/proliferation. All these cellular processes indicate an important role of KLF11 in maintaining systemic homeostasis and contributing to the development of several diseases, such as cardiovascular diseases, metabolic diseases, and cancer. Currently, most of the studies of KLF11 biology are focused on cancer. More studies on the KLF11 biology in the vascular wall and cardiovascular diseases may facilitate understanding the pathophysiology of these diseases and provide us with new therapeutic targets.

Table 1.1 Summary of KLF11 functions in normal cell types or tissues

Cell types or tissues	Function	Related disease	Reference
Pancreatic β cells	KLF11 activates insulin promoters in pancreatic β cells. KLF11 variants alter the binding capability and thus reduce insulin transcription.	Diabetes (MODY7)	[25, 27 26]
Pancreatic epithelial cells	KLF11 mediates the growth inhibition induced by TGF-β signaling.	Pancreatic cancer	[21]
Endothelial cells	KLF11 prevents vascular inflammation and inhibits leukocyte recruitment to the endothelium after lipopolysaccharide administration.	Sepsis	[28]
	KLF11 maintains the structure and integrity of the blood-brain barrier.	Ischemic stroke	[29, 30]
	KLF11 inhibits MMP9 activity and the production of reactive oxygen species. KLF11 deficiency induces dedifferentiation and apoptosis of smooth muscle cells.	Abdominal aortic aneurysm	[32]
Hepatocytes	KLF11 inhibits hepatic gluconeogenesis by directly suppressing the transcription of phosphoenolpyruvate carboxykinase (PEPCK) and PPARγ coactivator-1 alpha (PGC-1α).	Diabetes	[35]
	KLF11 deficiency altered gene clusters involved in the fatty acid biosynthetic process, partially by disrupting PPARγ target genes. KLF11 overexpression activates PPARα and its downstream targets involved in lipid oxidation, and thus alleviates lipid accumulation.	Steatosis/Fatty liver disease	[34, 36]

White adipose tissue	KLF11 is a direct transcription activator of uncoupling protein 1 (UCP1). KLF11 functions as a co-regulator of PPARγ to increase its activity (*e.g.*, enhancing oxidative capacity and adipose tissue browning)	Obesity	[29, 37, 38]

Chapter 2 KLF11 in Vascular Smooth Muscle Cells and Arterial Thrombosis

Introduction

Thrombosis is a common pathology underlying many cardiovascular diseases: myocardial infarction, stroke and venous thromboembolism, which collectively cause more than one-fourth of deaths worldwide.[43] The primary pathogenic process in arterial thrombosis is the rupture of the atherosclerotic plaque, which promotes platelet recruitment, adhesion, aggregation and activation and results in thrombus growth.[44] Given the importance of vascular smooth muscle cells (VSMCs) in vessel homeostasis and pathogenesis of vascular diseases,[45] it is of great interest to identify molecular signaling pathways that mediate the effects of both physiological and pathophysiological stimuli in VSMCs.

The Krüppel-like factor (KLF) family plays a critical role in maintaining vascular homeostasis and further affects multiple vascular diseases.[3, 46] Maturity-onset diabetes of the young type 7 (MODY7), an early-onset type 2 diabetes mellitus, is caused by mutations in the *KLF11* gene.[25] It was originally identified that KLF11 could regulate *INSULIN* transcription in pancreatic β cells. Apart from causing the metabolic disorder, diabetes accelerates vascular pathology and enhances thrombotic risk,[47, 48] which account for the major causes of morbidity and mortality in diabetic patients.[49]

As a transcription factor, KLF11 is expressed ubiquitously and is abundant in adipose tissue, testis, breast, artery and lung (GTEx database). RNA sequencing data show that the mRNA level of KLF11 is modest in human endothelium and moderate in human aortic smooth

muscle cells (HASMCs).[3] Prior studies from others and our group demonstrated that KLF11 plays an important role in maintaining vascular homeostasis.[28, 50] Specifically, KLF11 inhibits endothelial activation in the presence of inflammatory stimuli and functions as a peroxisome proliferator-activated receptor-γ co-regulator to attenuate middle cerebral artery occlusion-induced stroke in mice.[29] These *in vitro* and *in vivo* observations form the basis of the current view that KLF11 is a vessel protective factor. However, the role of KLF11 in VSMC biology and thrombosis has not been explored.

In the present study, we focused on VSMC KLF11 and, using *in vivo* VSMC-specific loss-of-function approaches, demonstrated that this factor is an inhibitor of experimental arterial thrombosis through transcriptional repression of tissue factor (TF, encoded by *F3* gene) in VSMCs.

Materials and methods

Animals

Conventional KLF11 knockout mice (*Klf11* KO) and wild type (WT) mice in the C57BL/6J background were previously described[28] and the KO was confirmed (**Figure 2.1**). The floxed-KLF11 ($Klf11^{fl/fl}$) mice were generated by injecting blastocysts developed from *Klf11* targeted ES cells ($Klf11^{tm2a(KOMP)Wtsi}$, UCDavis, KOMP) into C57BL/6J mice. Exon 3 of the *Klf11* gene was flanked by *LoxP* elements. The genotype was determined from mouse tail clippings and a pair of PCR primers flanking the downstream *LoxP* region (**Figure 2.2A**). The inducible smooth muscle cell-specific *Klf11* knockout (*Sm-Klf11* KO) mice were generated by cross-breeding $Klf11^{fl/fl}$ mice with *Myh11-CreER*^{T2} mice (019079, Jackson Laboratory).[51] The primer sequences for mouse genotyping are shown (**Table 2.1**). The *Myh11-CreER*^{T2}*-(+)/Klf11*$^{fl/fl}$ mice (*Sm-Cre/Klf11*$^{fl/fl}$ +TAM) and *Myh11-CreER*^{T2}*-(-)/Klf11*$^{fl/fl}$ mice ($Klf11^{fl/fl}$

+TAM) were treated with tamoxifen (intraperitoneal injections, 80mg/kg per day for 5 consecutive days, indicated as +TAM). *Myh11-CreER^{T2}-(+)/Klf11$^{fl/fl}$* mice treated with the same volume of vehicle corn oil (*Sm-Cre/Klf11$^{fl/fl}$* + Oil) were used as the control group. Fourteen days after tamoxifen or corn oil treatment, the reduction of KLF11 expression in the aorta was confirmed by real-time quantitative PCR and western blot (**Figure 2.2B-C**). Since the *Myh11-Cre/ER^{T2}* transgene is inserted on the Y chromosome,[52] only male *Sm-Cre/Klf11$^{fl/fl}$* mice can be generated using this approach. All animal care and experimental procedures were approved by the University of Michigan Animal Care and Use Committee.

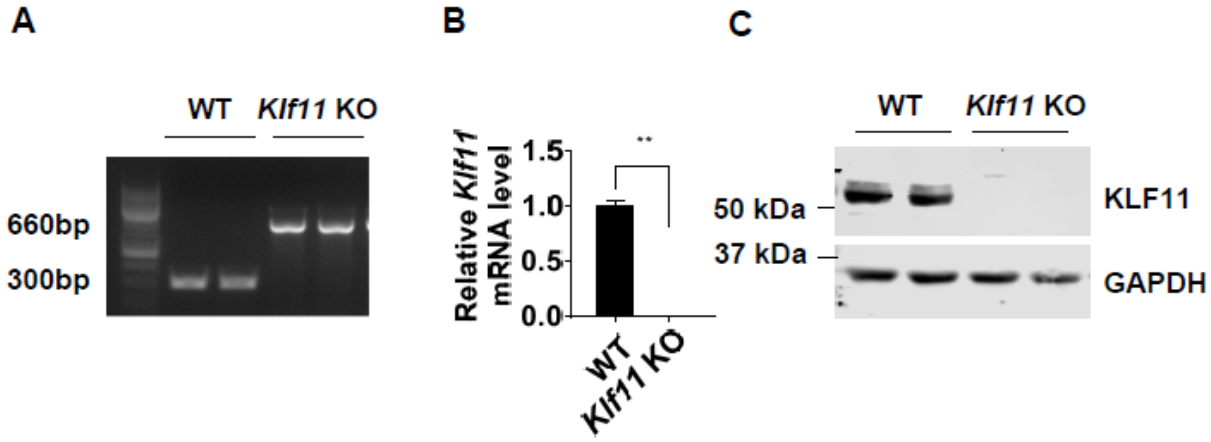

Figure 2.1 Characterization of the conventional *Klf11* KO (Krüppel-like Factor 11 knockout) mice.

A, Genotyping of wild type (WT) and *Klf11* KO mice by PCR. B, *Klf11* mRNA level was determined in the isolated mouse aorta by real-time quantitative PCR and normalized by 18S. Data are presented as mean ± SEM. n=5 per group. ***P*<0.01 using Student *t*-test. C, Representative western blots of KLF11 protein level in the mouse aorta from WT and *Klf11* KO mice.

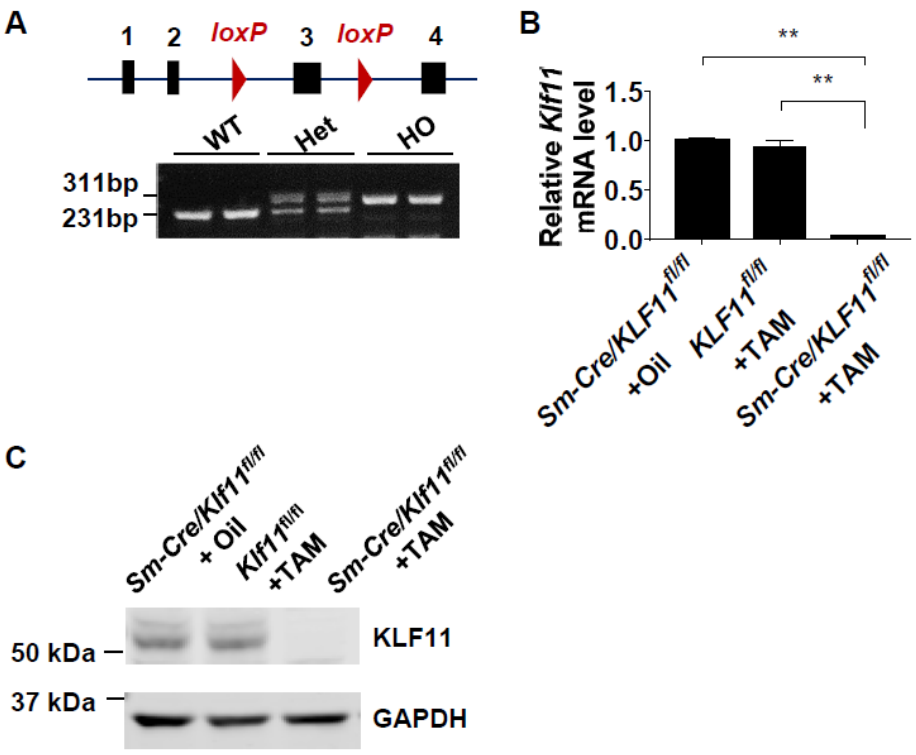

Figure 2.2 Characterization of the conventional *Klf11* KO (Krüppel-like Factor 11 knockout) mice.

A, Genotyping of wild type (WT) and *Klf11* KO mice by PCR. B, *Klf11* mRNA level was determined in the isolated mouse aorta by real-time quantitative PCR and normalized by 18S. Data are presented as mean ± SEM. n=5 per group. ***P*<0.01 using Student *t*-test. C, Representative western blots of KLF11 protein level in the mouse aorta from WT and *Klf11* KO mice.

Ferric Chloride-Induced Carotid Artery Thrombosis Model

Ferric chloride ($FeCl_3$)-induced carotid artery thrombosis was conducted as previously described. [53] Briefly, conventional *Klf11* KO mice and WT mice (8-10-week-old male mice; 6-8-week-old female mice) or *Sm-Klf11* KO mice and control mice (11-13-week-old male mice) were anesthetized by intraperitoneal injection of ketamine (100mg/kg)/xylazine (10mg/kg). The left common carotid artery was dissected, and the probe of a transonic flow meter was placed under the carotid artery (Mode T106; Transonic Systems, Ithaca, NY). Ten percent $FeCl_3$ was applied to a filter paper (1×2mm) that was placed above the carotid artery for 3 minutes. The blood flow was monitored, and the clotting time was recorded and statistically analyzed.

Bone Marrow Transplantation (BMT)

The protocol for syngeneic BMT was previously described.[54, 55] Briefly, recipient mice received 13 Gy (1300 rad) of total body irradiation (137Cs source) delivered in a single dose. Bone marrow (BM) cells were isolated from the femur of WT mice. A cell mixture of 5×10^6 bone marrow (BM) cells was resuspended in Leibovitz's L-15 medium (Thermo Fisher Scientific) and transplanted into syngeneic recipients via tail vein injection (total volume = 0.25 ml). Experiments with BMT mice were performed four weeks after BMT.

Preparation of Washed Murine Platelets and Platelet Aggregation Assay

The collection of washed murine platelets and platelet aggregation assay were performed as previously described.[56] Briefly, whole murine blood was collected from the inferior vena cava and mixed with Tyrode's buffer in equal volumes before centrifuging at 200 g to obtain the platelet-rich-plasma. The platelet-rich-plasma was supplemented with 10x acid citrate dextrose solution and apyrase (0.02 unit/ml) and centrifuged at 2,000 g. The platelet count was adjusted to

3×10^8 platelets/ml. Platelet aggregation was measured in a lumi-aggregometer (Chrono-log model 700D) under stirring conditions (1,100 rpm) at 37°C.

Isolation of Microvesicles (MV) from Plasma

We isolated MV following the protocol kindly provided by Dr. Nigel Mackman's lab with minor modifications. Briefly, mouse blood was collected from inferior vena cava (1:10 volume of 4% sodium citrate was used as an anticoagulant) and centrifuged at 5,000 g for 15 minutes at room temperature for collecting platelet-poor-plasma (PPP). PPP (100 µl) was washed by adding 1 ml HBSA-Ca^{2+}(-) (pH=7.4, 137 mM NaCl, 5.38 mM KCl, 5.55 mM Glucose, 10 mM Hepes, 0.1% BSA) and centrifuging at 20,000 g for 40 minutes at 4°C. After a second wash, the pellet was resuspended vigorously with 100 µl HBSA-Ca^{2+}(-) and underwent sonication (35% Amplitude, 5 seconds, 2 times).

Tissue Factor Activity Assay

The protocol for detecting tissue factor (TF) activity was kindly provided by Dr. Nigel Mackman's lab. The mouse aorta was homogenized in 50mM Tris-buffered saline (pH 8.0) with 1% Triton X-100 and centrifuged at 14000 g for 20 minutes at 4°C to collect the supernatant. Homogenized protein samples (aorta or MVs) (50 µl) were added to duplicate wells in a 96-well plate and incubated with TF 1H1 antibody or rat IgG (final concentration: 200 µg/ml) for 1 hour at room temperature. Next, 50 µl of HBSA containing 24.4 nM human FVIIa (HFVIIa, Enzyme Research Laboratories), 73 nM human FX (HFX 1010, Enzyme Research Laboratories) and 10 mM $CaCl_2$ was added to each well and incubated at 37°C for a certain time (80 minutes for aorta samples and 3 hours for MVs). The reaction was stopped by adding 25 µl EDTA (25 mM) and incubated at room temperature for 5 minutes. After that, 25 µl chromogenic substrate RGR-

XaChrom (4.6 mM, 100-03, Enzyme Research Laboratories) was added, and the plate was incubated at 37°C for 15 minutes. The generation of FXa was measured by reading the absorbance at 405 nm. The concentration was calculated by referring to a standard curve generated by recombinant human TF standard (ab108906, Abcam), at a range of 0.01 pM - 0.1 pM for MVs and 1.0 pM - 25.0 pM for aorta samples. The TF-dependent FXa generation was measured and calculated by subtracting the amount of FXa generated in the presence of TF 1H1 antibody from the total amount of FXa generated in the presence of IgG.

Prothrombin Time (PT) and Activated Partial Thromboplastin Time (aPTT) Measurements

Platelet-poor-plasma (PPP) was collected as previously described. [57] Eight to ten-week-old male conventional *Klf11* KO mice and WT mice were used in this experiment. Briefly, whole mouse blood was collected from the tail into tubes containing 3.8% sodium citrate and centrifuged at 1,500g for 15 minutes to collect the PPP. According to the manufacturer's manual, PT and aPTT were determined in a KC-4 Coagulation Analyzer (Sigma-Aldrich, St Louis, MO).

Tail-Bleeding Assay

Conventional *Klf11* KO mice and WT mice (8-10-week-old male) were used in this experiment. As previously described,[56] a transverse incision at the 5 mm distal end of the tail was performed and the tail was immersed in saline at 37°C. Bleeding time was recorded as the time to cessation of bleeding.

Thrombin-antithrombin (TAT) Complexes Measurements

Mouse plasma was collected from mice tails using 1:10 volume of 4% sodium citrate as an anticoagulant and centrifuged at 3000 g for 10 minutes. The level of thrombin-antithrombin (TAT) complexes in the plasma was determined by enzyme-linked immunosorbent assay

(ab137994, Abcam) in accordance with the manufacturer's protocol. Briefly, TAT complexes specific antibody has been precoated onto the 96-well plates. Plasma samples or TAT complexes standards were added in triplicate into this plate and incubated at room temperature for 2 hours, followed by adding a TAT complexes specific biotinylated detection antibody and incubating for 2 hours. Streptavidin-Peroxidases conjugate was added to induce an enzymatic reaction. The TAT complexes were visualized by adding chromogen substrate. After adding the stop solution, the absorbance at 450nm was recorded. The concentration was calculated by referring to a standard curve generated with a TAT complexes standard.

Adenoviral Constructs

Adenoviral vectors overexpressing human KLF11 or LacZ control were generated as previously described.[58] Briefly, the coding sequences were amplified by PCR and cloned into Ad-Easy vector via the AdTrack-CMV vector (Agilent Technologies). Adenoviruses were packaged in HEK293 cells and purified by $CsCl_2$ density gradient ultracentrifugation. The genomic DNA of adenovirus was purified with the NucleoSpin virus kit (Macherey Nagel) and the titration was performed with the Adeno-XTM quantitative PCR titration kit (#632252, Clontech).

Cell Culture

Human aortic smooth muscle cells (HASMCs, CC-2571, Lonza) were cultured in SmGM™-2 medium containing 5% FBS (CC-3182, Lonza) and used within 10 passages. Before thrombin stimulation, the HASMCs were made quiescent with DMEM/F12 with 0.5% fetal bovine serum (FBS) for 48 hours. A7r5 cells (CRL-1444™, ATCC) were cultured in DMEM/F12 supplemented with 10% FBS) and 50mg/ml of a penicillin/streptomycin mix.

Mouse aortic smooth muscle cells (MASMCs) were isolated from the conventional Klf11 KO mice and WT mice (3-4-week-old male) as previously described.[51] Briefly, the aorta was isolated and digested in an enzyme solution: Hank's balanced salt solution containing 1 mg/ml collagenase type 2 (LS004174), 0.744U/ml elastase (LS002279) and 1 mg/ml soybean trypsin inhibitor (LS003570, all enzymes were from Worthington Biochemical Cooperation) for 10 minutes. After the first digestion, the adventitia was removed, and the lumen was scraped to remove endothelium. The remaining aortic media was subjected to final digestion in the same enzyme solution at 37°C for 1 hour. The disaggregated mouse aortic smooth muscle cells were plated on 0.1% gelatin (ES-006-B, Millipore) coated plates and cultured in DMEM/F12 supplemented with 20% FBS and 50 mg/ml of a penicillin/streptomycin mix. The purity of MASMCs was validated by immunostaining for α-smooth muscle actin (SMA). All cells were cultured in a 5% CO_2 humidified incubator at 37°C. All cells were used within passages 6-10 for the experiments.

Reagents and Antibodies

Thrombin (T1063); for cell culture studies, the control group was treated with the same volume of the vehicle for thrombin [0.1% (w/v) BSA in PBS], Lipopolysaccharide (L3012) and Tamoxifen (T5648) were from Sigma-Aldrich. BAY 11-7082 (10010266) was from Cayman. Thrombin (HT 1002a) used in the platelet aggregation assay was from Enzyme Research Laboratories. For western blot, antibodies against GAPDH (sc-32233, 0.1 μg/ml) and tissue factor (sc-374441, 0.2 μg/ml) were from Santa Cruz Biotechnology. Antibodies against β-actin (#4967S, 0.014 μg/ml), histone 3 (#4499S, 0.01 μg/ml), p65 (#8242T, 0.212 μg/ml) and IκBα (#4814T, 0.463 μg/ml) were from Cell Signaling Technology. Antibody against mouse KLF11 was produced by Syd labs (targeted to the epitope CTKKIPGWQAEVGKLNR, 1 μg/ml).

Monoclonal antibody against human KLF11 was from Abnova (H00008462-M01, 1 μg/ml). The anti-flag antibody (#14793S, 2.82 μg/ml) and rabbit IgG (#2729S, 2.82 μg/ml) for ChIP assay were from Cell Signaling Technology. The rat anti-mouse tissue factor 1H1 antibody, kindly provided by Dr. Daniel Kirchhofer at Genentech,[59] was applied for immunostaining (20 μg/ml) and blocking TF activity (200 μg/ml). The α-smooth muscle actin (α-SMA) antibody for immunostaining was from Abcam (ab5694, 1 μg/ml).

Messenger RNA (mRNA) Isolation and Quantitative Polymerase Chain Reaction (PCR)

Total RNA from tissues or cells was extracted with the RNeasy Kit (QIAGEN) and was reverse-transcribed into cDNA with SuperScript III reverse transcriptase (Thermo Fisher Scientific). Gene expression was measured by real-time quantitative PCR with IQ SYBR Green Supermix (Bio-Rad). The primer sequences are listed in Table 2.1.

Protein Extracts and Western Blot

Homogenized tissues or cells were lysed in RIPA lysis buffer at 4°C for 30 minutes and centrifuged at 15000 rpm for 15 minutes to remove the insoluble material. Proteins (30 μg/lane) were separated by 10% SDS-PAGE in running buffer (25Mm Tris, 190mM glycine and 0.1% SDS) and electrophoretically transferred to 0.45 μm nitrocellulose membrane in transfer buffer (25mM Tris, 190mM glycine and 20% methanol). Membranes were blocked with 5% non-fat milk in Tris-buffered saline for 1 hour at room temperature. Blots were incubated with primary antibodies diluted in 5% non-fat milk at 4°C overnight (working concentration was described in "Reagents and Antibodies"), followed by incubation with IRDye secondary antibody (0.2 μg/ml, LI-COR) at room temperature for 1 hour. Odyssey infrared imaging system was used to scan the blots at 169 μm resolution. The blot intensity was quantified on a single channel with the Image Studio Analysis Software (LI-COR).

Small interfering RNA (siRNA)-mediated gene knockdown

HASMCs were transfected with siRNA-KLF11 (107176, Thermo Fisher Scientific) or non-targeting siRNA control (AM4611, Thermo Fisher Scientific) using Lipofectamine RNAiMAX Reagent (13778150, Thermo Fisher Scientific) according to the manufacturer's recommendations. Briefly, si-Control or si-KLF11 were diluted in Opti-MEM (final concentration: 40 nM) and incubated with Lipofectamine RNAiMAX (diluted in Opti-MEM) for 20 minutes at room temperature. The mix was added to HASMCs cultured in 6-well plates. After incubation with the reaction mix for 24 hours, the medium was changed to DMEM/F12 with 0.5% FBS for a 48-hours' serum starvation before thrombin stimulation. Data are from triplicates and from at least three independent experiments.

Immunostaining

Murine aortas were fixed in 4% paraformaldehyde and embedded in OCT. Cryostat aortic sections (7 μm) were permeabilized with 0.3% Triton-X100 and stained with primary antibody against mouse TF (20 μg/ml, Genentech) and α-SMA (1 μg/ml, Abcam) overnight, followed by immunostaining with the Alexa Fluor conjugated secondary antibody (1 μg/ml, Jackson ImmunoResearch) for 2 hours. MASMCs seeded on 0.1% gelatin-coated cell culture chamber slides, and grown to 70% confluence, were fixed with 4% paraformaldehyde and permeabilized with 0.3% Triton-X100, followed by incubating with anti-SMA (1 μg/ml) overnight and Alexa Fluor secondary antibody (1 μg/ml, Jackson ImmunoResearch) for 2 hours. Slides were mounted with ProLong™ Gold Antifade Mountant with DAPI (Thermo Fisher Scientific) and images were taken with an Olympus IX73 microscope. The exposure time was 3 ms for DAPI and α-SMA staining and 500 ms for TF staining. Quantification of the TF intensity was performed with

Image J. This process included 4 mice for each group and 3 randomly selected 40x objective microscopic fields for each specimen. The immunofluorescence signal of TF was calculated by subtracting nonspecific signal (determined by the control IgG staining) and then the values were divided by the total area of the medial layer (determined by α-SMA staining). Data were normalized to the control group (basal level of WT mice) set as 1. The individuals performing imaging and analysis were blinded to the identity of the specimens.

Chromatin Immunoprecipitation Assay (ChIP)

ChIP assays were performed using the SimpleChIP Enzymatic Chromatin IP Kit (Magnetic Beads) (9003S, Cell Signaling Technology) in accordance with the manufacturer's protocol. Briefly, serum-starved HASMCs were treated with 1% formaldehyde for 10 minutes at room temperature and the cross-linking was stopped with 0.1% glycine. The nuclei pellets were digested with Micrococcal Nuclease (1000 gel units/4×10^6 cells) at 37°C for 20 minutes, followed by sonication (35% Amplitude, 5 seconds, 3 times). After centrifugation, the supernatants were incubated with 1 μg anti-flag antibody or normal rabbit IgG at 4°C overnight. The DNA/protein complexes were immunoprecipitated with Protein G Magnetic Beads with rotation at 4°C for 2 hours, followed by washing in low-salt and high-salt buffer and elution at 65°C for 30 minutes. The cross-link of DNA-protein complexes was reversed at 65°C overnight. DNA was purified and used as a template for real-time quantitative PCR. The primer sequences for ChIP assay are forward: 5'-GGTGAGTCATCCCTTGCAG-3'; reverse: 5'-GGGAGCTCGCAGTCTTG-3' and correspond to the region of -170 to +41 base pairs, relative to the transcription start site of the tissue factor gene.

Luciferase Assay

A7r5 cells were co-transfected with plasmids using Lipofectamine 2000 (11668019, Thermo Fisher Scientific) according to the manufacturer's protocol. Briefly, A7r5 cells were cultured in 48-well plate and grown to approximately 80% confluence before transfection. Both the reporter plasmids (0.5 μg/well) and Lipofectamine 2000 Reagent were incubated with Opti-MEM separately and mixed for a 20 minutes' incubation. The mix was added to A7r5 cells cultured in DMEM/F12 containing 10% FBS. Three days after transfection, the *F3* promoter reporter activity was measured by firefly luciferase (Promega) and normalized against Renilla activity, co-transfected as a control.

Statistical Analysis

All quantitative data are presented as mean ± SEM. Statistical analysis was performed using the GraphPad Prism 7. All data were first subjected to Shapiro-Wilk normality test and *F* test to evaluate homogeneity of variances. For normally distributed data with similar variances among groups, unpaired Student *t*-test with Welch's correction was used for two-group comparisons and one-way analysis of variance (ANOVA) followed by Tukey's test was used for more than two groups' comparisons. Two-way ANOVA followed by Bonferroni test was applied for comparisons of grouped data under different conditions. A nonparametric Mann-Whitney test was used for data not normally distributed. All results were representative of at least four independent experiments.

Table 2.1 Primer Sequences Used for Genotyping and Real-time Quantitative PCR

Primers used for real-time quantitative PCR		
Gene*	Primer Sequences	
h*KLF11*	F	GACACACACCTCACGGACAG
	R	ATCATCTGGCAAAGGACAGG
h*F3*	F	GTACTTGGCACGGGTCTTCT
	R	AATTGTTGGCTGTCCGAGGT
h*TFPI*	F	GTTGGGCTATTCCCAACTGC
	R	TCGCTGCTGTCTGTTAGAGC
h*PAR-1*	F	CCACAAACGTCCTCCTGATT
	R	TGGGATCGGAACTTTCTTTG
h*MCP-1*	F	CAATCAATGCCCCAGTCACC
	R	TCGGAGTTTGGGTTTGCTTG
h*IL-1β*	F	GGAGAATGACCTGAGCACCT
	R	GGAGGTGGAGAGCTTTCAGT
h*GAPDH*	F	GTCAGTGGTGGACCTGACCT
	R	TGCTGTAGCCAAATTCGTTG
m*Klf11*	F	CAGGGAACTGTGATGCTGGT
	R	GCCATGACACTGGATGGACA
m*F3*	F	AAAGGGAAGAACACCCCGTC
	R	ATCAGAGCTCTCCGCAACAG
m*18S*	F	CGCGGTTCTATTTTGTTGGT
	R	AGTCGGCATCGTTTATGGTC
Primers used for mouse genotyping		
Conventional *Klf11* KO	F	GAACAAGATGGATTGCACGCAGGTTCTCCG
	R	AGGCGATAGAAGGCGATGCGCTGCGAATCG
Wild type	F	CCTGCAGCTGGGACGGCTGTGAC
	R	CCCACAGGTGACGGATGCCACAG
Floxed *Klf11*	F	GCCCCTTGCTCCCAGAAATA
	R	GGTGAATCTCCCGCCTGGC
Myh11-Cre	F	TGACCCCATCTCTTCACTCC
	R	AGTCCCTCACATCCTCAGGTT

* h: human. m: mouse.

Results

KLF11 Deficiency Aggravates Arterial Thrombosis In Vivo

To assess the role of KLF11 in arterial thrombosis, we used the conventional *Klf11* KO mice previously reported[28] and applied a $FeCl_3$-induced thrombosis model for studying arterial thrombosis.[53] The occlusion time in the *Klf11* KO male mice was significantly reduced to an average of 62% of that in WT C57BL/6J male mice (**Figure 2.3A***).* A similar pro-thrombotic phenotype was also observed in *Klf11* KO female mice, with the occlusion time reducing to 56% of that in the WT C57BL/6J female mice (**Figure 2.3B**). To exclude the effects of *Klf11* KO in blood cells (platelets, neutrophils, macrophages, *etc.*) in this pro-thrombotic phenotype, we performed bone marrow transplantation (BMT) in *Klf11* KO and WT mice. The reduced occlusion time in the *Klf11* KO group transplanted with WT bone marrow was not rescued when compared with WT mice transplanted with WT bone marrow (**Figure 2.3C**).

The hemostatic status in the *Klf11* KO male mice was evaluated by measuring the function of coagulation factors and platelets. Our results showed that KLF11 did not alter the prothrombin time (PT) and activated partial thromboplastin time (aPTT), which reflects the function of extrinsic/common or intrinsic coagulation pathways, respectively (**Figure 2.3D-E**). Bleeding time and thrombin-antithrombin (TAT) complexes were also unchanged in the *Klf11* KO mice, indicating that the general hemostatic status was normal in the conventional *Klf11*-deficient mice (**Figure 2.3F-G**). To evaluate whether the deficiency of KLF11 in megakaryocytes can affect the platelet function, we isolated washed platelets and performed a thrombin-induced platelet aggregation assay. The maximum platelet aggregation induced by thrombin did not show significant differences between WT and conventional *Klf11* KO mice (**Figure 2.4**).

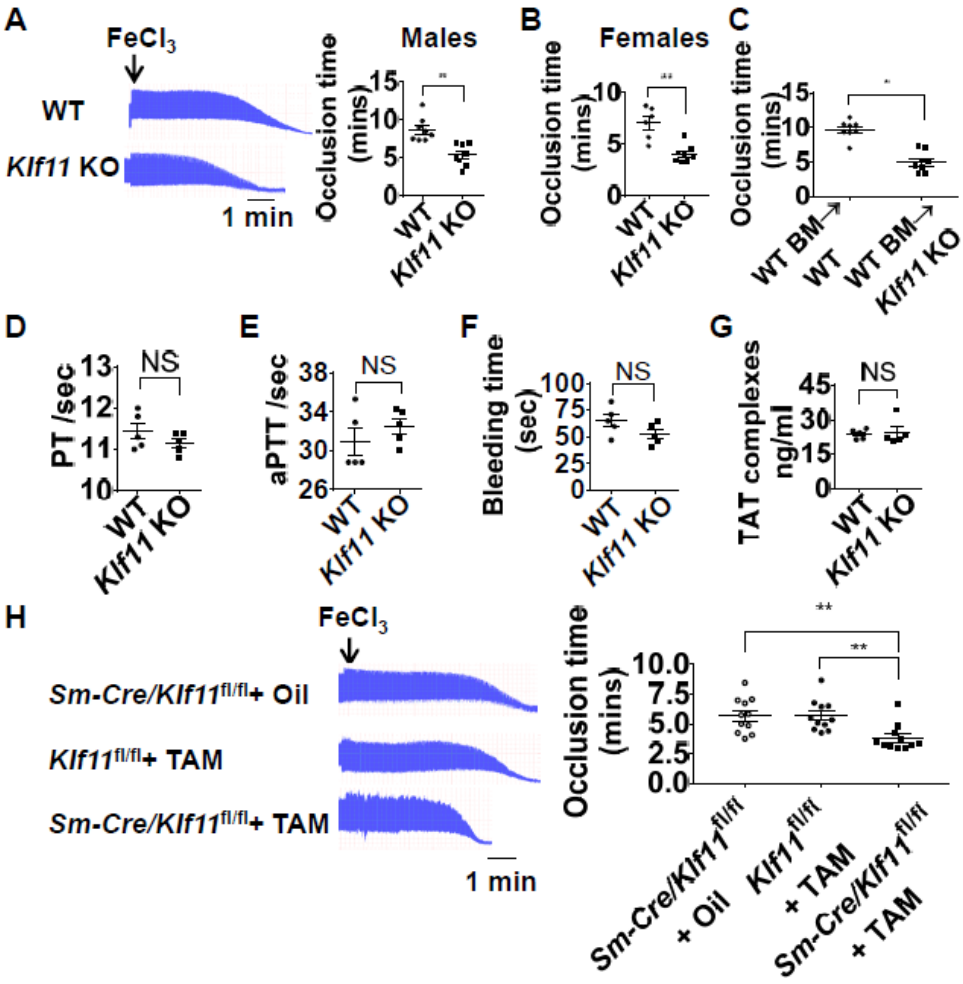
A
FeCl3
WT
Klf11 KO
1 min
Occlusion time (mins)
Males
WT
Klf11 KO
B
Females
C
WT BM→ WT
WT BM→ Klf11 KO
D
PT /sec
NS
E
aPTT /sec
F
Bleeding time (sec)
G
TAT complexes ng/ml
H
Sm-Cre/Klf11fl/fl+ Oil
Klf11fl/fl+ TAM
Sm-Cre/Klf11fl/fl+ TAM
Sm-Cre/Klf11fl/fl + Oil
Klf11fl/fl + TAM
Sm-Cre/Klf11fl/fl + TAM

Figure 2.3 KLF11 deficiency aggravates arterial thrombosis.

A-**C**, The left carotid arteries of WT (wild type) and conventional *Klf11* KO (knockout) mice were subjected to 10% $FeCl_3$ to induce arterial thrombosis. **A**, Representative images of blood flow detected by ultrasound are shown with each division representing 8 seconds (left) and the corresponding occlusion time (right) determined in WT and *Klf11* KO male mice (n=8/group). **B**, Occlusion time in WT and *Klf11* KO female mice (n=6-8/group). **C**, WT male mice transplanted with WT bone marrow were designated as WT BM→WT, *Klf11* KO male mice transplanted with WT bone marrow were designated as WT BM→*Klf11* KO mice. The carotid artery occlusion time after bone marrow transplantation was recorded as in **A** (n=8/group). $^{**}P<0.01$ or $^{*}P<0.05$ using unpaired Student *t-test*. **D**-**G**, PT (prothrombin time), aPTT (activated partial thromboplastin time), bleeding time and TAT (thrombin-antithrombin) complexes were measured from WT and *Klf11* KO male mice (n=5/group). NS, no significance using unpaired Student *t*-test (**D, F, G**) or nonparametric Mann-Whitney test (**E**). **H**, The left carotid arteries of *Sm-Cre/Klf11*$^{fl/fl}$+TAM (*Myh11-CreER*^{T2}*/Klf11*$^{fl/fl}$+tamoxifen) mice and controls: *Sm-Cre/Klf11*$^{fl/fl}$+ Oil (*Myh11-CreER*^{T2}*/Klf11*$^{fl/fl}$+ corn oi) and *Klf11*$^{fl/fl}$+TAM (*Klf11*$^{fl/fl}$+ tamoxifen) mice, were subjected to 10% $FeCl_3$ to induce thrombosis. Representative images of blood flow detected by ultrasound are shown and the occlusion time in control and *Sm-Klf11* KO mice was recorded (n=11/group). $^{**}P<0.01$ using one-way ANOVA followed by Tukey's test.

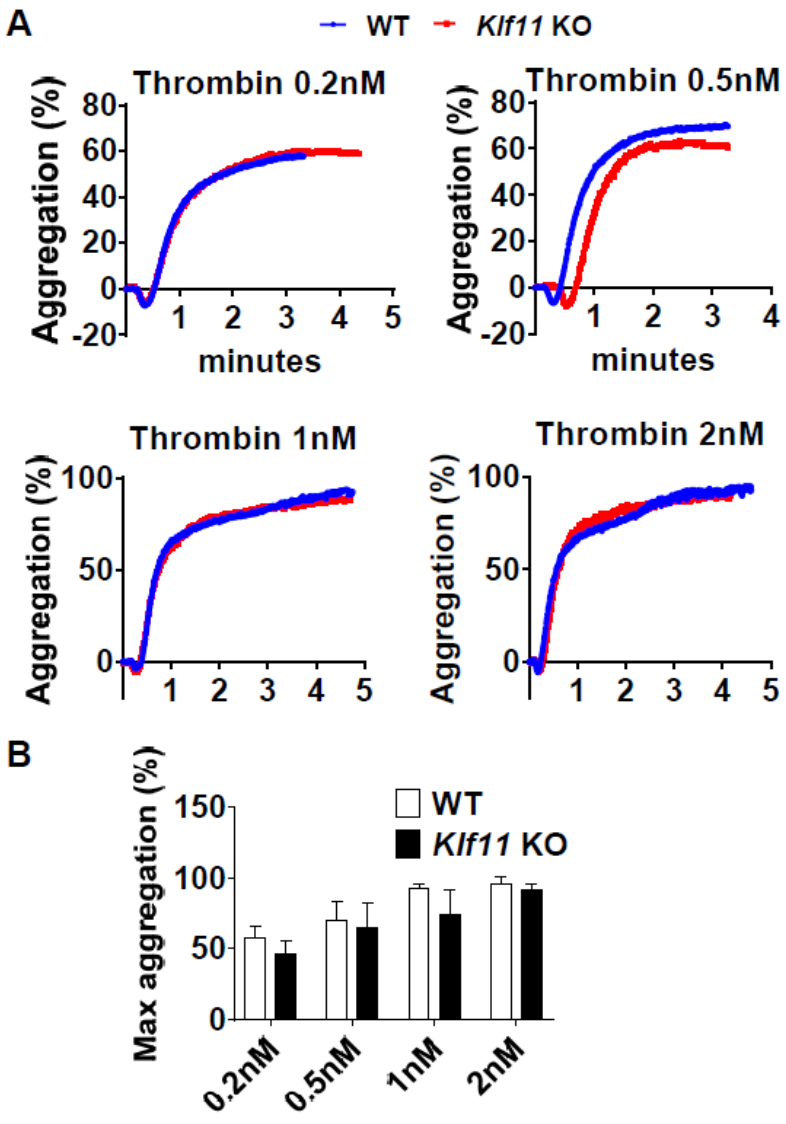

Figure 2.4 Thrombin-induced platelet aggregation response is not altered in *Klf11* KO mice.

Platelets were isolated from WT and conventional *Klf11* KO mice. **A,** Representative tracings of platelet aggregation. **B,** Maximum aggregation percent of platelets stimulated with different concentrations of thrombin. n=4 per group. Data are presented as mean ± SEM. Data between two groups were analyzed by two-way ANOVA followed by Bonferroni test.

Smooth Muscle Cell-Specific KLF11 Deficiency Aggravates $FeCl_3$-Induced Arterial Thrombosis

Considering that the hemostatic status in the circulation was not affected and the bone marrow transplantation cannot rescue the occlusion time in the conventional *Klf11* KO mice, the phenotype in *Klf11* KO mice might result from molecular changes specific to the vascular wall. To further identify the role of the vascular smooth muscle cell (VSMC) KLF11 in thrombosis, we generated tamoxifen-inducible *Sm-Klf11* KO (*Myh11-CreER^{T2}/Klf11$^{fl/fl}$* + TAM) mice (**Figure 2.2A**). *Klf11$^{fl/fl}$* mice treated with tamoxifen (*Klf11$^{fl/fl}$* + TAM) and *Myh11-CreER^{T2}/Klf11$^{fl/fl}$* mice treated with corn oil (*Sm-Cre/Klf11$^{fl/fl}$* + Oil) were used as controls. KLF11 deficiency in the aortic media of *Sm-Klf11* KO mice was confirmed at the mRNA and protein levels (**Figure 2.2B-C**). The specificity of the Myh11-CreER^{T2} in the aorta had been confirmed previously, as no expression was detected in cells from the blood and bone marrow.[60] In the $FeCl_3$ thrombosis model, *Sm-Klf11* KO mice exhibited a similar pro-thrombotic phenotype as that observed in the conventional *Klf11* KO mice. The occlusion time in the Sm-*Klf11* KO mice was significantly reduced to an average of 67% of that in the two control mouse groups (**Figure 2.3H**). Our data suggest that VSMC KLF11 protects against arterial thrombosis.

TF Expression is Increased in the Vascular Wall of Conventional Klf11 KO Mice

Tissue factor (TF) is an important initiator of the coagulation cascade, which can generate insoluble fibrin and form a thrombus. The vascular wall TF contributes to arterial thrombosis in cardiovascular diseases such as atherosclerotic plaque rupture and myocardial infarction.[61] VSMC TF is critical for arterial thrombus formation in the mouse $FeCl_3$ thrombosis model.[53] To determine whether TF is an effector mediating the enhanced thrombosis resulting from KLF11 deficiency, we measured TF expression in the aorta of conventional *Klf11* KO mice and WT

mice in basal conditions. First, circulating microvesicle-associated TF (MV-TF) activity showed no significant differences between *Klf11* KO and WT mice (**Figure 2.5A**). We applied anti-mouse TF 1H1 antibody[59] or rat IgG to validate the specificity of this assay. Next, we observed increased *F3* mRNA level and TF activity in the isolated carotid artery of conventional *Klf11* KO mice (**Figure 2.5B-C**). The elevated aortic TF activity can also be blocked by TF 1H1 antibody. Furthermore, the immunofluorescence staining data showed that TF protein was consistently upregulated in the vascular wall and co-localized with α-smooth muscle actin (α-SMA), a specific marker of VSMCs. Moreover, the *Klf11* KO mice also showed increased TF expression under lipopolysaccharide (LPS)-induced inflammatory conditions (**Figure 2.5D**). The relative TF intensity in the vascular wall was quantified and statistically analyzed. Collectively, our data suggest that KLF11 negatively regulates TF levels in VSMCs *in vivo*. Similar to the data in **Figure 2.3G**, no significant difference in TAT complexes was observed between WT and *Klf11* KO mice at basal conditions. However, there were higher TAT complexes in *Klf11* KO mice after LPS treatment (**Figure 2.6**).

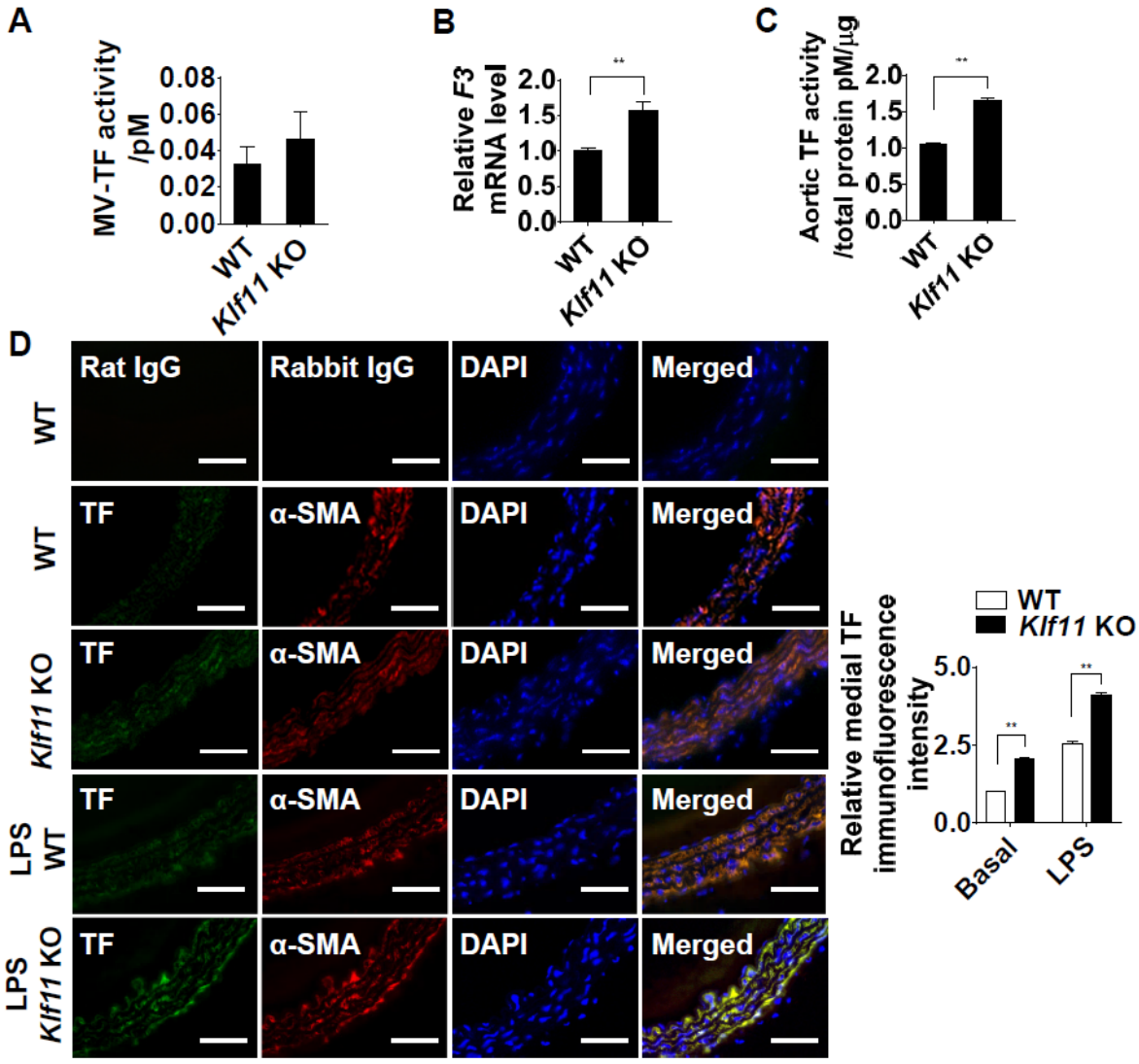
A
MV-TF activity /pM
0.08
0.06
0.04
0.02
0.00
WT
Klf11 KO
B
Relative F3 mRNA level
2.0
1.5
1.0
0.5
0.0
**
WT
Klf11 KO
C
Aortic TF activity /total protein pM/μg
2.0
1.5
1.0
0.5
0.0
**
WT
Klf11 KO
D
Rat IgG
Rabbit IgG
DAPI
Merged
WT
TF
α-SMA
DAPI
Merged
WT
TF
α-SMA
DAPI
Merged
Klf11 KO
TF
α-SMA
DAPI
Merged
LPS WT
TF
α-SMA
DAPI
Merged
LPS Klf11 KO
Relative medial TF immunofluorescence intensity
WT
Klf11 KO
5.0
2.5
0.0
**
**
Basal
LPS

Figure 2.5 KLF11 deficiency induces TF (tissue factor) expression in arterial wall.

A, Activity of microvesicles-associated tissue factor (MV-TF) in the plasma after preincubation with IgG or TF 1H1 antibody (n=6/group). Data are presented by subtracting the amount of FXa generated in the presence of TF 1H1 antibody from the amount of total FXa generated in the presence of IgG. **B,** *F3* mRNA level of carotid arteries from WT and *Klf11* KO mice. The mRNA level was normalized by *18S* and is presented relative to the WT group set as 1 (n=4/group). **C,** The aortic TF activity was measured and presented as in A, after preincubation with IgG or TF 1H1 antibody and normalized to the total protein quantity (n=6/group). ***P*<0.01 using unpaired Student *t*-test (**A-C**). **D**, Expression of TF (Alexa 647, displayed in green) and α-SMA (α-smooth muscle actin, Alexa 568, displayed in red) in mouse aorta at basal level or 4 hours after LPS (30 μg/kg) tail vein injection was visualized by immunofluorescence staining. Respective IgG staining was used as negative control. Scale bars=50 μm. Quantification was performed from 4 mice, randomly selecting 3 different medial regions from each specimen and dividing the TF immunofluorescence intensity by medial area (indicated by α-SMA positive cells). Data are presented relative to the basal level of WT group set as 1. ***P*<0.01 using two-way ANOVA followed by Bonferroni test.

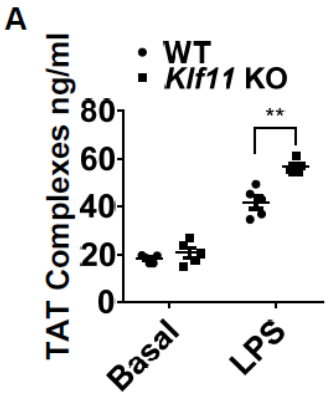

Figure 2.6 Characterization of the hemostatic condition in the conventional *Klf11* KO mice after LPS (lipopolysaccharides) treatment.

A, The TAT (thrombin-antithrombin) complexes were measured from WT and *Klf11* KO male mice, at basal level or 4 hours after LPS (30 µg/kg) tail vein injection. n=5/group. **P<0.01 using two-way ANOVA followed by Bonferroni test.

KLF11 Overexpression Rescues the TF Upregulation in KLF11-Deficient MASMCs

As a complementary and necessary approach, mouse aortic smooth muscle cells (MASMCs) were isolated from male and female conventional *Klf11* KO mice and WT mice. The isolated MASMCs were characterized by immunostaining for α-SMA (**Figure 2.7**). The *Klf11* deficiency was confirmed by real-time quantitative PCR (**Figure 2.8A, E**). A higher TF expression was observed in the MASMCs from both male and female *Klf11* KO mice compared with WT mice (**Figure 2.8B-D**, F-H, Ad-LacZ). In both genders, restoration of KLF11 can rescue the phenotype in *Klf11* KO MASMCs. As expected, the upregulated TF expression was significantly alleviated after KLF11 overexpression at both mRNA and protein levels (**Figure 2.8B-D, F-H,** Ad-KLF11). These results indicate that endogenous KLF11 is required to prevent excessive TF upregulation, a hallmark of VSMC involvement in thrombosis.[53]

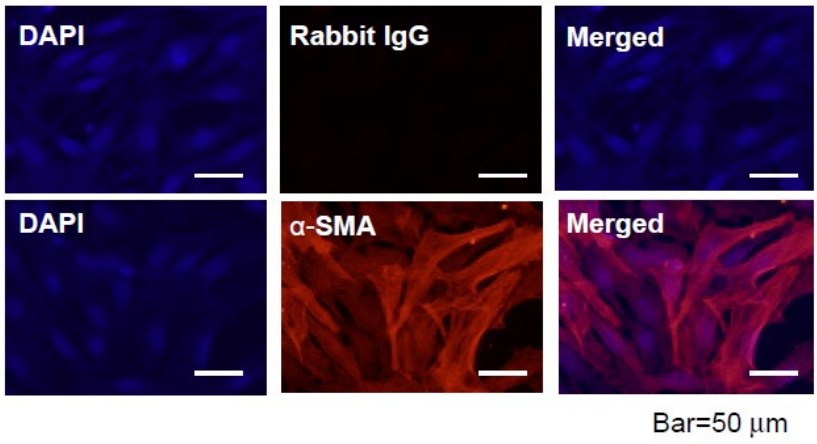

Figure 2.7 Characterization of freshly isolated mouse aortic smooth muscle cells.

Expression of α-SMA (α-smooth muscle actin, 1 μg/ml, Alexa 568 displayed in red) in mouse aortic smooth muscle cells was visualized by immunofluorescence staining. Rabbit IgG staining was used as the negative control. Scale bars=50 μm.

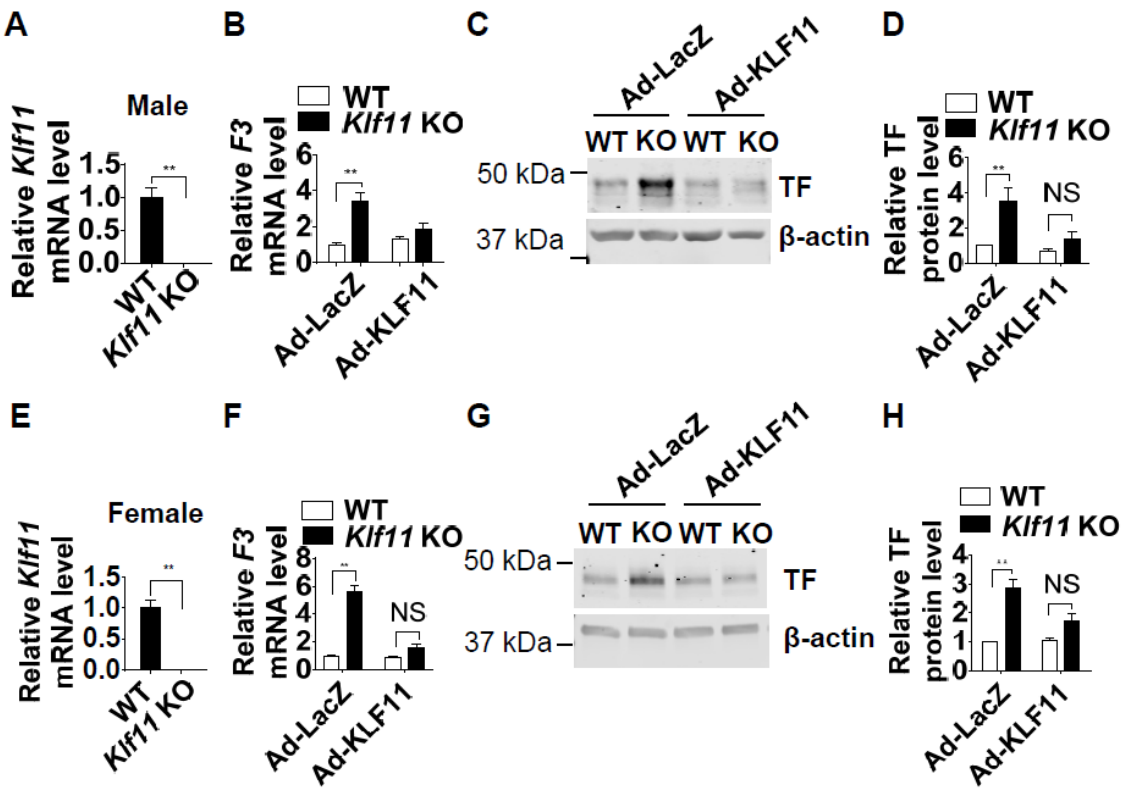

Figure 2.8 KLF11 overexpression rescues the TF (tissue factor) upregulation in KLF11-deficient MASMCs (mouse aortic smooth muscle cells).

MASMCs were isolated from male (**A-D**) and female (**E-H**) WT or *Klf11* KO mice. **A and E**, *Klf11* mRNA level of MASMCs from WT and *Klf11* KO mice. The mRNA level was normalized by 18S and is presented relative to the WT group set as 1 (n=4/group). **P<0.01 using unpaired Student t-test. B-H, MASMCs isolated from WT or *Klf11* KO mice were infected with Ad-LacZ or Ad-KLF11 (50 MOI). **B and F**, *F3* (the gene name of TF) mRNA level of MASMCs was normalized by 18S and is presented relative to the WT infected with Ad-LacZ group set as 1 (n=4/group). **C and G**, Representative western blot of TF protein level. **D and H**, Band density from 4 independent western blots was quantitatively analyzed and normalized against β-actin. The WT infected with Ad-LacZ group was set as 1. **P<0.01 or NS, no significance using two-way ANOVA followed by Bonferroni test (**B, D, F, H**).

KLF11 Inhibits TF Expression in HASMCs

To determine whether KLF11 is essential to regulate TF in VSMCs, we measured TF expression upon KLF11 knockdown in HASMCs. The efficiency of siRNA-mediated KLF11 knockdown was confirmed at the mRNA and protein levels (**Figure 2.9A**). The KLF11 knockdown in HASMCs increased both the basal and thrombin-induced expression of TF at mRNA and protein levels (**Figure 2.9B-D**). Similar effects were observed in HASMCs stimulated with 10% FBS-containing culture medium (**Figure 2.9E-G**).

Apart from TF, other factors can also affect the formation of arterial thrombus. In HASMCs, the expression of other thrombosis related factors such as tissue factor pathway inhibitor (*TFPI*) and protease-activated receptor-1 (*PAR-1*) and inflammatory genes such as monocyte chemoattractant protein-1 (*MCP-1*) and interleukin 1 beta (*IL-1β*) was not significantly changed in the KLF11-deficient HASMCs (**Figure 2.10**).

Further, we upregulated KLF11 in primary HASMCs to determine whether KLF11 regulates TF *in vitro*. In HASMCs, adenovirus-mediated overexpression of KLF11 (**Figure 2.11A**) significantly inhibited the thrombin-induced TF expression at both mRNA and protein levels (**Figure 2.11B-D**). Similarly, KLF11 also suppressed TF expression in HASMCs stimulated with 10% FBS-containing culture medium (**Figure 2.11E-G**). Thus, our data suggest that KLF11 potently inhibits TF in human VSMCs under either thrombin stimulation or normal serum conditions.

Interestingly, KLF11 overexpression also decreased tumor necrosis factor alpha (TNF-α)-induced TF expression in human umbilical vein endothelial cells (HUVECs) at both mRNA and protein levels (**Figure 2.12**), implicating that endothelial KLF11 also may have an important role in thrombosis.

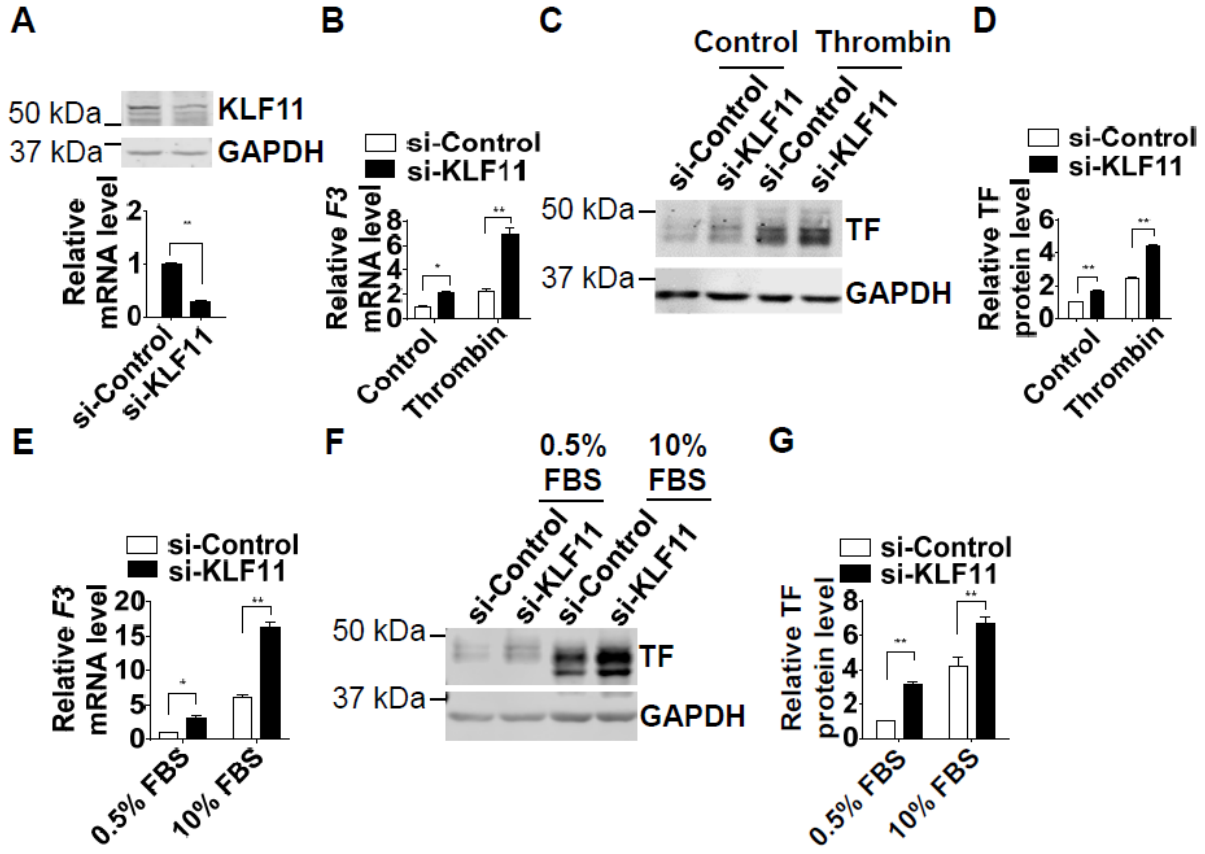

Figure 2.9 TF (Tissue factor) expression is increased upon KLF11 knockdown in HASMCs (human aortic smooth muscle cells).

HASMCs were transfected with si-Control or si-KLF11 (40 nM) and 24 hours later, serum starved with 0.5% FBS (fetal bovine serum) for 48 hours. Three days after transfection, HASMCs were exposed to thrombin (3.24 μg/ml) (**B-D**) or 10% FBS (**E-G**) for 4 hours. **A**, The knockdown efficiency of KLF11 was determined by real-time quantitative PCR and western blot. The mRNA level was normalized by GAPDH and is presented relative to HASMCs transfected with si-Control group set as 1 (n=4/group). **P<0.01 using unpaired Student's t-test. **B and E,** *F3* (the gene name of TF) mRNA level of HASMCs was normalized by GAPDH and is presented relative to HASMCs transfected with si-Control group set as 1 (n=4/group). **C and F,** Representative western blot showing the protein level of TF. **D and G,** Band density from 4 independent western blots was quantitatively analyzed and normalized against GAPDH. HASMCs transfected with si-Control group was set as 1. *P<0.05, **P<0.01 using two-way ANOVA followed by Bonferroni test (**B, D, E, G**).

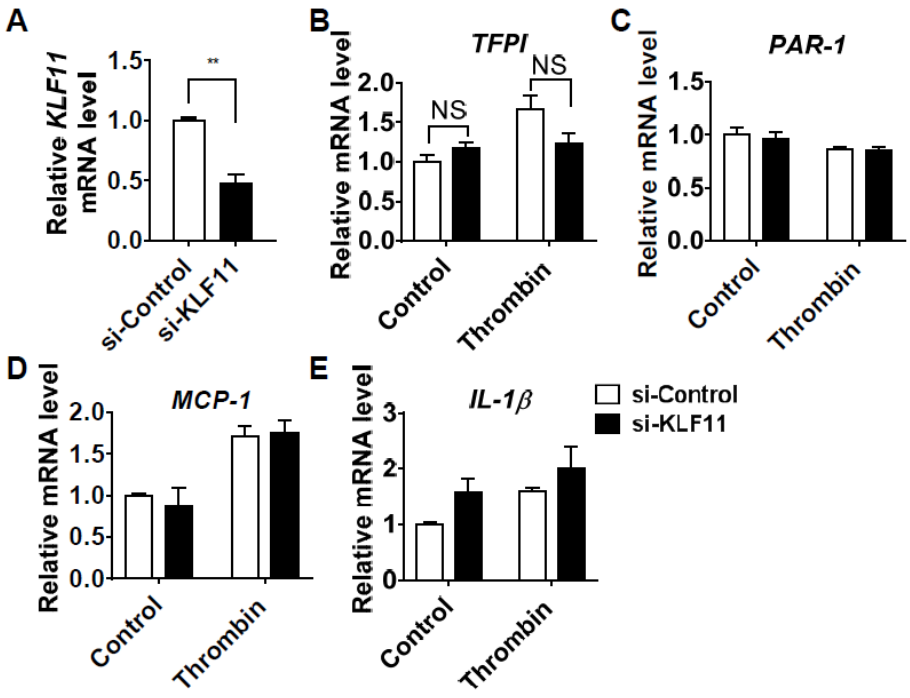

Figure 2.10 Expression of thrombosis related genes in HASMCs (human aortic smooth muscle cells) upon KLF11 knockdown.

HASMCs were transfected with si-Control or si-KLF11 (40 nM) in 6-well plates and 24 hours later serum starved with 0.5% FBS (fetal bovine serum) for 48 hours. Three days after transfection, HASMCs were treated with thrombin (3.24 μg/ml) for 4 hours. **A,** The KLF11 mRNA level was normalized by GAPDH and is presented relative to the si-Control group set as 1. Data are presented as mean ± SEM. n=4 per group. **P<0.01 using unpaired Student t-test. **B-E,** The expression of tissue factor pathway inhibitor (TFPI) (**B**), protease activated receptor-1 (PAR-1) (**C**), monocyte chemoattractant protein-1 (MCP-1) (**D**) and interleukin 1 beta (IL-1β) (**E**) was determined by real-time quantitative PCR and normalized by GAPDH. The data are presented relative to the si-Control group set as 1. Data are from 4 independent experiments and presented as mean ± SEM. NS, no significance using two-way ANOVA followed by Bonferroni test.

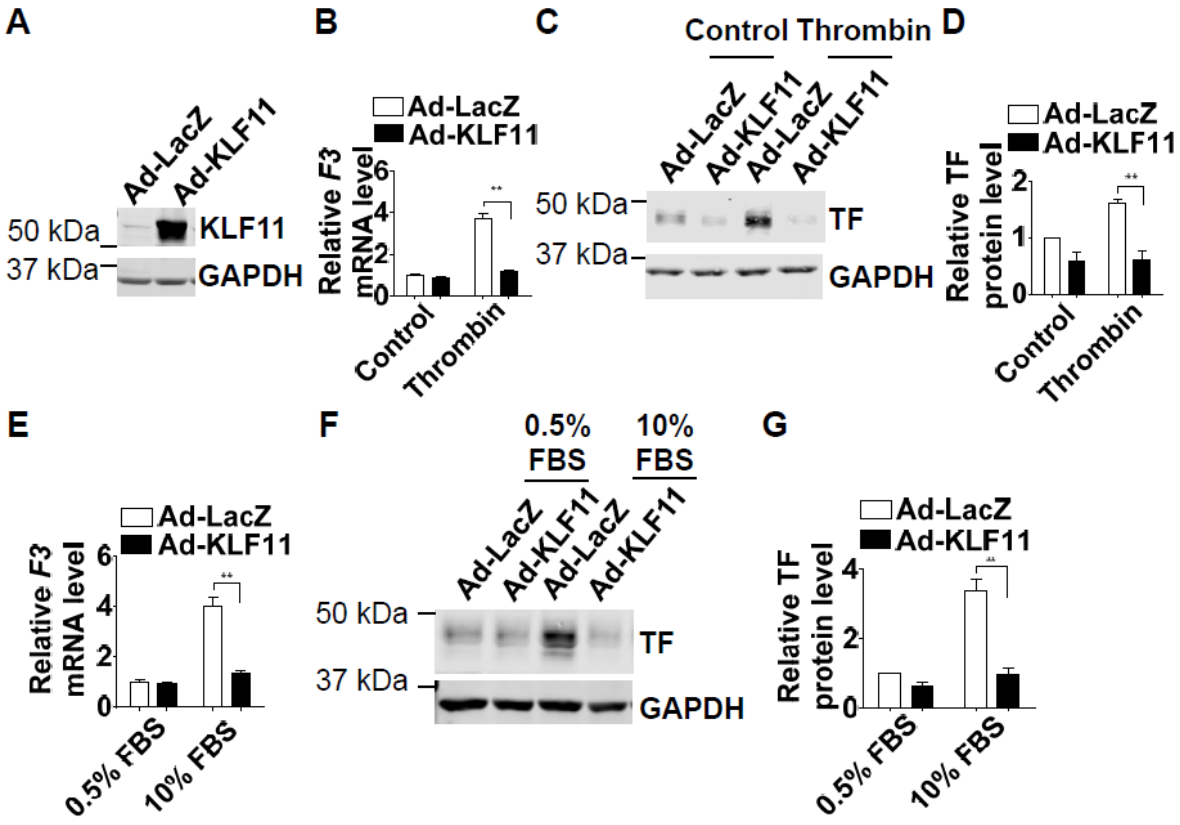

Figure 2.11 TF (Tissue factor) expression is decreased upon KLF11 overexpression in HASMCs (human aortic smooth muscle cells).

HASMCs were infected with Ad-LacZ or Ad-KLF11 (50 MOI). Twelve hours after infection, HASMCs were serum starved with 0.5% FBS (fetal bovine serum) for 48 hours and then stimulated to thrombin (3.24 μg/ml) (**B-D**) or 10% FBS (**E-G**) for 4 hours. **A,** The overexpression of KLF11 was determined by western blot. **B and E**, *F3* (the gene name of TF) mRNA level of HASMCs from each group was normalized by GAPDH and is presented relative to HASMCs infected with Ad-LacZ group set as 1 (n=4/group). **C and F,** Representative western blot showed the protein level of TF. **D and G,** Band density from 4 independent western blots was quantitatively analyzed and normalized against GAPDH. HASMCs infected with Ad-LacZ group was set as 1. **P<0.01 using two-way ANOVA followed by Bonferroni test (B, D, E, G).

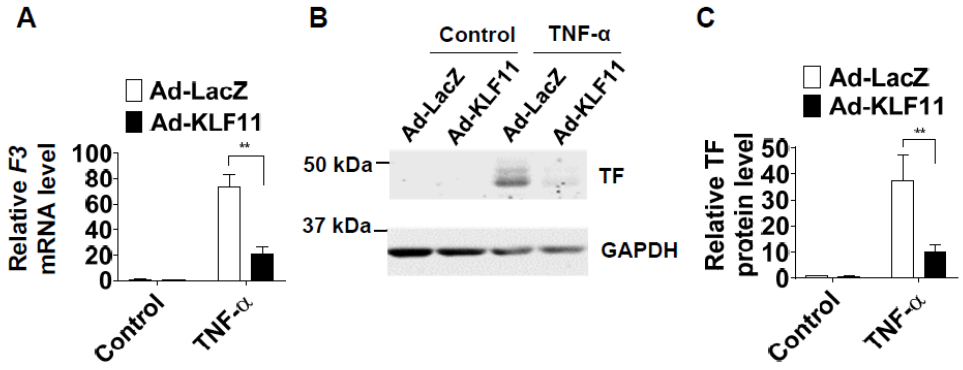

Figure 2.12 KLF11 inhibits TNF (Tumor necrosis factor)-α-induced *F3* (tissue factor) transcription in HUVECs (human umbilical vein endothelial cells).

HUVECs were infected with Ad-LacZ or Ad-KLF11 (10 MOI). Forty-eight hours after infection, HUVECs were stimulated with TNF-α (5 ng/ml) for 4 hours. **A,** *F3* (the gene name of TF) mRNA expression from each group was normalized by GAPDH and is presented relative to HUVECs infected with Ad-LacZ group set as 1. Data are presented as mean ± SEM. n=4 per group. **P<0.01 using two-way ANOVA followed by Bonferroni test. **B,** Representative western blot showed the protein level of TF. **C,** Band density from 4 independent western blots was quantitatively analyzed and normalized against GAPDH. HUVECs infected with Ad-LacZ group was set as 1. Data are presented as mean ± SEM. **P<0.01 using two-way ANOVA followed by Bonferroni test.

KLF11 Inhibits F3 Transcription

Next, we determined the mechanism that mediates the regulation of *F3* (the gene name of TF) by KLF11. *KLF11* was originally identified as the transforming growth factor-β-inducible early gene 2 (*TIEG2*), with a preference to bind at GC-rich sequences (GGGTG*).*[62] Transcription factor binding site analysis of the human *F3* gene (Genomatix) revealed a relatively conserved TIEG binding site (-177 to -161 base pairs) upstream of the *F3* transcription start site (**Figure 2.13A**). The TIEG binding site is conserved among human, mouse, rat and rabbit (**Figure 2.13B**). To determine whether this TIEG binding site is a functional KLF11 binding region, we performed chromatin immunoprecipitation (ChIP) assay in the HASMCs infected with Ad-flag-KLF11 or Ad-LacZ. Our data suggest that KLF11 can bind to the region containing this TIEG binding site (**Figure 2.13C**). To determine whether KLF11 regulates *F3* at the transcriptional level, we generated luciferase reporter constructs, which were under the control of different lengths (-906/+162 and -556/+162) of the human *F3* promoter. In A7R5 cells, a rat aortic smooth muscle cell line, transfected with different reporter constructs, KLF11 overexpression significantly reduced the luciferase activity (**Figure 2.13D**). Next, we deleted the TIEG bind site (-177 to -161) in the *F3* promoter-driven luciferase construct. As expected, the deletion of the TIEG binding site significantly attenuated the KLF11 inhibition of *F3* luciferase activity (**Figure 2.13E**) from the reporter plasmid. In conclusion, we identified that KLF11 inhibits *F3* expression at the transcription level through direct binding to the *F3* promoter (**Figure 2.13F**).

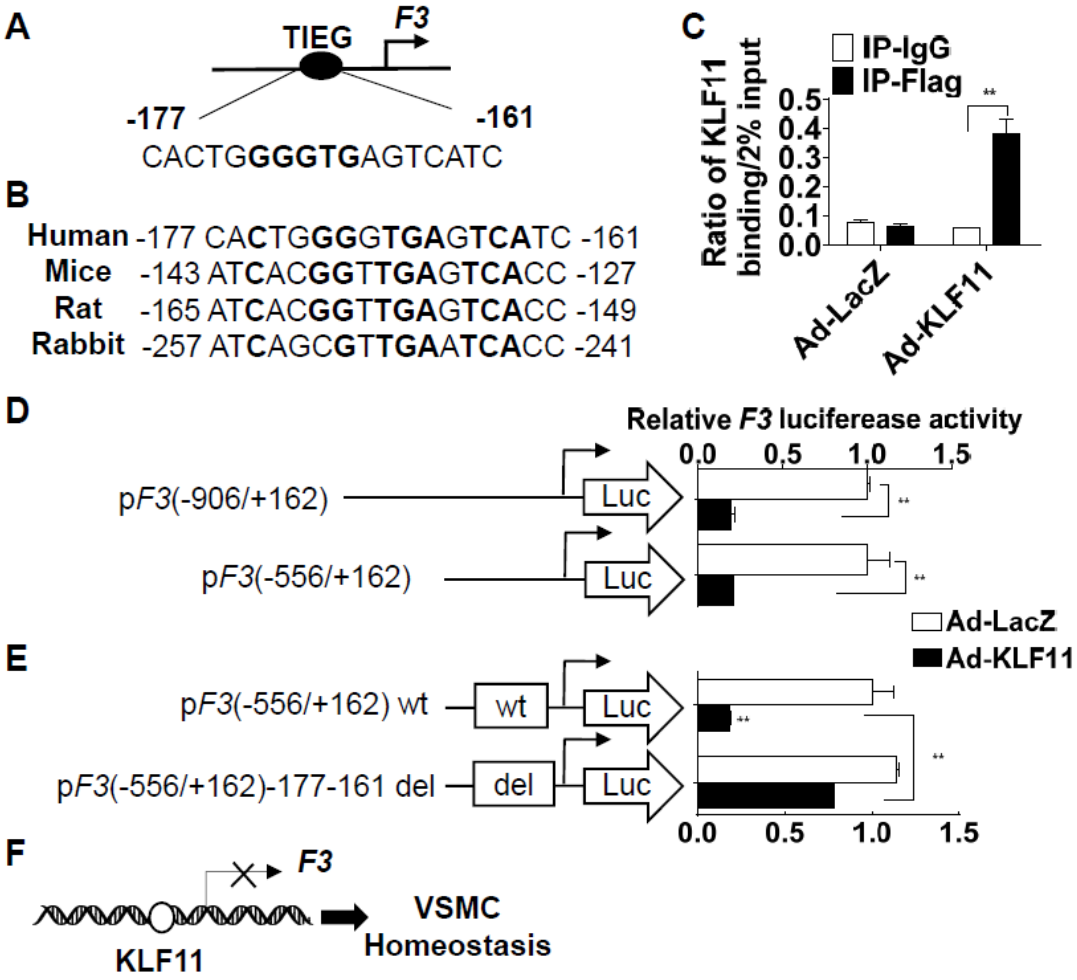

Figure 2.13 KLF11 inhibits *F3* (gene name of tissue factor) transcription.

A, A diagram showing the simplified structure of the human *F3* promoter region with an illustration of the TIEG (transforming growth factor-beta-inducible early gene) binding site. KLF binding region is shown in bold. **B,** The bold bases indicate the conservation of the TIEG binding site among species. **C,** HASMCs were infected with Ad-LacZ or Ad-Flag KLF11. Forty-eight hours after infection, the binding of KLF11 to the *F3* promoter was determined by ChIP assays using an antibody against Flag (n=4/group). **D-E,** A7r5 cells were transfected with two different lengths (**D**), or wt (wild type) or del (region deleted) (**E**) luciferase reporter driven by the *F3* promoter and then infected with Ad-LacZ or Ad-KLF11 (50 MOI). Two days later, the luciferase activity was measured and normalized by Renilla activity. The results are presented relative to A7r5 transfected with p*F3* (-906/+162) (**D**) or wt (**E**) and infected with Ad-LacZ group set as 1 (n=4/group). **P<0.01 using two-way ANOVA followed by Bonferroni test (**C, D, E**). **F**, Schematic summary: KLF11 inhibits *F3* transcription by directly binding to the *F3* promoter region.

Discussion

In the current study, we observed an increase in arterial thrombosis in both genetically engineered conventional *Klf11* KO mice and VSMC-specific *Klf11* KO mice. In cultured human aortic smooth muscle cells, we demonstrated that KLF11 inhibits TF expression. Mechanistically, KLF11 directly binds to the *F3* promoter region and thereby suppresses the transcription of *F3*. This study demonstrated a potential role for VSMC KLF11 in arterial thrombosis.

The KLF family modulates cardiovascular activity through regulation of metabolism and inflammation in the cardiovascular system.[3, 4, 46] Endothelial KLF2 and KLF4 have been reported to inhibit thrombus formation by inhibiting the transcription of pro-thrombotic factors (*e.g.*, plasminogen activator inhibitor one and TF) and increasing the expression of anti-thrombotic factors (*e.g.*, thrombomodulin) under inflammatory conditions.[3, 63-65]

We previously identified that KLF11 inhibits endothelial activation[28] and attenuates endothelial dysfunction in the mouse middle cerebral artery occlusion-induced stroke model.[29] Our current finding that VSMC KLF11 inhibits arterial thrombosis advances the understanding of the protective role of KLF11 in vascular diseases. Population genetics studies identified that mutations in the *KLF11* gene are positively associated with type 2 diabetes.[25] Cardiovascular events are the major causes of death in diabetes.[66] Our study points to a potentially beneficial effect of KLF11 on cardiovascular complications in diabetic patients. Follow-up studies are warranted to determine the role of VSMC KLF11 in diabetes-associated cardiovascular diseases such as atherosclerosis, thrombosis, and angiogenesis.

In this study, we used the $FeCl_3$ thrombosis model, a widely used mouse arterial thrombosis model,[67] to study the role of KLF11 in the vascular wall *in vivo*. The penetration of

$FeCl_3$ from adventitia triggers thrombosis.[68] In this study, we found that conventional *Klf11* KO mice were more pro-thrombotic. The bone marrow transplantation study and the measurement of MV-TF activity excluded a potential involvement of KLF11 from blood cells and circulation-derived TF. A similar pro-thrombotic phenotype was observed in the *Sm-Klf11* KO mice, which further demonstrated the anti-thrombotic effects of KLF11 in the vascular wall under basal conditions.

TF is critical in maintaining the balance between hemostasis and thrombosis.[69] VSMCs in human atherosclerotic plaques express high levels of TF.[70-72] Interestingly, a previous study using a low-TF mouse demonstrated that the vascular wall derived TF, rather than leukocytes derived TF, is responsible for the macrovascular thrombosis.[73] Therefore, the lower expression of TF in the vascular wall, especially in the VSMCs, can limit the initiation of the TF-dependent coagulation cascade and thus be a potentially protective mechanism for the prolonged occlusion time *in vivo.* Compared with endothelial cells (ECs), VSMCs have a higher constitutive expression of TF and are considered the primary TF source in the arterial wall.[74] The expression of TF can be rapidly induced in VSMCs after artery injury[75] and contributes to thrombosis events after plaque rupture.[70, 76] The *SM22*-driven VSMC-specific TF-deficient mice showed an increase in occlusion time in $FeCl_3$-induced arterial thrombosis, indicating a key role of VSMC-derived TF in arterial thrombosis.[53] Although TF is not the only key factor in thrombosis formation, inhibition of TF activity by a monoclonal antibody[77] or administration of its counterpart recombinant TFPI[78] showed beneficial effects, which make inhibition of TF a potential pharmaceutical target for thrombosis. In addition, it has been reported that the deficiency of TFPI in smooth muscle cells can reduce the occlusion time in the $FeCl_3$ model.[79] However, in this study, we found that *TFPI* expression was not significantly changed in the

KLF11-deficient VSMCs. Therefore, the increased TF can at least partially account for the pro-thrombotic phenotype in the KLF11-deficient VSMCs.

It is well known that thrombin causes positive feedback effects on the coagulation cascade, including promoting the contact activation pathway.[80] However, numerous studies indicated that thrombin can also induce TF expression in VSMCs.[81-84] Thrombin can bind to protease-activated receptors (PARs) on human aortic SMCs and activate protein kinase B (PKB), protein kinase C (PKC) and mitogen-activated protein kinase (MAPK) pathways, which could induce TF expression.[85-87] Our data demonstrated that KLF11 directly binds to the *F3* promoter and inhibits its activity in VSMCs, which account for the KLF11-dependent decreased *F3* transcription under thrombin stimulation. The effect of KLF11 on thrombin-activated signaling pathways (*e.g.*, PARs, PKB, PKC, and MAPK) warrants future investigation.

In the present study, we demonstrated that KLF11 binds to the *F3* promoter to inhibit its transcription (**Figure 2.13**). In basal conditions (serum starvation), TF is expressed at a very low level in VSMCs, and endogenous KLF11 is abundant enough to maintain the low level of TF by direct binding to the *F3* promoter. Thus, overexpression of KLF11 did not further inhibit *F3* transcription (**Figure 2.11**). The ChIP (**Figure 2.13C**) and luciferase (**Figure 2.13D-E**) experiments were performed in normal growth conditions (10% FBS). Under these conditions, we observed the inhibitory effect of KLF11 on *F3* transcription (**Figure 2.11**). Upon thrombin or serum stimulation, overexpressed KLF11 may compete with other transcription factors such as activator protein-1 (AP-1),[88] whose binding region (-172-160bp) at the *F3* promoter overlaps with the KLF11 binding region (-177-161bp). On the other hand, KLF11 deficiency may vacate the KLF11 binding site and abolish the repressive effect of KLF11 on *F3* promoter activity.

Therefore, KLF11 deficiency can increase *F3* transcription even under basal conditions (**Figure 2.9**).

The $FeCl_3$ model is a commonly used experimental model to study arterial thrombosis.[89] However, whether the endothelium is denudated and internal elastic lamina is intact in this model are still controversial.[90, 91] The mechanisms mediating the VSMC derived effect on arterial thrombosis in the $FeCl_3$ model remain to be investigated. Noteworthy, despite an intact internal elastic lamina upon $FeCl_3$ infiltration,[90, 91] VSMC-specific TF KO inhibited the thrombus formation in the $FeCl_3$ model.[53] In the present study, we found that smooth muscle cell-specific *Klf11* KO mice had a pro-thrombotic phenotype in association with increased TF, indicating that VSMC KLF11 can maintain an anti-thrombotic state through transcriptional control of *F3*. We also found that KLF11 overexpression potently inhibited tumor necrosis factor-alpha (TNF-α)-induced TF expression in HUVECs at both the mRNA and protein levels (**Figure 2.12**), although it should be highlighted that endogenous levels of KLF11 in ECs are low.[3] Since the contribution of endothelium is unclear in the $FeCl_3$ model,[90, 91] the function of EC KLF11 in thrombosis warrants further investigation independently in other appropriate thrombosis models.

Interestingly, although there was no significant difference in TAT complexes between WT and *Klf11* KO mice at basal conditions, there was a higher TAT complex in *Klf11* KO mice after LPS treatment (**Figure 2.3** and **Figure 2.6**). At basal conditions, TF is constitutively expressed in the vascular wall and expressed much less in circulation. [92, 93] After LPS stimulation, TF expression is significantly induced not only in the vascular wall, but also in monocytes. [94, 95] We have demonstrated that KLF11 inhibits TF expression in VSMCs and ECs. Whether KLF11 also has inhibitory effects on TF expression in monocytes and thereby inhibits the pro-thrombotic status under LPS conditions warrants future investigations. Moreover, the

conversion of prothrombin to thrombin is the common pathway in the coagulation cascade. [93] Under LPS-treated conditions, apart from the increased TF expression, the abnormality of other coagulation factors may also contribute to the elevated TAT complexes in *Klf11* KO mice.

In summary (**Figure 2.14**), utilizing gain- and loss-of-function strategies, we demonstrated an important homeostatic role of KLF11 as an anti-thrombotic factor in the vascular wall. Furthermore, we uncovered KLF11-dependent transcriptional inhibition of *F3* in VSMCs as the potential mechanism underlying this anti-thrombotic effect. Our findings extend the current understanding of the roles of KLF11 in the vascular system. Manipulation of this novel molecular target could contribute to therapeutic strategies aimed at controlling thrombosis under pathological conditions and diabetic vascular pathologies at large.

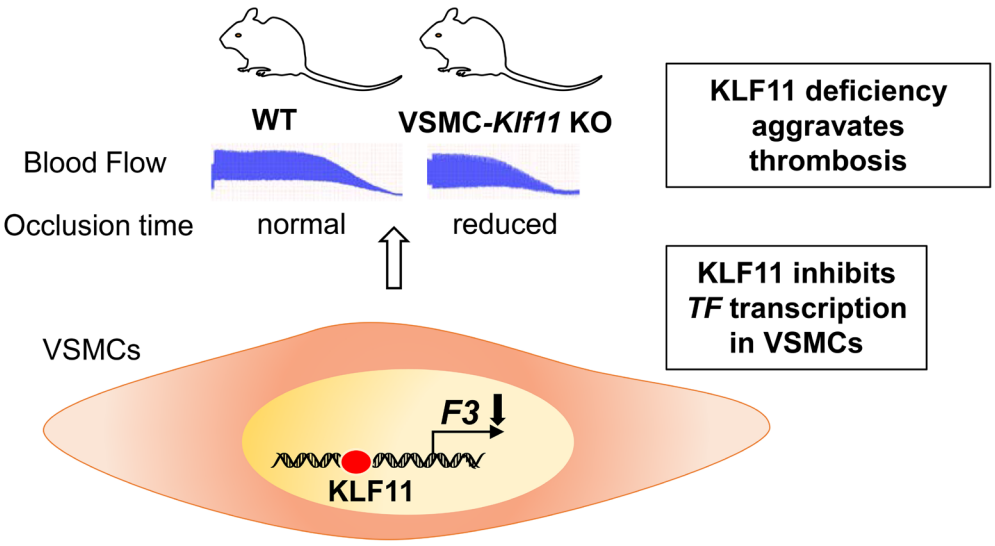

WT, wild type mice; VSMC-*Klf11* KO mice, *v*ascular smooth muscle cell specific krüppel-like factor 11 knockout mice; VSMCs, vascular smooth muscle cells; TF, tissue factor.

Figure 2.14 Summary

In vascular smooth muscle cells (VSMCs), KLF11 binds at tissue factor (*F3* gene) promoter to inhibit *F3* transcription. This can result in the protection against arterial thrombosis in VSMC-*Klf11* KO mice.

Chapter 3 KLF11 in Endothelial Cells and Deep Vein Thrombosis

Introduction

Venous thromboembolism (VTE), ranked as the third leading vascular disease after myocardial infarction and stroke,[96] is a major threat to global health with 10 million cases occurring each year.[97] In the USA, the prevalence of VTE is still on the rise, and its annual economic cost is estimated to be $7–10 billion.[98] Although VTE contributes to a high disease burden, it is considered a preventable disease, which drives the need for a deeper understanding of the mechanism underlying thrombus initiation and propagation. The endothelium plays a critical role in this process as it functions as the intersection point between inflammation and thrombus formation. Inflammation caused by either local vessel injury or systemic disease conditions (*e.g.*, sepsis, dyslipidemia) can induce many endothelial gene expression changes.

The KLF (Krüppel-like factor) family, a group of transcription factors with Cys2/His2 zinc-finger DNA-binding domain,[4] plays essential roles in the maintenance of vascular homeostasis and the pathology of various vascular diseases.[3, 46] Among them, *KLF11* gene was initially discovered from a human genetic study that identified several *KLF11* gene polymorphisms associated with diabetes.[25] Maturity-onset diabetes mellitus of the young type 7 (MODY7), a particular type of early-onset type 2 diabetes mellitus, is defined by harboring mutations in the *KLF11* gene.[25] Diabetes is commonly complicated with vascular dysfunction, including thrombosis, contributing to one of its leading causes of mortality.[49] Others and our lab proved that KLF11 is critical in maintaining vascular hemostasis. Endothelial KLF11 has been demonstrated to maintain vascular homeostasis in many diseases, including sepsis, stroke,

abdominal aortic aneurysm, and type 2 diabetes mellitus.[28-30, 32, 99, 100] We also recently identified that selectively deficiency of KLF11 in vascular smooth muscle cells (VSMCs) aggravated arterial thrombosis formation.[101] In line with the known protective effects of KLF11 in vascular diseases, in this study, we further found that KLF11 inhibits deep vein thrombosis (DVT) formation.

Materials and Methods

Mice

Conventional KLF11 knockout mice (*Klf11* KO) and littermate control mice were generated, and the fidelity of KLF11 deficiency was confirmed as previously described.[101-103] Briefly, the *Klf11* KO mice were backcrossed with C57BL/6J mice (The Jackson Laboratory, Stock No: 000664) for six generations, then heterozygous *Klf11* KO mice were interbred to produce homozygous *Klf11* KO along with wild-type littermate control (Wt) mice for experiments. All experimental procedures were approved by the Institutional Animal Care and Use Committee (IACUC) at the University of Michigan.

Reagents

TNF-α (210-TA) was purchased from R&D Systems. Thrombin (T1063) and lipopolysaccharide (L3012) were purchased from Sigma-Aldrich. BAY 11-7082 (10010266) and SP600125 (10010466) were obtained from Cayman.

Deep Vein Thrombosis Mouse Model

A complete stasis mouse model of inferior vena cava (IVC) was conducted as previously described.[104] Briefly, *Klf11* KO and Wt mice (8-10 weeks old male mice) were anesthetized with 5% isoflurane and placed in a supine position. A ventral midline incision (2 cm) was made

through the skin and peritoneum to expose the abdomen. After laparotomy, the small intestine was exteriorized and covered with a wet sterile pad. Sterile saline was applied during the whole procedure to prevent drying. After gentle separation from the aorta, IVC was ligated by a 7-0 polypropylene suture immediately below the renal vein branch (toward the tail) to obtain complete blood stasis. All visible side branches were ligated or cauterized. After surgery, the peritoneum was closed by monofilament sutures, and the skin was closed by clips. Mice were sacrificed 48 hours after ligation to harvest the thrombus, which was statistically analyzed by weight and length.

Histology and Immunohistochemistry of IVC

Histology and immunohistochemistry were performed as previously described.[105, 106] In stasis-induced deep vein thrombosis mouse model or baseline condition, murine vessels (IVC + abdominal aorta) were harvested, and the thrombus was collected for analysis. The vessels were fixed in 10% buffered formalin in PBS (245685, Fisher Healthcare) overnight, embedded in paraffin, and mounted to slides at 5 μm thickness. After deparaffinization and rehydration, the slides were treated with 3% hydrogen peroxide for 15 minutes to block endogenous peroxidase activity and subjected to 10 mM citrate buffer for heat-mediated antigen retrieval. The slides were incubated with diluted rat anti-mouse tissue factor 1H1 antibody (TF, 20 μg/ml, Genentech) or control isotypic rat IgG at 4°C overnight, followed by goat anti-rat IgG with HRP conjugated secondary antibody (31470, Invitrogen, 1:500 dilution) at room temperature for 1 hour. The color was developed by DAB staining system (Thermo Fisher Scientific). Slides were counterstained by hematoxylin, examined and photographed in a blinded fashion. The expression of TF was quantified by dividing the area of TF positive endothelial region by the total endothelial area of

IVC in ImageJ software. Data were collected from 3 mice/group and presented with the Wt group at the baseline level set as 1.

Immunofluorescence Staining

The procedures were performed as previously described[32, 101]. In brief, after 48-hour ligation-induced deep vein thrombosis or sham operation, murine vessels (IVC + abdominal aorta) were collected, fixed in 4% paraformaldehyde, and embedded in OCT. Cryostat sections (8 μm thick) were stained with primary antibody against mouse Klf11 (X1710, Sydlab, 1:50 dilution) and PECAM1 (DIA-310, Dianova, 1:100 dilution), or normal rabbit or rat IgG overnight. Alexa Fluor conjugated secondary antibodies (code number 711-585-152 and 112-605-143, Jackson ImmunoResearch Laboratories, 1:500 dilution) were applied for 1 hour. Slides were mounted with ProLong™ Gold Antifade Mountant with DAPI (P36935, Thermo Fisher Scientific), and images were taken with an Olympus IX73 microscope. Quantification of KLF11 expression in endothelial cells was performed with ImageJ software (NIH). Data were collected from 3 mice/group and presented with the comparison to the Sham group.

Culture of Human and Bovine Endothelial Cells

Human umbilical vein endothelial cells (HUVECs) (Lonza) were cultured in M199 medium (Gibco) supplemented with 16% fetal bovine serum (FBS) (Sigma-Aldrich), 24 mM HEPES (Gibco), 0.5 mg/ml penicillin/streptomycin (Gibco), 100 μg/ml heparin (Sagent Pharmaceuticals), and 1 ng/ml recombinant human fibroblast growth factor (Sigma-Aldrich) as previously described.[107] Bovine aortic endothelial cells (BAECs) (American Type Culture Collection) were cultured in Dulbecco's modified Eagle's medium (DMEM) (Gibco) with 10% FBS. All cells were cultured in a 5% CO_2 humidified incubator at 37°C.

Isolation and Culture of Mouse Aortic Endothelial Cell

The mouse aortic endothelial cells (MAECs) were isolated and cultured according to previous protocol.[108] Briefly, mice were anesthetized with ketamine (50 mg/kg) and xylazine (5 mg/kg). The mouse aorta from the aortic arch to the abdominal aorta was dissected and immersed with DMEM containing 20% FBS and 100 μg/ml heparin. The surrounding fat and connective tissues were removed, and the lumen was flushed with serum-free DMEM. The aorta was then fused with DMEM containing collagenase Type 2 (2 mg/ml, LS004174, Worthington). After 45-minute incubation at 37°C, the aorta was flushed with DMEM containing 20% FBS to harvest the MAECs. Cells from the same genotype (n=3/group) were mixed, centrifuged (1200 rpm, 5 minutes), re-suspended (DMEM containing 20% FBS), and cultured in Collagen Type 1-coated plate at 37°C for 2 hours. After PBS wash, MAECs were incubated with culture medium (DMEM containing 20% FBS, 2 mM L-Glutamine, non-essential amino acid, 1 mM sodium pyruvate, 25 mM HEPES, 100 μg/ml heparin, 0.5 mg/ml penicillin/streptomycin) for about one week. After reaching 80-100% confluence, MAECs were stimulated with TNF-α (2 ng/ml) or vehicle for 4 hours, and protein was extracted to measure TF expression.

***Ex Vivo* Clot Assay**

The *ex vivo* clot assay was developed based on a previous report detecting the procoagulant activity of endothelial cells.[109] HUVECs were cultured in a 96-well plate and infected with Ad-LacZ or Ad-KLF11 for 48 hours, followed by stimulated with TNF-α (10 ng/ml) or vehicle for 4 hours. Before coagulation induction, the medium was removed, and cells were washed with warm PBS. Pre-warmed human plasma (50 μl, P9523, Sigma) and calcium chloride (25 mM, 50 μl) were added to each well. Clot formation was determined by kinetic detection of OD value at 405 nm at 37°C (Molecular Devices, Spectra Max Plus).

Messenger RNA (mRNA) Isolation and Quantitative Polymerase Chain Reaction (qPCR)

Total RNA from tissues or cells was extracted (RNeasy Kit, QIAGEN) and reverse-transcribed into cDNA with SuperScript III reverse transcriptase (Thermo Fisher Scientific). Gene expression was measured by real-time quantitative PCR (qPCR) with IQ SYBR Green Supermix (Bio-Rad). Primers used in qPCR were listed in **Table 3.1**.

Table 3.1 Primer Sequences Used for Real-time Quantitative PCR and Chromatin Immunoprecipitation

Gene[a]	**Primer Sequences**	
h*KLF11*	F	GACACACACCTCACGGACAG
	R	ATCATCTGGCAAAGGACAGG
h*TF*	F	GTACTTGGCACGGGTCTTCT
	R	AATTGTTGGCTGTCCGAGGT
h*TFPI*	F	GTTGGGCTATTCCCAACTGC
	R	TCGCTGCTGTCTGTTAGAGC
h*THBD*	F	CCTAATGACAGTGCGCTCCT
	R	TCTCCCGTAACCCACTGGAA
h*VWF*	F	CAAGCTGGAGTGCAGGAAGA
	R	CCATCCTGGAGCGTCTCATC
h*SELP*	F	TGAAGAAAAAGCACGCATTG
	R	GGGAGCTCAAGTTCTCCACA
h*PECAM1*	F	CAAGCCTTGAGGGTCAAGAA
	R	TGCTCTTCATGGAGGAGATG
h*PLAU*	F	GCCATCCCGGACTATACAGA
	R	ACACAGCATTTTGGTGGTGA
h*PLAUR*	F	TGAAGAACAGTGCCTGGATG
	R	TGTTGCAGCATTTCAGGAAG
h*PLAT*	F	TCTTACCAAGGTTGCAGCGA
	R	AGGCTGACCCATTCCCAAAG
h*SERPINE1*	F	TCAGACCAAGAGCCTCTCCA
	R	TTGTGCCGGACCACAAAGAG
h*NFKB1*	F	CCTGGATGACTCTTGGGAAA
	R	TCAGCCAGCTGTTTCATGTC
h*RELA*	F	GCGAGAGGAGCACAGATACC
	R	CTGATAGCCTGCTCCAGGTC
h*JUN*	F	CCCCAAGATCCTGAAACAGA
	R	CCGTTGCTGGACTGGATTAT
h*FOS*	F	AGAATCCGAAGGGAAAGGAA
	R	CTTCTCCTTCAGCAGGTTGG
h*EGR1*	F	CACCTGACCGCAGAGTCTTT
	R	CTGACCAAGCTGAAGAGGGG
h*GAPDH*	F	GTCAGTGGTGGACCTGACCT
	R	TGCTGTAGCCAAATTCGTTG
m*Klf11*	F	CAGGGAACTGTGATGCTGGT
	R	GCCATGACACTGGATGGACA
m*TF*	F	AAAGGGAAGAACACCCCGTC
	R	ATCAGAGCTCTCCGCAACAG
h*TF* (ChIP)	F	AGGGTCCCGGAGTTTCCTAC

	R	GGGGAGCTCGCAGTCTTG

[a] h: human. m: mouse.

Abbreviations of gene names:

KLF11, Krüppel-like factor; *TF*, tissue factor (also known as coagulation factor III); *TFPI*, tissue factor pathway inhibitor; *THBD*, thrombomodulin; *VWF*, von Willebrand factor; *SELP*, selectin P; *PECAM1*, platelet endothelial cell adhesion molecule 1; *PLAU*, plasminogen activator, urokinase (also known as u-PA); *PLAUR*, plasminogen activator, urokinase receptor; *PLAT*, plasminogen activator, tissue type (also known as t-PA); *SERPINE1*, plasminogen activator inhibitor-1 (also known as PAI-1); *NFKB1*, nuclear factor kappa B subunit 1 (also known as p50); *RELA*, RELA proto-oncogene, NF-κB subunit (also known as p65); *JUN*, Jun proto-oncogene, AP-1 transcription factor subunit; *FOS*, Fos proto-oncogene, AP-1 transcription factor subunit; *EGR1*, early growth response 1; GAPDH, glyceraldehyde 3-phosphate dehydrogenase; ChIP, Chromatin Immunoprecipitation Assay.

Protein Extracts and Western Blot

Total protein from cells was extracted as previously reported.[101] Primary antibodies used in Western blot: GAPDH (sc-32233, Santa Cruz Biotechnology, 1:1000 dilution), tissue factor (sc-374441, Santa Cruz Biotechnology, 1:1000 dilution), KLF11 (H00008462-M01, Abnova, 1:1000 dilution) and EGR1 (4153s, Cell Signaling Technology, 1:1000 dilution).

Adenovirus-Mediated Gene Overexpression and Small Interfering RNA (siRNA)-Mediated Gene Knockdown

These were performed as previously reported.[101] For knockdown experiments, si-Control or si-KLF11 were diluted in Opti-MEM (40 nM) and incubated with Lipofectamine RNAiMAX for 20 minutes at room temperature, and then added to cultured HUVECs. After 24 hours of incubation, the medium was changed to M199 with 0.5% FBS for 48 hours of serum starvation before thrombin stimulation. Data were calculated from triplicates and at least three independent experiments.

Co-Immunoprecipitation

HUVECs were co-infected with Ad-EGR1 (5 MOI) and Ad-KLF11 (5 MOI) for 48 hours. The cells were lysed with Pierce IP Lysis Buffer (87788, Thermo Fisher Scientific) and incubated with primary antibody against EGR1 (4153, Cell Signaling Technology, 1:50 dilution), KLF11 (H00008462-M01, Abnova, 1:50 dilution), or normal respective IgG separately at 4°C overnight with rotation. The immunocomplexes were precipitated with Protein A/G PLUS-Agarose (sc-2003, Santa Cruz Biotechnology), followed with Western blot analysis using antibodies against KLF11 and EGR1.

Chromatin Immunoprecipitation Assay (ChIP)

ChIP assays were performed using the SimpleChIP Enzymatic Chromatin IP Kit (9003s, Cell Signaling Technology) following the manufacturer's protocol. Briefly, serum-starved HUVECs were fixed with 1% formaldehyde and quenched before enzymatic digestion. The DNA/protein complex was immunoprecipitated with control immunoglobulin G or anti-Flag antibody (14793, Cell Signaling Technology) conjugated to Protein G magnetic beads. Purified DNA was used as the template for qPCR analysis with primers (listed in **Table 3.1**) flanking the putative EGR1 binding region in the tissue factor gene promoter.

Luciferase Assay

Bovine aortic endothelial cells (BAECs) were co-transfected with plasmids using Lipofectamine 2000 (11668019, Thermo Fisher Scientific) as previously described.[101] Briefly, BAECs were cultured in a 48-well plate and grown to approximately 80% confluence before transfection. The reporter plasmids (0.5 μg/well) and Lipofectamine 2000 Reagent were incubated with Opti-MEM separately and mixed to set 20 minutes. Then, the mix was added to cultured BAECs in DMEM containing 10% FBS. Seventy-two hours after transfection, the *TF* gene promoter activity was measured by firefly luciferase (Promega) and normalized against *Renilla* activity which was co-transfected as a control.

Statistical Analysis

All quantitative data are presented as mean ± SEM. Statistical analyses were performed using the GraphPad Prism 7. The homogeneity of variances was first evaluated by Shapiro-Wilk normality test and *F* test. For data distributed normally with similar variances among groups, unpaired Student *t*-test with Welch's correction was used for two-group comparisons. Comparisons among more than two groups were analyzed by one-way analysis of variance (ANOVA) followed by Tukey's test. Grouped data under different conditions were analyzed

with two-way ANOVA followed by Bonferroni test. All results were representative and collected from at least three independent experiments.

Results

KLF11 Expression is Upregulated in Endothelial Cells under Pro-Thrombotic Conditions

Firstly, we performed the stasis-induced DVT model in C57BL/6 wild-type (Wt) male mice and compared KLF11 expression in the inferior vena cava (IVC) with that in the sham-operated mice. The immunofluorescence staining shows that the induced KLF11 expression was mainly located in the endothelium (**Figure 3.1A-B**). The mRNA level of KLF11 was significantly doubled in the vascular wall of the DVT group (**Figure 3.1C**). These data suggest that vascular KLF11 may play an important role in venous thrombosis. Consistent with the *in vivo* results, KLF11 expression was also enhanced in the human umbilical vein endothelial cells (HUVECs) treated with different pro-thrombotic stimuli, including tumor necrosis factor-alpha (TNF-α), lipopolysaccharide (LPS) and thrombin, as was measured by both qPCR and Western blot (**Figure 3.1D-F**). These data indicate that KLF11 is a thrombosis-responsive gene in endothelial cells (ECs).

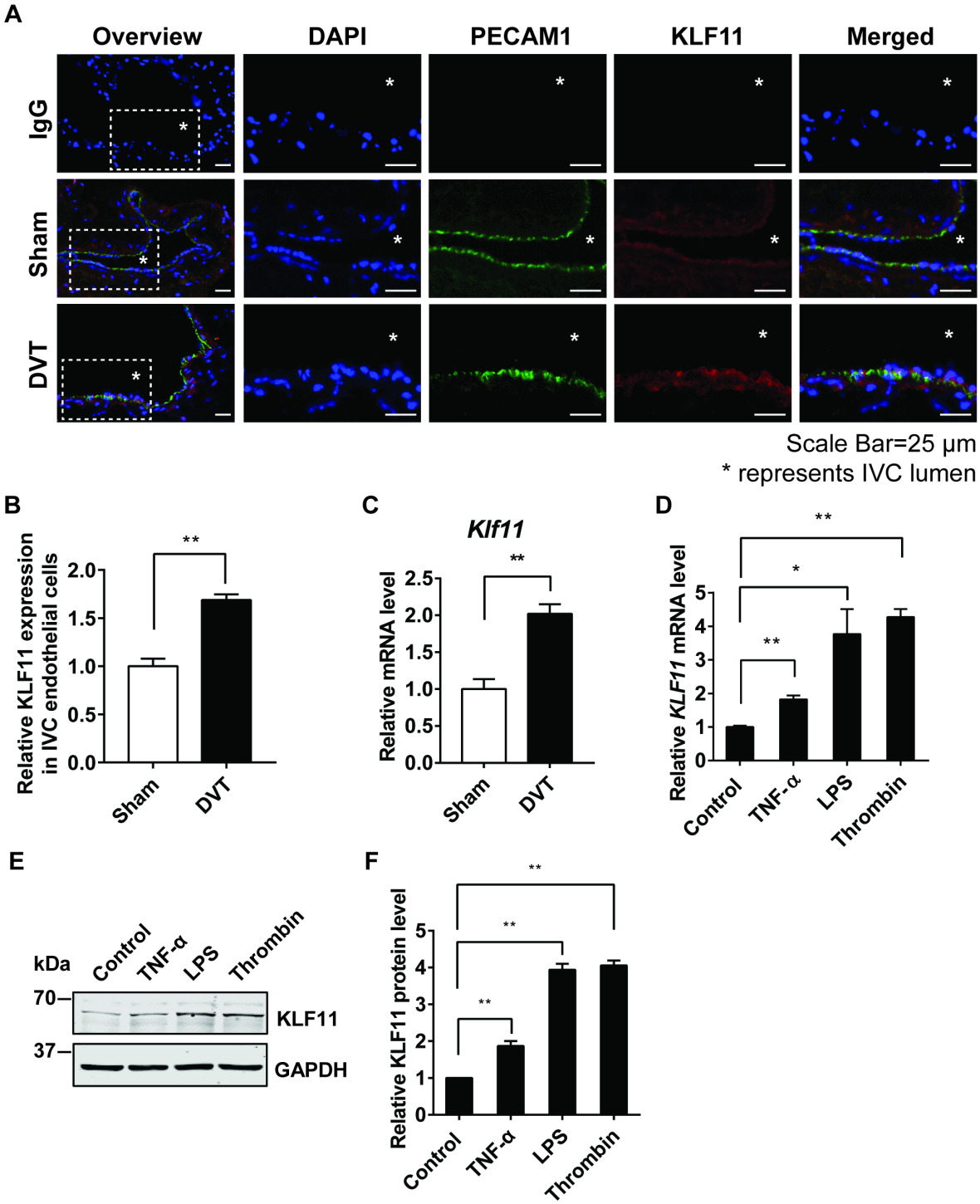
A
Overview
DAPI
PECAM1
KLF11
Merged
IgG
Sham
DVT
Scale Bar=25 μm
* represents IVC lumen
B
Relative KLF11 expression in IVC endothelial cells
Sham
DVT
C
Klf11
Relative mRNA level
Sham
DVT
D
Relative KLF11 mRNA level
Control
TNF-α
LPS
Thrombin
E
kDa
Control
TNF-α
LPS
Thrombin
70
KLF11
37
GAPDH
F
Relative KLF11 protein level
Control
TNF-α
LPS
Thrombin

Figure 3.1 KLF11 expression is upregulated in endothelial cells under pro-thrombotic conditions.

A-C, In the stasis-induced deep vein thrombosis model (DVT), the inferior vena cava (IVC) from C57BL/6 male mice were either sham-operated or ligated for 48 hours to induce DVT (n=3/group). The cryostat IVC sections were stained with antibodies against PECAM1 (DIA-310, Dianova, 1:100; Alexa 647, Jackson ImmunoResearch, 1:500, displayed in green) and KLF11 (X1710, Sydlab, 1:50; Alexa 568, Jackson ImmunoResearch, 1:500, displayed in red). DAPI (4′,6-diamidino-2-phenylindole) stained for nuclear acid. Respective IgG staining was used as the negative control. Scale bars=25 μm. * represents IVC lumen. The representative images are presented (**A**) and the expression of KLF11 in the endothelial cells of IVC was quantified by Image J (**B**). The vascular wall of IVC was isolated to measure *Klf11* mRNA level (**C**). **D-F**, Human umbilical vein endothelial cells (HUVECs) were treated with different stimuli for 4 hours to induce endothelial inflammation. The stimuli included: TNF-α (10 ng/ml), Lipopolysaccharides (LPS, 100 ng/ml), and thrombin (5 U/ml). The mRNA level of *KLF11* (**D**) was normalized to GAPDH and is presented relative to the control group. The representative Western blot (**E**) and quantification (**F**) of the KLF11 level are presented. N=3/group. Data are presented as mean±SEM. **p*<0.05, ***p*<0.01 using unpaired Student *t*-test.

The Expression Profiles of Thrombosis-related Genes in Response to Altered KLF11 Levels in ECs

Under inflammatory conditions, the endothelium is activated to express a plethora of genes regulating hemostasis and thrombosis.[110, 111] To gain a general view on the role of endothelial KLF11 in this process, adenovirus-mediated KLF11 overexpression and siRNA-mediated KLF11 knockdown were applied to cultured HUVECs, followed with TNF-α stimulation. The expression of the genes that are both highly expressed in ECs and related to thrombosis was measured by qPCR. KLF11 overexpression reduced TNF-α-induced *TF* gene transcription by 84.6%. Consistently, downregulation of KLF11 enhanced *TF* gene transcription by 1.93-fold. However, there was no significant change in anti-coagulative genes, including tissue factor pathway inhibitor (*TFPI*) and thrombomodulin (*THBD*) (**Figure 3.2A, D**). Next, we analyzed genes mediating the interaction between ECs and platelets. KLF11 knockdown increased TNF-α-induced transcription of von Willebrand factor (*VWF*), while there was no significant change after KLF11 overexpression (**Figure 3.2B, E**). For fibrinolysis-related genes, although the transcription of urokinase type plasminogen activator receptor (*PLAUR*) was increased by KLF11 overexpression, it was not regulated by KLF11 knockdown (**Figure 3.2C, F**). The expression of other platelet adhesion-related genes [platelet endothelial cell adhesion molecule 1 (*PECAM1*), selectin P (*SELP*)] (**Figure 3.2B, E**) and fibrinolysis-related genes (**Figure 3.2C, F**) did not show significant change. Altogether, these data indicate that KLF11 is a negative regulator of *TF* gene transcription in ECs, thereby contributing to the anti-thrombotic phenotype.

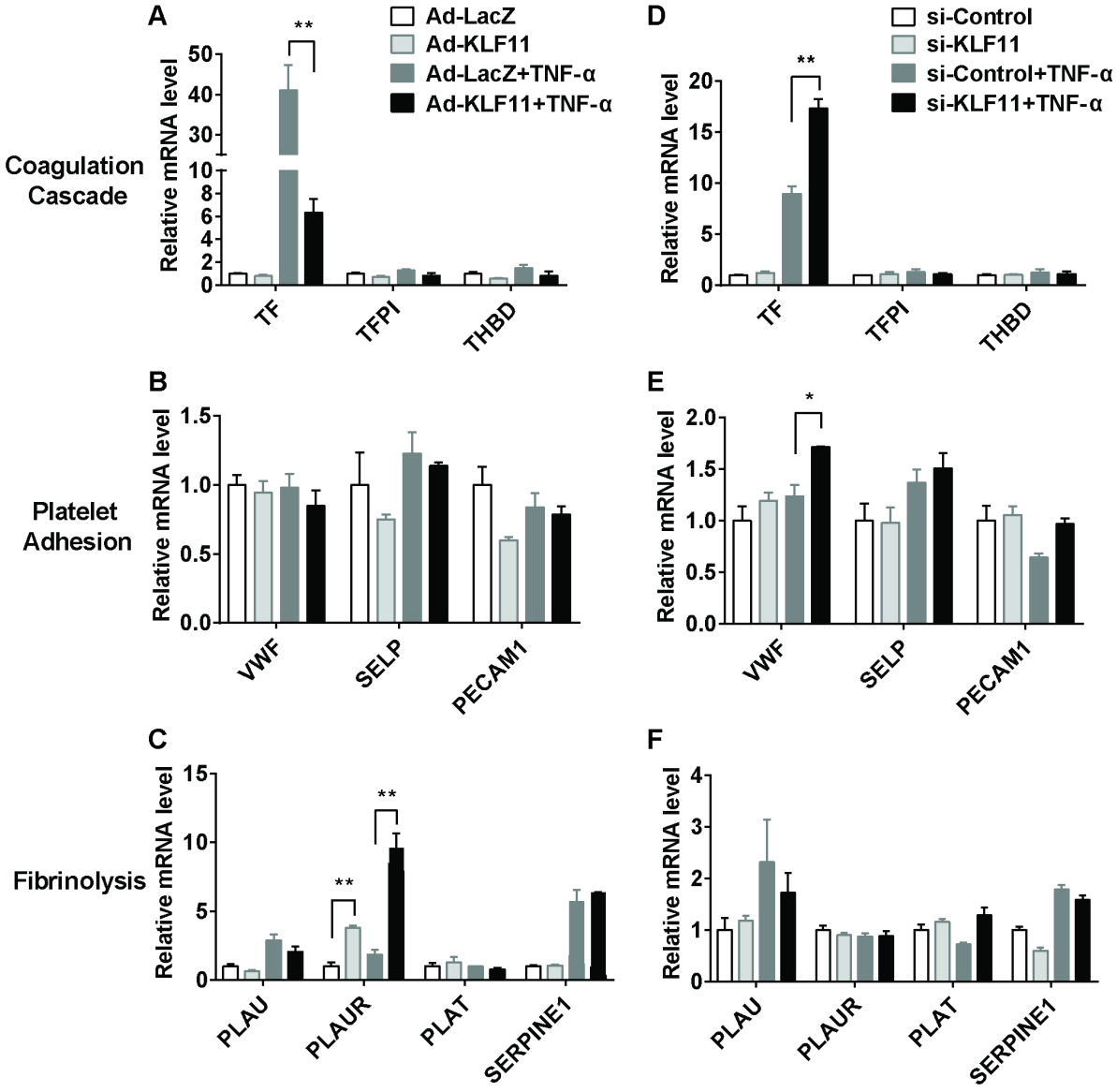
A
Ad-LacZ
Ad-KLF11
Ad-LacZ+TNF-α
Ad-KLF11+TNF-α
Coagulation Cascade
Relative mRNA level
TF
TFPI
THBD
D
si-Control
si-KLF11
si-Control+TNF-α
si-KLF11+TNF-α
B
Platelet Adhesion
VWF
SELP
PECAM1
E
C
Fibrinolysis
PLAU
PLAUR
PLAT
SERPINE1
F

Figure 3.2 The expression profiles of thrombosis-related genes in response to altered KLF11 levels in endothelial cells.

A-C, Human umbilical vein endothelial cells (HUVECs) were infected with Ad-LacZ or Ad-KLF11 (10 MOI) for 48 hours, followed by TNF-α (10 ng/ml) stimulation for 4 hours. **D-F,** HUVECs were transfected with si-Control or si-KLF11 (20 nM). Seventy-two hours after transfection, HUVECs were stimulated with TNF-α (10 ng/ml) for 4 hours. The mRNA level of thrombosis-related genes was normalized to GAPDH and is presented relative to HUVEC infected with Ad-LacZ group. N=3/group. Data are presented as mean±SEM. *p<0.05, **p<0.01 using two-way ANOVA followed by Bonferroni test. Abbreviations of gene names: *TF,* tissue factor; *TFPI*, tissue factor pathway inhibitor; *THBD*, thrombomodulin; *VWF*, von Willebrand factor; *SELP*, selectin P; *PECAM1*, platelet endothelial cell adhesion molecule 1; *PLAU*, plasminogen activator, urokinase (also known as u-PA); *PLAUR*, plasminogen activator, urokinase receptor; *PLAT*, plasminogen activator, tissue type (also known as t-PA); *SERPINE1*, plasminogen activator inhibitor-1 (also known as PAI-1).

KLF11 Negatively Regulates TNF-α-Induced Tissue Factor Protein Expression in ECs

We further analyzed TF protein expression under a similar experimental setting as was performed in **Figure 3.2**. Adenovirus-mediated KLF11 overexpression was confirmed by qPCR (**Figure 3.3A**). Consistent with the qPCR data, KLF11 overexpression reduced TNF-α-induced TF protein expression by 83.9% in ECs (**Figure 3.4A, B**). Similarly, siRNA-mediated KLF11 knockdown (**Figure 3.3B**) increased TF protein level after TNF-α stimulation by 1.44-fold (**Figure 3.4C, D**). Moreover, a higher TF expression was observed in the isolated mouse aortic endothelial cells (MAECs) from *Klf11* knockout (*Klf11* KO) mice compared with Wt mice (**Figure 3.4E**). Collectively, KLF11 negatively regulates TNF-α-induced TF expression in ECs.

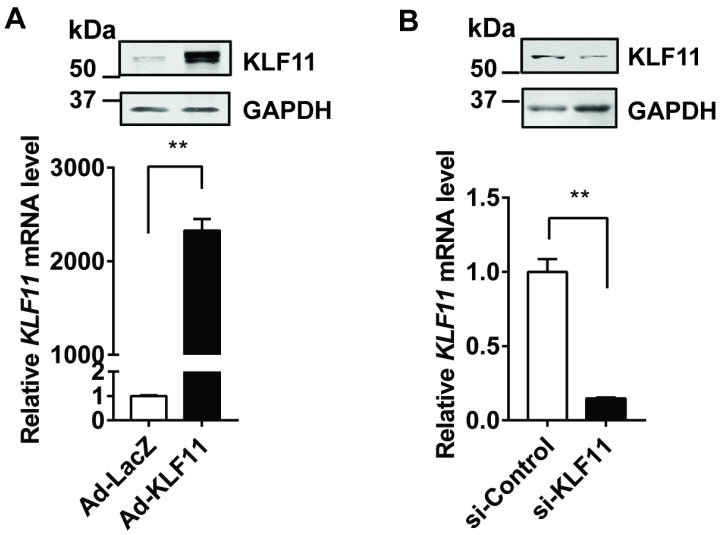

Figure 3.3 The confirmation of KLF11 expression in the gain-of-function and loss-of-function modified endothelial cells.

Human umbilical vein endothelial cells (HUVECs) were infected with Ad-LacZ or Ad-KLF11 (10 MOI) for 48 hours, followed by TNF-α (10 ng/ml) stimulation for 4 hours. The mRNA level and representative Western blot of KLF11 are presented (**A**). HUVECs were transfected with si-Control or si-KLF11 (20 nM) for 72 hours, followed by stimulation with TNF-α (10 ng/ml) for 4 hours. The mRNA level and representative Western blot of KLF11 are presented (**B**). The mRNA level was normalized to GAPDH and is presented relative to the control group set as 1. N=3/group. Data are presented as mean±SEM. $^{**}p<0.01$ using unpaired Student *t*-test.

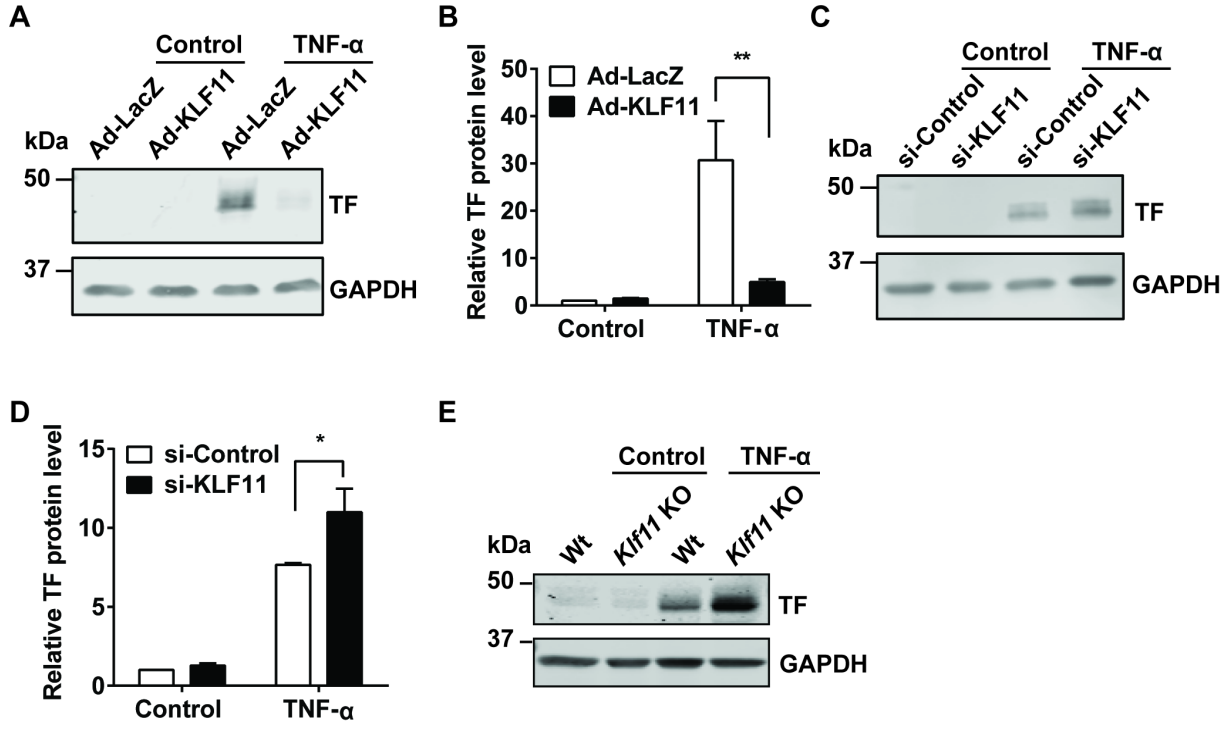

Figure 3.4 KLF11 negatively regulates TNF-α-induced tissue factor protein expression in endothelial cells.

A-B, Human umbilical vein endothelial cells (HUVECs) were infected with Ad-LacZ or Ad-KLF11 (10 MOI) for 48 hours, followed by TNF-α (10 ng/ml) stimulation for 4 hours. The representative Western blot of tissue factor (TF) protein level (**A**) and quantification (**B**) are presented. **C-D,** HUVECs were transfected with si-Control or si-KLF11 (20 nM). Seventy-two hours after transfection, HUVECs were stimulated with TNF-α (10 ng/ml) for 4 hours. The representative Western blot of TF protein level (**C**) and quantification (**D**) are presented. Mouse aortic endothelial cells (MAECs) were isolated from wild type (Wt) or *Klf11* knockout (*Klf11* KO) male mice (n=3/group) and stimulated with TNF-α (2ng/ml) for 4 hours. The representative Western blot of TF expression is presented (**E**). The mRNA level was normalized to GAPDH and is presented relative to the control group. N=3/group. Data are presented as mean±SEM. **p*<0.05, ***p*<0.01 using two-way ANOVA followed by Bonferroni test. Antibodies: GAPDH (sc-32233, Santa Cruz Biotechnology, 1:1000 dilution), tissue factor (sc-374441, Santa Cruz Biotechnology, 1:1000 dilution).

The Early Growth Response 1, Rather than Nuclear Factor Kappa B and Activating Protein-1, is Responsive to KLF11-Dependent Inhibition of TF gene Transcription

Under basal conditions, TF expression in the endothelium is undetectable, preventing activation of the extrinsic coagulation cascade. However, endothelial TF expression can be significantly induced upon vascular injury and thus initiates coagulation. Several proinflammatory transcription factors, including nuclear factor kappa B (NF-κB), activating protein-1 (AP-1) and early growth response protein 1 (EGR1), have been well established in this process.[112, 113 114] Accordingly, we first determined whether KLF11 regulates the expression of these pathways. HUVECs infected with Ad-LacZ or Ad-KLF11 were stimulated with TNF-α for 60 minutes to evaluate the rapid gene expression changes in these three pathways. TNF-α-induced *TF* gene expression was increased more than 20-fold at 1-hour, which was significantly reduced in the KLF11 overexpression group (**Figure 3.5A**). These expression levels were either not affected (*p50*, *c-Jun*, *AP-1*) or slightly changed (*p65* increased and *EGR1* reduced) upon KLF11 overexpression compared with the LacZ control (**Figure 3.5B-D**). Therefore, the levels of AP-1, NF-κB, and EGR1 in ECs may not be responsible for the inhibitory effects of KLF11 on the early phase *TF* gene expression (**Figure 3.5A**). We next determined whether KLF11 might affect their function by applying the respective inhibitors of these signal pathways. BAY11-7082 was applied to block TNF-α-induced IκB-α phosphorylation (an essential step for NF-κB activation) (**Figure 3.6A**). SP600125 was used to inhibit c-Jun N-terminal kinase (**Figure 3.6B**). NGFI-A binding protein 2 (NAB2) was known to suppress EGR1-induced transcription (**Figure 3.6C**).[115] Consistent with the data in **Figure 3.4**, overexpression of KLF11 reduced TNF-α-induced *TF* gene transcription in HUVECs (**Figure 3.6A-C**, **compare the 5th and 6th column**). Of note, in the conditions of blocking a single signaling, KLF11 overexpression could

still further inhibit *TF* gene transcription, indicating that KLF11 effects involved multiple signaling pathways (**Figure 3.6A-C, compare the last two columns**). In addition, with KLF11 overexpression, the NF-κB or AP-1 inhibitors but not EGR1 inhibition could further reduce *TF* gene transcription (**Figure 3.6A-C, compare the 6th and 8th columns**). As EGR1 can induce *TF* gene expression and contribute to thrombus formation,[113, 114] we determined if KLF11 inhibits the inflammation-induced EGR1 signaling. Indeed, KLF11 suppressed EGR1 overexpression-induced *TF* gene expression at both mRNA and protein levels (**Figure 3.6D, E**). Collectively, our data indicate that EGR1, at least partially, mediates the KLF11-dependent inhibition of *TF* gene transcription in ECs under proinflammatory conditions.

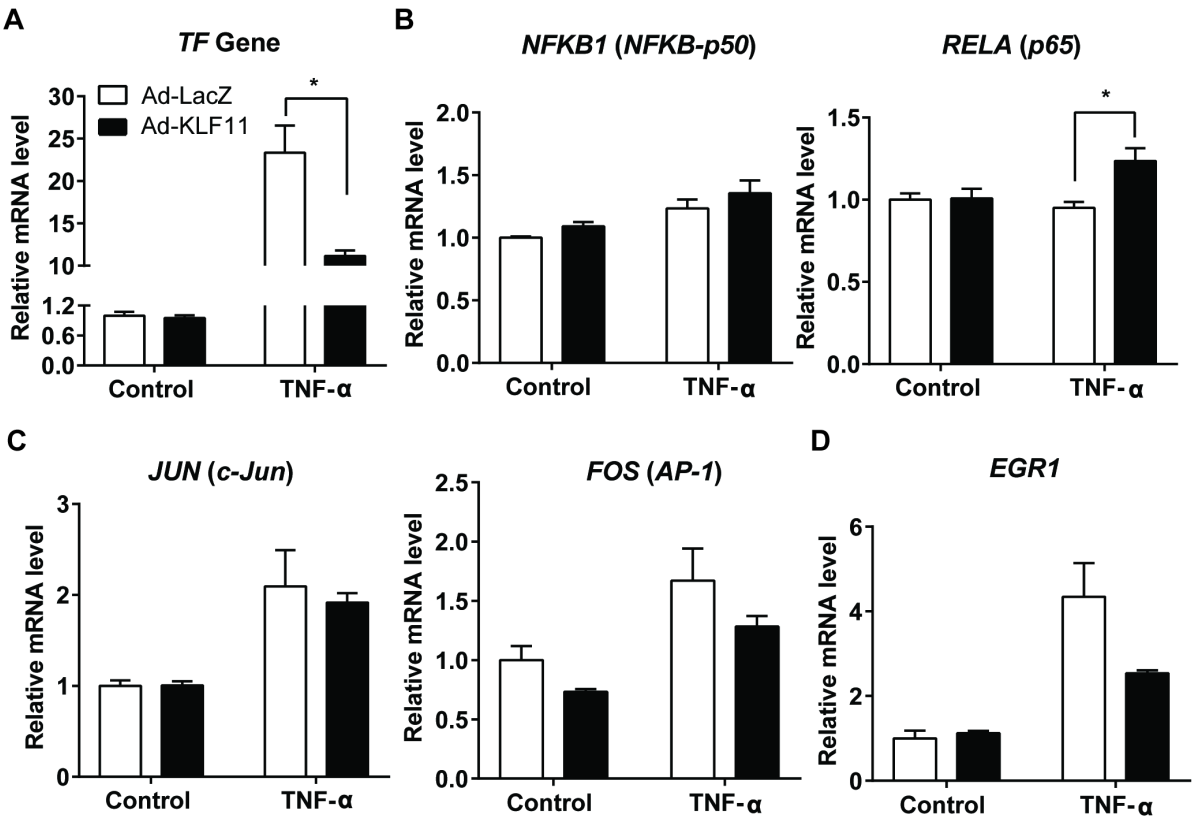

Figure 3.5 Overexpression of KLF11 cannot reduce the gene expression level of NF-κB, AP-1 and EGR1 signaling.

Human umbilical vein endothelial cells (HUVECs) were infected with Ad-LacZ or Ad-KLF11 (10 MOI) for 48 hours, followed by TNF-α (10 ng/ml) stimulation for 60 minutes. The mRNA level of *TF* gene (**A**), key factors in NF-κB signaling (*NFKB1* and *RELA*) (**B**), AP-1 signaling (*JUN, FOS*) (**C**), and *EGR1* (**D**) is presented. The mRNA level was normalized to GAPDH and is presented relative to the control group. N=3/group. Data are presented as mean±SEM. **p*<0.05 using unpaired Student *t*-test.

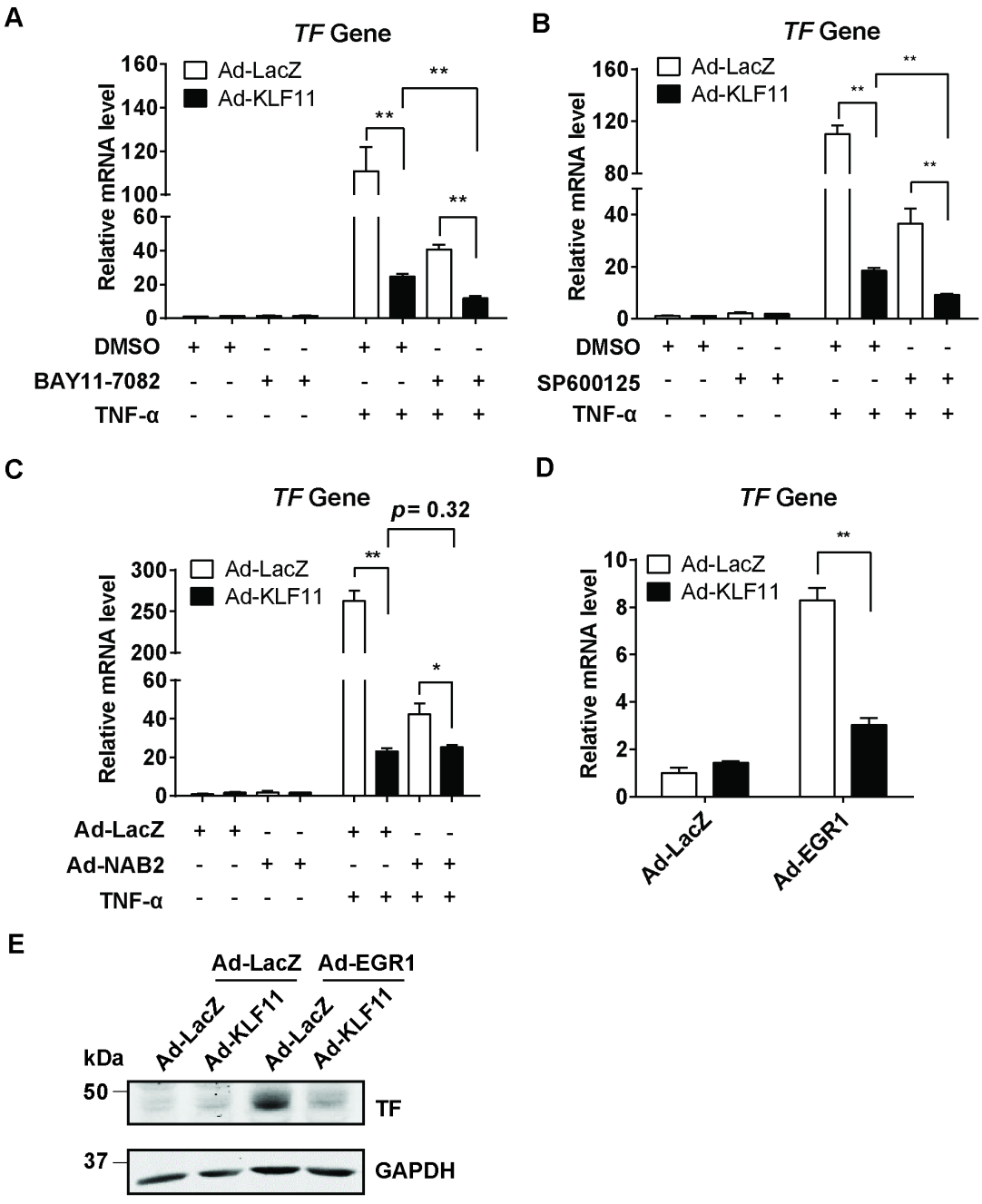
A
TF Gene
Ad-LacZ
Ad-KLF11
Relative mRNA level
DMSO
BAY11-7082
TNF-α
B
TF Gene
Ad-LacZ
Ad-KLF11
Relative mRNA level
DMSO
SP600125
TNF-α
C
TF Gene
p= 0.32
Ad-LacZ
Ad-KLF11
Relative mRNA level
Ad-LacZ
Ad-NAB2
TNF-α
D
TF Gene
Ad-LacZ
Ad-KLF11
Relative mRNA level
Ad-LacZ
Ad-EGR1
E
Ad-LacZ
Ad-EGR1
kDa
Ad-LacZ
Ad-KLF11
Ad-LacZ
Ad-KLF11
50
TF
37
GAPDH

Figure 3.6 The early growth response 1 (EGR1), rather than nuclear factor kappa B (NF-κB) and activating protein-1 (AP-1), is responsive to KLF11-dependent inhibition of *TF* gene transcription.

A-B, Human umbilical vein endothelial cells (HUVECs) were infected with Ad-LacZ or Ad-KLF11 (10 MOI). Forty-eight hours later, cells were treated with different compounds: BAY11-7082 (0.5 μM, **A**) or SP600125 (5 μM, **B**) for 1 hour, followed by TNF-α (10 ng/ml) stimulation for 4 hours. DMSO serves as the vehicle control for these compounds. **C,** HUVECs were co-infected with Ad-NAB2 (5 MOI) and Ad-LacZ or Ad-KLF11 (5 MOI) for 48 hours, followed by TNF-α (10 ng/ml) stimulation for 4 hours. The transcription of *TF* gene was determined by qPCR. **D-E,** HUVECs were co-infected with Ad-EGR1 (5 MOI) and Ad-LacZ or Ad-KLF11 (5 MOI) for 48 hours, and then the transcription of *TF* gene was determined by qPCR (**D**), the protein level of TF was detected by Western blot and the representative results are presented (**E**). The mRNA level was normalized to GAPDH and is presented relative to the control group. N=3/group. Data are presented as mean±SEM. **p*<0.05, ***p*<0.01 using two-way ANOVA followed by Bonferroni test. Antibodies: GAPDH (sc-32233, Santa Cruz Biotechnology, 1:1000 dilution), tissue factor (sc-374441, Santa Cruz Biotechnology, 1:1000 dilution).

KLF11 Inhibits EGR1-Induced TF Gene Transcription

To further determine the underlying mechanism, we transfected luciferase reporter plasmids driven by different lengths of *TF* gene promoter into bovine aortic endothelial cells (BAECs) (**Figure 3.7A**). Under both basal and TNF-α treatment conditions, KLF11 overexpression significantly reduced all three *TF* gene promoter-driven luciferase activities (**Figure 3.7B**). These results suggest that KLF11 downregulates *TF* gene at the transcriptional level. Although our previous study identified that KLF11 directly binds at *TF* gene promoter and inhibits its transcription in VSMCs at basal condition,[101] deletions of the potential KLF11 binding region (-177/-161 bp) failed to abolish the TNF-α-induced *TF* gene promoter activity in ECs (**Figure 3.8**). By using chromatin immunoprecipitation (ChIP) assay, we found that KLF11 overexpression abolished TNF-α-induced EGR1 binding to *TF* gene promoter (-154/+58 bp) (**Figure 3.7C**). To specifically test if KLF11 is important to counteract EGR1-induced *TF* gene transcription, we generated *TF* gene promoter-driven reporter plasmids with mutations at four putative EGR1 binding regions (predicted by online software MatInspector, **Figure 3.7D**, and **Table 3.2**). EGR1 overexpression-induced *TF* gene promotor activity can be inhibited by KLF11 overexpression, while these effects were interrupted when the EGR1 binding site was mutated at -63/-60 bp, -39/-34 bp, or -24/-21 bp, but not at -126/-123 bp region (**Figure 3.7E**). Furthermore, co-immunoprecipitation (Co-IP) followed by Western blot verified that KLF11 binds with EGR1 in ECs (**Figure 3.7F**). Therefore, KLF11 inhibits *TF* gene transcription *via* interacting with and suppressing EGR1.

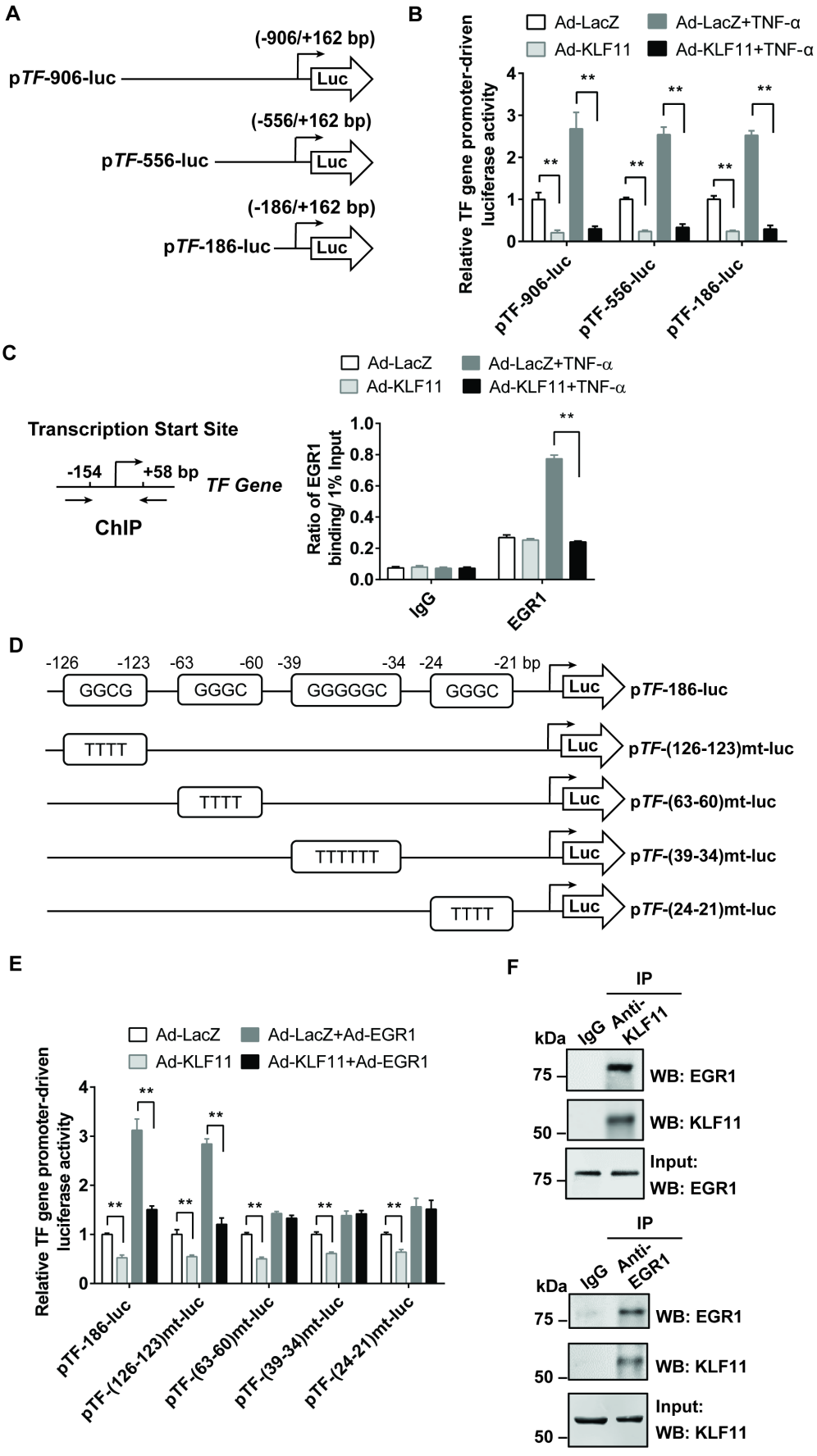
A
(-906/+162 bp)
pTF-906-luc
Luc
(-556/+162 bp)
pTF-556-luc
Luc
(-186/+162 bp)
pTF-186-luc
Luc
B
Ad-LacZ
Ad-LacZ+TNF-α
Ad-KLF11
Ad-KLF11+TNF-α
Relative TF gene promoter-driven luciferase activity
pTF-906-luc
pTF-556-luc
pTF-186-luc
C
Ad-LacZ
Ad-LacZ+TNF-α
Ad-KLF11
Ad-KLF11+TNF-α
Transcription Start Site
-154
+58 bp
TF Gene
ChIP
Ratio of EGR1 binding/ 1% Input
IgG
EGR1
D
-126
-123
-63
-60
-39
-34
-24
-21 bp
GGCG
GGGC
GGGGGC
GGGC
Luc
pTF-186-luc
TTTT
pTF-(126-123)mt-luc
TTTT
pTF-(63-60)mt-luc
TTTTTT
pTF-(39-34)mt-luc
TTTT
pTF-(24-21)mt-luc
E
Ad-LacZ
Ad-LacZ+Ad-EGR1
Ad-KLF11
Ad-KLF11+Ad-EGR1
Relative TF gene promoter-driven luciferase activity
pTF-186-luc
pTF-(126-123)mt-luc
pTF-(63-60)mt-luc
pTF-(39-34)mt-luc
pTF-(24-21)mt-luc
F
IP
kDa
IgG
Anti-KLF11
75
WB: EGR1
50
WB: KLF11
75
Input:
WB: EGR1
IP
kDa
IgG
Anti-EGR1
75
WB: EGR1
50
WB: KLF11
50
Input:
WB: KLF11

Figure 3.7 KLF11 inhibits EGR1-induced TF gene transcription.

A, The simplified structure illustration of luciferase reporters driven by different lengths of human *TF* gene promoter (p*TF*). **B,** Bovine aortic endothelial cells (BAECs) were transfected with p*TF*- luciferase reporters with varying sizes of promotor (**A**) for 24 hours and then infected with Ad-LacZ or Ad-KLF11 (10 MOI). Forty-eight hours after infection, BAECs were stimulated with TNF-α (10 ng/ml) for 12 hours. The luciferase activity was measured and normalized by Renilla activity. The results are presented relative to the group infected with Ad-LacZ(**B**). **C,** Human umbilical vein endothelial cells (HUVECs) were infected with Ad-LacZ or Ad-KLF11 (10 MOI) for 48 hours, followed by TNF-α (10 ng/ml) stimulation for 4 hours. The binding of EGR1 to the *TF* gene promoter was determined by chromatin immunoprecipitation (ChIP) assay using an antibody against EGR1. **D,** *TF* gene promoter-driven luciferase reporters p*TF*-186-luc with wild-type (wt) or different EGR1 binding region mutants are shown in the simplified illustration. **E,** BAECs were transfected with p*TF*-wt-luc or several p*TF*-mt-luc luciferase reporters for 24 hours and then co-infected with Ad-EGR1 (5 MOI) with Ad-LacZ or Ad-KLF11 (5 MOI) for 48 hours. The luciferase activity was measured and normalized by Renilla activity. The results are presented relative to the group infected with Ad-LacZ. $^{**}p<0.01$ using two-way ANOVA followed by Bonferroni test. **F,** HUVECs were co-infected with Ad-EGR1 (5 MOI) and Ad-KLF11 (5 MOI) for 48 hours. The cell lysates were subjected to immunoprecipitation (IP) with antibodies against KLF11 or IgG (**upper panel**), or EGR1 or IgG (**lower panel**). The precipitates were analyzed by Western blot (WB) using antibodies against KLF11 and EGR1. The co-immunoprecipitated EGR1 or KLF11 are presented. Data are presented as mean±SEM.

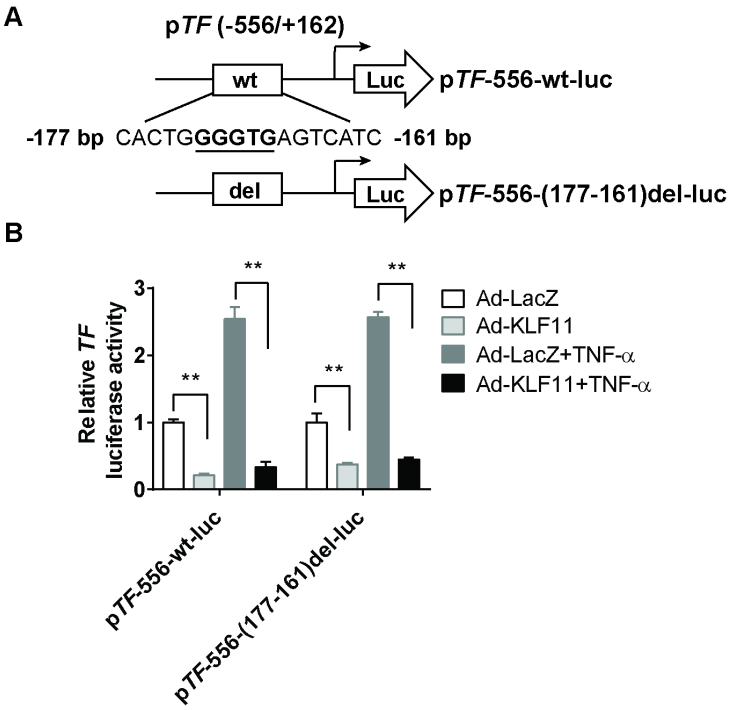

Figure 3.8 The inhibition of KLF11 on TNF-α-induced *TF* gene transcription is independent of the direct binding between KLF11 and *TF* gene promoter.

A, TF gene promoter-driven luciferase reporters with wild-type (wt) or KLF11 binding region deleted (del) are shown in the simplified illustration. The bold and underlined region represents the key KLF11 binding sites. **B,** Bovine aortic endothelial cells (BAECs) were transfected with wt or del TF gene promoter-driven luciferase reporters for 24 hours and then infected with Ad-LacZ or Ad-KLF11 (10 MOI). Forty-eight hours after infection, BAECs were stimulated with TNF-α (10 ng/ml) for 12 hours. The luciferase activity was measured and normalized by Renilla activity. The results are presented relative to the group infected with Ad-LacZ. **p<0.01 using two-way ANOVA followed by Bonferroni test.

Table 3.2 Predicted EGR1 Binding Sites and *TF* Gene Promoter-Driven Luciferase Constructs

Five Predicted EGR1 Binding Sites			***TF* Gene Promoter-Driven Luciferase Constructs**		
Start position	End position	Sequence (Capital letters denote the core sequence)	Plasmid (with mutation start and end site)	Original sequence	Mutant sequence
-134	-116	ccgggaggaGGCGg ggcag	p*TF*-(126-123)mt-luc	GGCG	TTTT
-70	-52	cgggccggGGGCgg ggagt	p*TF*-(63-60)mt-luc	GGGC	TTTT
-47	-29	aggagcggcGGGGg cgggc	p*TF*-(39-34)mt-luc	GGGGGC	TTTTTT
-44	-26	agcggcggGGGCgg gcgcc			
-31	-13	ggcgccggGGGCgg gcaga	p*TF*-(24-21)mt-luc	GGGC	TTTT

The EGR1 binding sites within -154/+58 bp in the human *TF* gene promoter were predicted by online software "MatInspector". To test if these sites mediate KLF11 function, we generated plasmid containing *TF* gene promoter-driven luciferase construct, with mutation in each binding site (-126/-123 bp, -63/-60 bp, -24/-21 bp) or an overlapped binding site (-39/-34 bp).

Endothelial KLF11 Protects against Thrombus Formation

To explore whether KLF11 affects venous thrombus formation, we performed *ex vivo* clot assay and *in vivo* DVT model in *Klf11* KO mice. With the *ex vivo* clot assay, we found that KLF11 overexpression significantly reduced TNF-α-induced clot formation (**Figure 3.9A**). Next, we investigated the effect of KLF11 on the development of DVT *in vivo*. Compared to Wt mice, *Klf*11 KO mice were more susceptible to stasis-induced DVT formation, as was evidenced by increased thrombus length (Wt 5.51 ± 0.50 mm vs. *Klf11* KO 7.44 ± 0.36 mm, p=0.004) and weight (Wt 14.6 ± 1.86 mg vs. *Klf11* KO 21.2 ± 1.73 mg, p=0.017), after 48-hour IVC ligation (**Figure 3.9B, C**). Moreover, the immunohistochemistry staining showed that *Klf*11 KO mice had higher TF expression in the IVC endothelium under stasis conditions than Wt mice (**Figure 3.9D, E**). As expected, there were no significant differences for endothelial TF expression in the baseline (**Figure 3.9D, E**). The increased *TF* gene expression in the ligated IVC of *Klf11* KO mice was further confirmed by qPCR (**Figure 3.9F**).

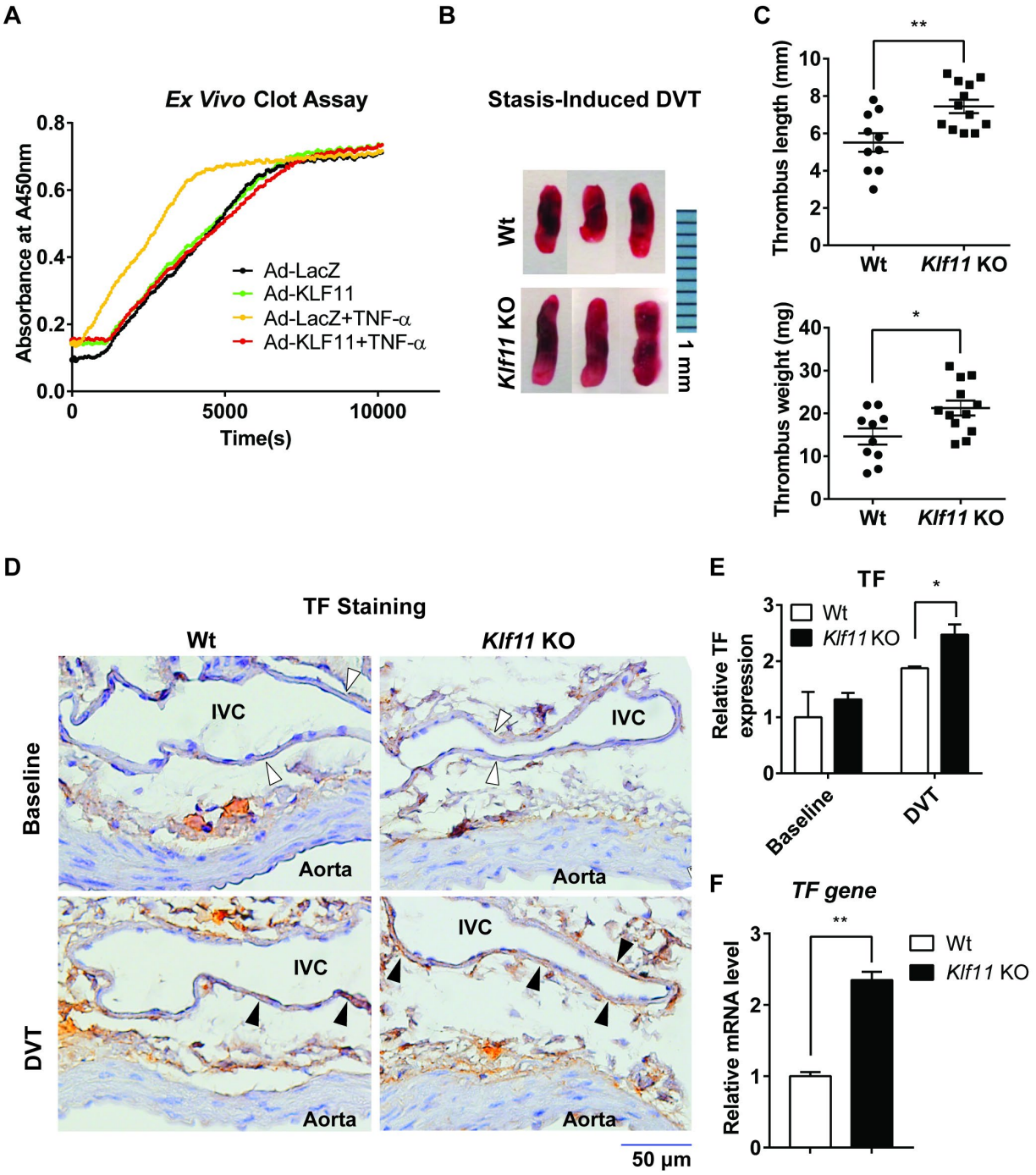
A
Ex Vivo Clot Assay
Absorbance at A450nm
0.8
0.6
0.4
0.2
0.0
0
5000
10000
Time(s)
Ad-LacZ
Ad-KLF11
Ad-LacZ+TNF-α
Ad-KLF11+TNF-α
B
Stasis-Induced DVT
Wt
Klf11 KO
1 mm
C
Thrombus length (mm)
10
8
6
4
2
0
**
Wt
Klf11 KO
Thrombus weight (mg)
40
30
20
10
0
*
Wt
Klf11 KO
D
TF Staining
Wt
Klf11 KO
Baseline
DVT
IVC
Aorta
50 μm
E
TF
*
Wt
Klf11 KO
Relative TF expression
3
2
1
0
Baseline
DVT
F
TF gene
**
Wt
Klf11 KO
Relative mRNA level
3
2
1
0

Figure 3.9 Endothelial KLF11 protects against thrombus formation.

A, Human umbilical vein endothelial cells (HUVECs) were infected with Ad-LacZ or Ad-KLF11 (10 MOI). Forty-eight hours after infection, HUVECs were stimulated with TNF-α (10 ng/ml) for 4 hours. Human plasma and calcium chloride were added, and the time of clot formation was measured. **B-C,** The stasis-induced deep vein thrombosis model (DVT) was applied in 8-10 weeks old male wild-type (Wt, n=10) or *Klf11* KO (n=12) mice by ligation of inferior vena cava (IVC) for 48 hours. Representative images of thrombus were shown. Bar=1mm (**B**). The length and weight of thromboses were measured (**C**). **D-F,** The cross-sections of a combination of the abdominal aorta and IVC from Wt and *Klf11* KO mice at baseline and in DVT condition (48-hour-ligation) were prepared. (**D**) The tissue factor (TF) expression was determined by immunohistochemistry staining (filled arrowheads). The lumen of the aorta and IVC are labeled, and the endothelium of DVT was indicated with empty arrowheads. Bar=50 μm. (**E**) The expression of TF was quantified by dividing the TF positive endothelial area by the total endothelial area of IVC in ImageJ software. Data were analyzed with the Wt group at the baseline level set as 1. (**F**) The IVC from Wt and *Klf11* KO mice were harvested after 48-hour ligation procedure to detect *TF* gene mRNA level (n=4/group). *$p<0.05$, **$p<0.01$ using the unpaired Student *t*-test.

Discussion

The endothelium is a dynamically changing barrier that is critically involved in the maintenance of vascular hemostasis. As endothelial injury is one of the major factors leading to thrombosis development, accumulating studies focus on the role of endothelium in DVT pathology. In this study, our data showed that KLF11 is an inflammation-responsive gene in ECs and inhibits DVT *in vivo*. KLF11 downregulates aberrant *TF* gene transcription *via* suppressing induced-EGR1 signaling in ECs. Based on the *in vitro* and *in vivo* data, we identified that KLF11 is a protector against DVT.

As a transcription factor, KLF11 regulates insulin expression in pancreatic β cells,[27, 33] and increases fatty acid oxidation in hepatic cells.[29] Our previous studies demonstrated that KLF11 deficiency upregulates the expression of proinflammatory adhesion molecules (*e.g.* ICAM1, VCAM1) by inhibiting NF-κB in ECs and thus aggravates leukocyte adhesion to vascular wall in mice.[28] In this paper, we discovered that KLF11 expression is induced under pro-thrombotic conditions, indicating KLF11 may modulate the pro-thrombotic response in endothelial cells. To extend our knowledge on the role of KLF11 in endothelial biology and deep vein thrombosis, we grouped the essential genes highly expressed in ECs and involved in thrombus formation into three groups according to their functions: coagulation cascade, platelet adhesion, and fibrinolysis (**Figure 3.2**). Among these genes, only *TF* gene was consistently and significantly downregulated by KLF11 under TNF-α-induced inflammation. Other genes are either not affected or only changed in one condition (*i.e.*, KLF11 overexpression or knockdown). As a whole, we discovered *TF* gene as the potential downstream target of KLF11 that prevents thrombus formation under inflammatory conditions in the endothelium.

In fact, the primary mechanism by which ECs regulate the coagulation cascade lies in its upregulation of TF expression (*i.e.*, *TF* gene transcription), especially upon vascular injury.[110] TF is the initiator of the extrinsic coagulation cascade. Although the expression of endothelial TF is low, it is highly inducible under pathological conditions. The primary transcription factors regulating TF expression in ECs include Sp1 transcription factor (SP1), NF-κB, AP-1, and EGR1.[112, 113, 116] In ECs, SP1 families bind at AP-1 and contribute to the constitutive *TF* gene transcription.[112] Upon stimulation (*e.g.*, inflammation), the NF-κB, AP-1 and EGR1 signaling can be activated and recruited to *TF* gene promoter, inducing TF expression.[113, 117]

However, KLF11 does not downregulate the key factors in NF-κB, AP-1 and EGR1 signaling (**Figure 3.5**), though KLF11 overexpression can significantly inhibit *TF* gene expression as early as one hour after TNF-α stimulation. This early phase transcriptional suppression may result from the altered activity rather than the expression level of these three pathways. To test this, we applied inhibitor studies and found that KLF11 further inhibited *TF* gene transcription in conditions of blocking NF-κB, AP-1 or EGR1 signaling, indicating that KLF11 effects are not mediated by a single pathway (**Figure 3.6A-C, compare the last two columns**). However, after KLF11 overexpression, the inhibition of NF-κB and AP-1 showed additive effects on suppressing *TF* gene transcription (**Figure 3.6A, B, compare the 6th and 8th columns**), which was not observed in the EGR1 inhibition group (**Figure 3.6C, compare the 6th and 8th columns**). These drove us to evaluate if KLF11 counteracts EGR1 signaling, which at least partially mediates the inflammation-induced *TF* gene transcription and contributes to thrombus formation.[114]

Employing multiple approaches, we demonstrated that KLF11 inhibits *TF* gene transcription *via* interrupting the binding between EGR1 and *TF* gene promoter. Consistent with

the previous report, there are multiple EGR1 binding sites in the *TF* gene promoter.[117] Although the mutation of three out of four EGR1 binding sites (-63/-60 bp, -39/-34 bp, and -24/-21 bp) cannot entirely abolish EGR1-induced *TF* gene promoter activity, it is enough to abolish KLF11 effects (no further reduction in **Figure 3.7E, compare the last two columns**). Combining this data with ChIP and Co-IP results, we propose that KLF11 can at least partially interrupt the induced-EGR1 binding to the *TF* gene promoter.

Although our previous paper identified that KLF11 binds at *TF* gene promoter (-177/-161 bp) and inhibits *TF* gene transcription in VSMCs,[101] we did not observe similarly direct regulation in ECs (**Figure 3.8**). TF is constitutively expressed in VSMCs but is almost undetectable in ECs at baseline. Upon inflammatory stimulation, endothelial TF is significantly induced and thus contributes to thrombus formation. Therefore, we demonstrated a novel mechanism in which KLF11, functioning as an inflammation inducible co-repressor *via* binding with EGR1, inhibits EGR1-induced *TF* gene transcription.

DVT, characterized by clot formation in the deep veins (*e.g.*, lower extremities), is triggered by hypercoagulative blood contents, disruption of blood flow, or endothelial damage. Inflammation, initiated by either systemic inflammatory status or local vascular injury, is an important mechanism contributing to thrombus formation.[118] In the present study, we applied this model in *Klf11* KO and Wt mice and found KLF11 deficiency aggravated DVT formation (**Figure 3.9B, C**). This is in line with the data that KLF11 deficiency enhanced TF expression in ECs (**Figure 3.4**) and endothelium (**Figure 3.9D-F**). The induced endothelial TF initiates extrinsic coagulation cascades and further triggers vascular inflammation (*e.g.*, leukocyte adhesion), all of which can accelerate DVT formation. Apart from ECs, circulating components such as platelets, coagulation factors, monocyte-derived TFs can also contribute to DVT. Our

previous study has shown that platelet activity (evaluated by *ex vivo* platelet activity assay) and coagulation cascade activity (assessed by prothrombin time and activated partial thromboplastin time) were not different between *Klf11* KO and Wt mice.[101] The overall hemostasis condition, measured by bleeding time, was also comparable between the two groups.[101] These indicate that KLF11 deficiency may not affect hemostatic status. Based on our current study, the aggravated DVT formation in *Klf11* KO mice can at least partially resulted from upregulated TF expression in ECs. The function of KLF11 in macrophages and monocyte-derived TF particles warrants further investigations in the future.

In summary, we demonstrated that KLF11 inhibits the EGR1-induced *TF* gene transcription in ECs under inflammatory conditions but not at baseline (**Figure 3.10**). Therefore, modulating endothelial KLF11 will be beneficial in the prevention of DVT.

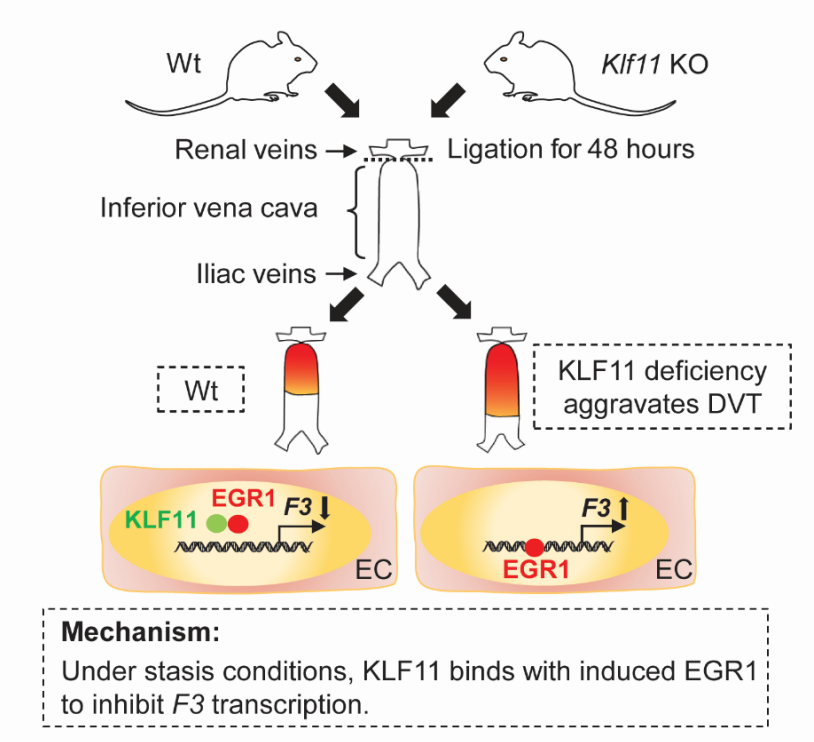

Figure 3.10 Summary

KLF11 inhibits the EGR1-induced *F3* transcription in endothelial cells (ECs) under inflammatory conditions but not at baseline and thus protects against thrombus formation.

Chapter 4 Summary and Perspectives

Summary

Vascular smooth muscle cells (VSMCs) and endothelial cells (ECs) are the two major vascular cell types that maintain vascular homeostasis. In the current study, we identified the importance of KLF11 in regulating the vascular biology in these two cell types (**Figure 4.1**). We found that both conventional and VSMC-selective *Klf11* KO mice were more susceptible to ferric chloride-induced arterial thrombosis *in vivo*, resulting from increased tissue factor expression in the tunica media of *Klf11* KO mice. No change after bone marrow transplantation and the normal plasma hemostasis parameters excluded the involvement of bone marrow-derived cells in this phenotype. In VSMCs, we applied gain- and loss-of-function approaches to demonstrate that KLF11 inhibits tissue factor expression. Chromatin immunoprecipitation (ChIP) assay and tissue factor promoter-driven luciferase assay further verified the direct binding of KLF11 to tissue factor promoter. Therefore, VSMC KLF11 functions as a transcription repressor to suppress tissue factor expression. We also performed the stasis-induced deep vein thrombosis (DVT) model in conventional *Klf11* KO mice. Comparing to the littermate control, *Klf11* KO mice had an increase in DVT. We found that KLF11 can inhibit the pro-thrombotic condition-induced early growth response 1 (EGR1) binding to tissue factor promoter, reducing the induced tissue factor expression in ECs.

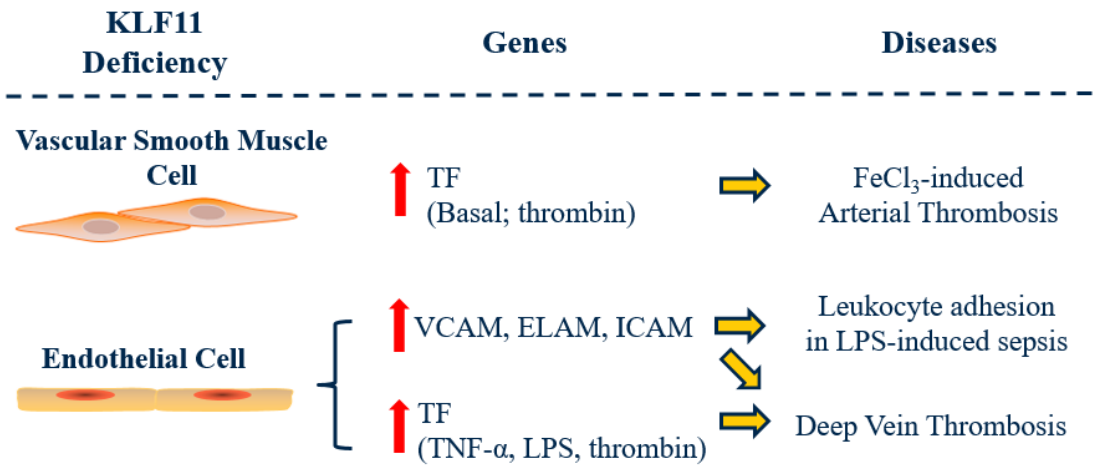

Abbreviations:
VCAM1, Vascular cell adhesion protein 1
ICAM1, Intercellular adhesion molecule 1
ELAM, E-selectin
TF, Tissue factor
LPS, Lipopolysaccharide

Figure 4.1 Overall Summary: KLF11 deficiency aggravates thrombosis formation.

Perspective

The Role of KLF11 in Other Vascular Diseases

KLF11 is originally identified as the causal gene of a monogenic subtype of diabetes, MODY7. Previous studies have reported that KLF11 can regulate pancreatic insulin secretion, peripheral insulin sensitivity, hepatic gluconeogenesis, and fatty acid oxidation. Metabolic disorders (*e.g.*, hyperlipidemia, hyperglycemia) can be strong risk factors for thrombotic diseases. Given our current studies that KLF11 inhibits both arterial and venous thrombosis, it would be of great clinical relevance to study if KLF11 dysfunction mediates the detrimental vascular events in metabolic diseases, such as diabetes.

Apart from thrombosis, atherosclerosis is another important pathological process disrupting vascular homeostasis. Endothelial inflammation and smooth muscle cell dysfunction can contribute to atherosclerotic plaque formation and development. In addition, atherosclerosis can also be aggravated under hyperlipidemia or hyperglycemia conditions. Based on these, investigating the role of KLF11 in atherosclerosis would provide more understanding of this common disease.

We recently identified the protective role of endothelial KLF11 in abdominal aortic aneurysms[32]. Besides the anti-inflammation function, endothelial KLF11 can inhibit MMP9 expression, suppress the NADPH oxidase 2-mediated reactive oxygen species production, and prevent the dedifferentiation of VSMCs and apoptosis. Given the high expression of KLF11 in VSMCs and the identified anti-thrombosis function, we will study the role of VSMC KLF11 in aneurysm development in the future.

Although the current studies focus on vascular KLF11, it would be promising to study the function of KLF11 in immune cells, such as macrophages. Our preliminary data indicated that

KLF11 deficiency aggravates lipopolysaccharide-induced inflammatory gene transcription in macrophages. With the success of the "CANTOS" clinical trial using a monoclonal antibody targeting interleukin-1β to prevent adverse cardiac events, a better knowledge of the inflammation regulation machinery in macrophages is in urgent demand[119]. In the future, we will investigate the role of KLF11 in regulating macrophages inflammation and its function in multiple vascular diseases.

KLF11 as a New Therapeutic Target

Considering the essential functions of KLFs in various diseases, therapeutic targeting selective KLFs may achieve desirable biomedical effects. However, some big obstacles, including the highly conserved sequences and the functional redundancy within this family, might impede efforts for drug development. Alternative strategies focusing on directly regulating KLF gene expression or modifying its DNA-binding capacity are applied to solve these problems.

One alternative strategy is to develop a compound that disrupts the DNA-binding of KLFs. For example, a region within the middle zinc finger domain of KLF10 has been identified as a "pocket". Once a compound blocks this "pocket", the binding ability of KLF10 is impaired. Based on this discovery, scientists have applied computer-aided drug design screens of chemical libraries and found small molecular compounds inhibiting KLF10-DNA binding activity[120].

KLFs can also be the downstream targets of several commonly prescribed drugs. For example, KLF2 and KLF4 can mediate the function of statins and facilitates the vascular protective effects of statins [63, 121]. Similarly, KLF11 has been identified as required for the therapeutic effects of PPARγ agonist (rosiglitazone, one of the commonly prescribed diabetes drugs) in improving oxidative capacity and adipose tissue browning[38].

Overall, the accumulating studies on the functions and regulation of KLFs can provide novel therapeutic strategies for treating cardiovascular diseases.

Bibliography

1. Schuh R, Aicher W, Gaul U, Cote S, Preiss A, Maier D, Seifert E, Nauber U, Schroder C, Kemler R and et al. A conserved family of nuclear proteins containing structural elements of the finger protein encoded by Kruppel, a Drosophila segmentation gene. *Cell*. 1986;47:1025-32.
2. Miller IJ and Bieker JJ. A novel, erythroid cell-specific murine transcription factor that binds to the CACCC element and is related to the Kruppel family of nuclear proteins. *Mol Cell Biol*. 1993;13:2776-86.
3. Fan Y, Lu H, Liang W, Hu W, Zhang J and Chen YE. Kruppel-like factors and vascular wall homeostasis. *J Mol Cell Biol*. 2017;9:352-363.
4. McConnell BB and Yang VW. Mammalian Kruppel-like factors in health and diseases. *Physiol Rev*. 2010;90:1337-81.
5. Nandan MO, Yoon HS, Zhao W, Ouko LA, Chanchevalap S and Yang VW. Kruppel-like factor 5 mediates the transforming activity of oncogenic H-Ras. *Oncogene*. 2004;23:3404-13.
6. Buckley AF, Kuo CT and Leiden JM. Transcription factor LKLF is sufficient to program T cell quiescence via a c-Myc-dependent pathway. *Nat Immunol*. 2001;2:698-704.
7. Chen C, Benjamin MS, Sun X, Otto KB, Guo P, Dong XY, Bao Y, Zhou Z, Cheng X, Simons JW and Dong JT. KLF5 promotes cell proliferation and tumorigenesis through gene regulation and the TSU-Pr1 human bladder cancer cell line. *Int J Cancer*. 2006;118:1346-55.
8. Rowland BD, Bernards R and Peeper DS. The KLF4 tumour suppressor is a transcriptional repressor of p53 that acts as a context-dependent oncogene. *Nat Cell Biol*. 2005;7:1074-82.
9. Rowland BD and Peeper DS. KLF4, p21 and context-dependent opposing forces in cancer. *Nat Rev Cancer*. 2006;6:11-23.
10. Drissen R, von Lindern M, Kolbus A, Driegen S, Steinlein P, Beug H, Grosveld F and Philipsen S. The erythroid phenotype of EKLF-null mice: defects in hemoglobin metabolism and membrane stability. *Mol Cell Biol*. 2005;25:5205-14.
11. Hodge D, Coghill E, Keys J, Maguire T, Hartmann B, McDowall A, Weiss M, Grimmond S and Perkins A. A global role for EKLF in definitive and primitive erythropoiesis. *Blood*. 2006;107:3359-70.
12. McConnell BB, Ghaleb AM, Nandan MO and Yang VW. The diverse functions of Kruppel-like factors 4 and 5 in epithelial biology and pathobiology. *Bioessays*. 2007;29:549-57.
13. Adam PJ, Regan CP, Hautmann MB and Owens GK. Positive- and negative-acting Kruppel-like transcription factors bind a transforming growth factor beta control element required for expression of the smooth muscle cell differentiation marker SM22alpha in vivo. *The Journal of biological chemistry*. 2000;275:37798-806.
14. Birsoy K, Chen Z and Friedman J. Transcriptional regulation of adipogenesis by KLF4. *Cell Metab*. 2008;7:339-47.
15. Cook T, Gebelein B, Mesa K, Mladek A and Urrutia R. Molecular Cloning and Characterization of TIEG2Reveals a New Subfamily of Transforming Growth Factor-β-inducible

Sp1-like Zinc Finger-encoding Genes Involved in the Regulation of Cell Growth*. *Journal of Biological Chemistry*. 1998;273:25929-25936.
16. Wang Z, Peters B, Klussmann S, Bender H, Herb A and Krieglstein K. Gene structure and evolution of Tieg3, a new member of the Tieg family of proteins. *Gene*. 2004;325:25-34.
17. Spittau B, Wang Z, Boinska D and Krieglstein K. Functional domains of the TGF-β-inducible transcription factor Tieg3 and detection of two putative nuclear localization signals within the zinc finger DNA-binding domain. *Journal of Cellular Biochemistry*. 2007;101:712-722.
18. Buttar NS, DeMars CJ, Lomberk G, Rizvi S, Bonilla-Velez J, Achra S, Rashtak S, Wang KK, Fernandez-Zapico ME and Urrutia R. Distinct role of Kruppel-like factor 11 in the regulation of prostaglandin E2 biosynthesis. *The Journal of biological chemistry*. 2010;285:11433-44.
19. Zhang J-S, Moncrieffe MC, Kaczynski J, Ellenrieder V, Prendergast FG and Urrutia R. A Conserved α-Helical Motif Mediates the Interaction of Sp1-Like Transcriptional Repressors with the Corepressor mSin3A. *Molecular and Cellular Biology*. 2001;21:5041-5049.
20. Johnsen SA, Subramaniam M, Janknecht R and Spelsberg TC. TGFβ inducible early gene enhances TGFβ/Smad-dependent transcriptional responses. *Oncogene*. 2002;21:5783-5790.
21. Buck A, Buchholz M, Wagner M, Adler G, Gress T and Ellenrieder V. The Tumor Suppressor KLF11 Mediates a Novel Mechanism in Transforming Growth Factor β–Induced Growth Inhibition That Is Inactivated in Pancreatic Cancer. *Molecular Cancer Research*. 2006;4:861-872.
22. Ellenrieder V, Zhang JS, Kaczynski J and Urrutia R. Signaling disrupts mSin3A binding to the Mad1-like Sin3-interacting domain of TIEG2, an Sp1-like repressor. *Embo j*. 2002;21:2451-60.
23. Potapova A, Hasemeier B, Römermann D, Metzig K, Göhring G, Schlegelberger B, Länger F, Kreipe H and Lehmann U. Epigenetic inactivation of tumour suppressor gene KLF11 in myelodysplastic syndromes*. *European Journal of Haematology*. 2010;84:298-303.
24. Faryna M, Konermann C, Aulmann S, Bermejo JL, Brugger M, Diederichs S, Rom J, Weichenhan D, Claus R, Rehli M, Schirmacher P, Sinn HP, Plass C and Gerhauser C. Genome-wide methylation screen in low-grade breast cancer identifies novel epigenetically altered genes as potential biomarkers for tumor diagnosis. *Faseb j*. 2012;26:4937-50.
25. Neve B, Fernandez-Zapico ME, Ashkenazi-Katalan V, Dina C, Hamid YH, Joly E, Vaillant E, Benmezroua Y, Durand E, Bakaher N, Delannoy V, Vaxillaire M, Cook T, Dallinga-Thie GM, Jansen H, Charles MA, Clement K, Galan P, Hercberg S, Helbecque N, Charpentier G, Prentki M, Hansen T, Pedersen O, Urrutia R, Melloul D and Froguel P. Role of transcription factor KLF11 and its diabetes-associated gene variants in pancreatic beta cell function. *Proceedings of the National Academy of Sciences of the United States of America*. 2005;102:4807-12.
26. Ushijima K, Narumi S, Ogata T, Yokota I, Sugihara S, Kaname T, Horikawa Y, Matsubara Y, Fukami M, Kawamura T, Childhood TJSGoITf and Diabetes A. KLF11 variant in a family clinically diagnosed with early childhood-onset type 1B diabetes. *Pediatric Diabetes*. 2019;20:712-719.
27. Bonnefond A, Lomberk G, Buttar N, Busiah K, Vaillant E, Lobbens S, Yengo L, Dechaume A, Mignot B, Simon A, Scharfmann R, Neve B, Tanyolac S, Hodoglugil U, Pattou F, Cave H, Iovanna J, Stein R, Polak M, Vaxillaire M, Froguel P and Urrutia R. Disruption of a novel Kruppel-like transcription factor p300-regulated pathway for insulin biosynthesis revealed

by studies of the c.-331 INS mutation found in neonatal diabetes mellitus. *J Biol Chem*. 2011;286:28414-24.
28. Fan Y, Guo Y, Zhang J, Subramaniam M, Song CZ, Urrutia R and Chen YE. Kruppel-like factor-11, a transcription factor involved in diabetes mellitus, suppresses endothelial cell activation via the nuclear factor-kappaB signaling pathway. *Arteriosclerosis, thrombosis, and vascular biology*. 2012;32:2981-8.
29. Yin KJ, Fan Y, Hamblin M, Zhang J, Zhu T, Li S, Hawse JR, Subramaniam M, Song CZ, Urrutia R, Lin JD and Chen YE. KLF11 mediates PPARgamma cerebrovascular protection in ischaemic stroke. *Brain : a journal of neurology*. 2013;136:1274-87.
30. Zhang X, Tang X, Ma F, Fan Y, Sun P, Zhu T, Zhang J, Hamblin MH, Chen YE and Yin KJ. Endothelium-targeted overexpression of Krüppel-like factor 11 protects the blood-brain barrier function after ischemic brain injury. *Brain Pathol*. 2020;30:746-765.
31. Glineur C, Gross B, Neve B, Rommens C, Chew GT, Martin-Nizard F, Rodríguez-Pascual F, Lamas S, Watts GF and Staels B. Fenofibrate Inhibits Endothelin-1 Expression by Peroxisome Proliferator–Activated Receptor α–Dependent and Independent Mechanisms in Human Endothelial Cells. *Arteriosclerosis, thrombosis, and vascular biology*. 2013;33:621-628.
32. Zhao G, Chang Z, Zhao Y, Guo Y, Lu H, Liang W, Rom O, Wang H, Sun J, Zhu T, Fan Y, Chang L, Yang B, Garcia-Barrio MT, Chen YE and Zhang J. KLF11 protects against abdominal aortic aneurysm through inhibition of endothelial cell dysfunction. *JCI Insight*. 2021;6.
33. Fernandez-Zapico ME, van Velkinburgh JC, Gutierrez-Aguilar R, Neve B, Froguel P, Urrutia R and Stein R. MODY7 gene, KLF11, is a novel p300-dependent regulator of Pdx-1 (MODY4) transcription in pancreatic islet beta cells. *J Biol Chem*. 2009;284:36482-90.
34. Mathison A, Escande C, Calvo E, Seo S, White T, Salmonson A, Faubion WA, Jr, Buttar N, Iovanna J, Lomberk G, Chini EN and Urrutia R. Phenotypic Characterization of Mice Carrying Homozygous Deletion of KLF11, a Gene in Which Mutations Cause Human Neonatal and MODY VII Diabetes. *Endocrinology*. 2015;156:3581-3595.
35. Zhang H, Chen Q, Jiao T, Cui A, Sun X, Fang W, Xie L, Liu Y, Fang F and Chang Y. Involvement of KLF11 in Hepatic Glucose Metabolism in Mice via Suppressing of PEPCK-C Expression. *PLOS ONE*. 2014;9:e89552.
36. Zhang H, Chen Q, Yang M, Zhu B, Cui Y, Xue Y, Gong N, Cui A, Wang M, Shen L, Zhang S, Fang F and Chang Y. Mouse KLF11 regulates hepatic lipid metabolism. *Journal of hepatology*. 2013;58:763-70.
37. Yamamoto K-i, Sakaguchi M, Medina RJ, Niida A, Sakaguchi Y, Miyazaki M, Kataoka K and Huh N-h. Transcriptional regulation of a brown adipocyte-specific gene, UCP1, by KLF11 and KLF15. *Biochemical and Biophysical Research Communications*. 2010;400:175-180.
38. Loft A, Forss I, Siersbæk MS, Schmidt SF, Larsen A-SB, Madsen JGS, Pisani DF, Nielsen R, Aagaard MM, Mathison A, Neville MJ, Urrutia R, Karpe F, Amri E-Z and Mandrup S. Browning of human adipocytes requires KLF11 and reprogramming of PPARγ superenhancers. *Genes & Development*. 2015;29:7-22.
39. Lin L, Mahner S, Jeschke U and Hester A. The Distinct Roles of Transcriptional Factor KLF11 in Normal Cell Growth Regulation and Cancer as a Mediator of TGF-β Signaling Pathway. *International journal of molecular sciences*. 2020;21:2928.

40. Han M, Wang Y, Guo G, Li L, Dou D, Ge X, Lv P, Wang F and Gu Y. microRNA-30d mediated breast cancer invasion, migration, and EMT by targeting KLF11 and activating STAT3 pathway. *Journal of Cellular Biochemistry*. 2018;119:8138-8145.
41. Son B, Jeon J, Lee S, Kim H, Kang H, Youn H, Jo S and Youn B. Radiotherapy in combination with hyperthermia suppresses lung cancer progression via increased NR4A3 and KLF11 expression. *Int J Radiat Biol*. 2019;95:1696-1707.
42. Ji Q, Li Y, Zhao Q, Fan LQ, Tan BB, Zhang ZD, Zhao XF, Liu Y, Wang D and Jia N. KLF11 promotes gastric cancer invasion and migration by increasing Twist1 expression. *Neoplasma*. 2019;66:92-100.
43. Raskob GE, Angchaisuksiri P, Blanco AN, Buller H, Gallus A, Hunt BJ, Hylek EM, Kakkar A, Konstantinides SV, McCumber M, Ozaki Y, Wendelboe A, Weitz JI and Day ISCfWT. Thrombosis: a major contributor to global disease burden. *Arteriosclerosis, thrombosis, and vascular biology*. 2014;34:2363-71.
44. Wolberg AS, Aleman MM, Leiderman K and Machlus KR. Procoagulant activity in hemostasis and thrombosis: Virchow's triad revisited. *Anesthesia and analgesia*. 2012;114:275-85.
45. Michel JB, Li Z and Lacolley P. Smooth muscle cells and vascular diseases. *Cardiovasc Res*. 2012;95:135-7.
46. Alaiti MA, Orasanu G, Tugal D, Lu Y and Jain MK. Kruppel-like factors and vascular inflammation: implications for atherosclerosis. *Curr Atheroscler Rep*. 2012;14:438-49.
47. Hess K and Grant PJ. Inflammation and thrombosis in diabetes. *Thromb Haemost*. 2011;105 Suppl 1:S43-54.
48. Pechlivani N and Ajjan RA. Thrombosis and Vascular Inflammation in Diabetes: Mechanisms and Potential Therapeutic Targets. *Front Cardiovasc Med*. 2018;5:1.
49. Vazzana N, Ranalli P, Cuccurullo C and Davi G. Diabetes mellitus and thrombosis. *Thrombosis research*. 2012;129:371-7.
50. Glineur C, Gross B, Neve B, Rommens C, Chew GT, Martin-Nizard F, Rodriguez-Pascual F, Lamas S, Watts GF and Staels B. Fenofibrate inhibits endothelin-1 expression by peroxisome proliferator-activated receptor alpha-dependent and independent mechanisms in human endothelial cells. *Arteriosclerosis, thrombosis, and vascular biology*. 2013;33:621-8.
51. Cherepanova OA, Gomez D, Shankman LS, Swiatlowska P, Williams J, Sarmento OF, Alencar GF, Hess DL, Bevard MH, Greene ES, Murgai M, Turner SD, Geng YJ, Bekiranov S, Connelly JJ, Tomilin A and Owens GK. Activation of the pluripotency factor OCT4 in smooth muscle cells is atheroprotective. *Nat Med*. 2016;22:657-65.
52. Chen F, Shao F, Hinds A, Yao S, Ram-Mohan S, Norman TA, Krishnan R and Fine A. Retinoic acid signaling is essential for airway smooth muscle homeostasis. *JCI Insight*. 2018;3:e120398.
53. Wang L, Miller C, Swarthout RF, Rao M, Mackman N and Taubman MB. Vascular smooth muscle-derived tissue factor is critical for arterial thrombosis after ferric chloride-induced injury. *Blood*. 2009;113:705-13.
54. Tilley RE, Pedersen B, Pawlinski R, Sato Y, Erlich JH, Shen Y, Day S, Huang Y, Eitzman DT, Boisvert WA, Curtiss LK, Fay WP and Mackman N. Atherosclerosis in mice is not affected by a reduction in tissue factor expression. *Arteriosclerosis, thrombosis, and vascular biology*. 2006;26:555-62.

55. Luo W, Wang H, Ohman MK, Guo C, Shi K, Wang J and Eitzman DT. P-selectin glycoprotein ligand-1 deficiency leads to cytokine resistance and protection against atherosclerosis in apolipoprotein E deficient mice. *Atherosclerosis*. 2012;220:110-7.
56. Yeung J, Tourdot BE, Adili R, Green AR, Freedman CJ, Fernandez-Perez P, Yu J, Holman TR and Holinstat M. 12(S)-HETrE, a 12-Lipoxygenase Oxylipin of Dihomo-gamma-Linolenic Acid, Inhibits Thrombosis via Galphas Signaling in Platelets. *Arteriosclerosis, thrombosis, and vascular biology*. 2016;36:2068-77.
57. Sun H, Wang X, Degen JL and Ginsburg D. Reduced thrombin generation increases host susceptibility to group A streptococcal infection. *Blood*. 2009;113:1358-64.
58. Fan Y, Lu H, Liang W, Garcia-Barrio MT, Guo Y, Zhang J, Zhu T, Hao Y, Zhang J and Chen YE. Endothelial TFEB (Transcription Factor EB) Positively Regulates Postischemic Angiogenesis. *Circ Res*. 2018;122:945-957.
59. Kirchhofer D, Moran P, Bullens S, Peale F and Bunting S. A monoclonal antibody that inhibits mouse tissue factor function. *J Thromb Haemost*. 2005;3:1098-9.
60. Shankman LS, Gomez D, Cherepanova OA, Salmon M, Alencar GF, Haskins RM, Swiatlowska P, Newman AA, Greene ES, Straub AC, Isakson B, Randolph GJ and Owens GK. KLF4-dependent phenotypic modulation of smooth muscle cells has a key role in atherosclerotic plaque pathogenesis. *Nat Med*. 2015;21:628-37.
61. Taubman MB, Wang L and Miller C. The role of smooth muscle derived tissue factor in mediating thrombosis and arterial injury. *Thrombosis research*. 2008;122 Suppl 1:S78-81.
62. Pollak NM, Hoffman M, Goldberg IJ and Drosatos K. Kruppel-like factors: Crippling and un-crippling metabolic pathways. *JACC Basic Transl Sci*. 2018;3:132-156.
63. Lin Z, Kumar A, SenBanerjee S, Staniszewski K, Parmar K, Vaughan DE, Gimbrone MA, Jr., Balasubramanian V, Garcia-Cardena G and Jain MK. Kruppel-like factor 2 (KLF2) regulates endothelial thrombotic function. *Circ Res*. 2005;96:e48-57.
64. Boon RA, Fledderus JO, Volger OL, van Wanrooij EJ, Pardali E, Weesie F, Kuiper J, Pannekoek H, ten Dijke P and Horrevoets AJ. KLF2 suppresses TGF-beta signaling in endothelium through induction of Smad7 and inhibition of AP-1. *Arteriosclerosis, thrombosis, and vascular biology*. 2007;27:532-9.
65. Zhou G, Hamik A, Nayak L, Tian H, Shi H, Lu Y, Sharma N, Liao X, Hale A, Boerboom L, Feaver RE, Gao H, Desai A, Schmaier A, Gerson SL, Wang Y, Atkins GB, Blackman BR, Simon DI and Jain MK. Endothelial Kruppel-like factor 4 protects against atherothrombosis in mice. *The Journal of clinical investigation*. 2012;122:4727-31.
66. Tancredi M, Rosengren A, Svensson AM, Kosiborod M, Pivodic A, Gudbjornsdottir S, Wedel H, Clements M, Dahlqvist S and Lind M. Excess Mortality among Persons with Type 2 Diabetes. *The New England journal of medicine*. 2015;373:1720-32.
67. Sachs UJ and Nieswandt B. In vivo thrombus formation in murine models. *Circ Res*. 2007;100:979-91.
68. Westrick RJ, Winn ME and Eitzman DT. Murine models of vascular thrombosis (Eitzman series). *Arteriosclerosis, thrombosis, and vascular biology*. 2007;27:2079-93.
69. Grover SP and Mackman N. Tissue Factor: An Essential Mediator of Hemostasis and Trigger of Thrombosis. *Arteriosclerosis, thrombosis, and vascular biology*. 2018;38:709-725.
70. Marmur JD, Thiruvikraman SV, Fyfe BS, Guha A, Sharma SK, Ambrose JA, Fallon JT, Nemerson Y and Taubman MB. Identification of active tissue factor in human coronary atheroma. *Circulation*. 1996;94:1226-32.

71. Annex BH, Denning SM, Channon KM, Sketch MH, Jr., Stack RS, Morrissey JH and Peters KG. Differential expression of tissue factor protein in directional atherectomy specimens from patients with stable and unstable coronary syndromes. *Circulation*. 1995;91:619-22.
72. Tremoli E, Camera M, Toschi V and Colli S. Tissue factor in atherosclerosis. *Atherosclerosis*. 1999;144:273-83.
73. Day SM, Reeve JL, Pedersen B, Farris DM, Myers DD, Im M, Wakefield TW, Mackman N and Fay WP. Macrovascular thrombosis is driven by tissue factor derived primarily from the blood vessel wall. *Blood*. 2005;105:192-8.
74. Mackman N and Taubman MB. Does tissue factor expression by vascular smooth muscle cells provide a link between C-reactive protein and cardiovascular disease? *Arteriosclerosis, thrombosis, and vascular biology*. 2008;28:601-3.
75. Marmur JD, Rossikhina M, Guha A, Fyfe B, Friedrich V, Mendlowitz M, Nemerson Y and Taubman MB. Tissue factor is rapidly induced in arterial smooth muscle after balloon injury. *The Journal of clinical investigation*. 1993;91:2253-9.
76. Wilcox JN, Smith KM, Schwartz SM and Gordon D. Localization of tissue factor in the normal vessel wall and in the atherosclerotic plaque. *Proceedings of the National Academy of Sciences of the United States of America*. 1989;86:2839-43.
77. Morrow DA, Murphy SA, McCabe CH, Mackman N, Wong HC and Antman EM. Potent inhibition of thrombin with a monoclonal antibody against tissue factor (Sunol-cH36): results of the PROXIMATE-TIMI 27 trial. *European heart journal*. 2005;26:682-8.
78. Abraham E, Reinhart K, Opal S, Demeyer I, Doig C, Rodriguez AL, Beale R, Svoboda P, Laterre PF, Simon S, Light B, Spapen H, Stone J, Seibert A, Peckelsen C, De Deyne C, Postier R, Pettila V, Sprung CL, Artigas A, Percell SR, Shu V, Zwingelstein C, Tobias J, Poole L, Stolzenbach JC, Creasey AA and Group OTS. Efficacy and safety of tifacogin (recombinant tissue factor pathway inhibitor) in severe sepsis: a randomized controlled trial. *Jama*. 2003;290:238-47.
79. Yang J, Jin K, Xiao J, Ma J and Ma D. Endogenous tissue factor pathway inhibitor in vascular smooth muscle cells inhibits arterial thrombosis. *Front Med*. 2017;11:403-409.
80. Spronk H, Borissoff J and ten Cate H. New Insights into Modulation of Thrombin Formation. *Curr Atheroscler Rep*. 2013;15:363.
81. Taubman MB, Marmur JD, Rosenfield CL, Guha A, Nichtberger S and Nemerson Y. Agonist-mediated tissue factor expression in cultured vascular smooth muscle cells. Role of Ca2+ mobilization and protein kinase C activation. *The Journal of clinical investigation*. 1993;91:547-52.
82. Herkert O, Diebold I, Brandes RP, Hess J, Busse R and Gorlach A. NADPH oxidase mediates tissue factor-dependent surface procoagulant activity by thrombin in human vascular smooth muscle cells. *Circulation*. 2002;105:2030-6.
83. BelAiba RS, Djordjevic T, Bonello S, Artunc F, Lang F, Hess J and Gorlach A. The serum- and glucocorticoid-inducible kinase Sgk-1 is involved in pulmonary vascular remodeling: role in redox-sensitive regulation of tissue factor by thrombin. *Circ Res*. 2006;98:828-36.
84. Gorlach A, BelAiba RS, Hess J and Kietzmann T. Thrombin activates the p21-activated kinase in pulmonary artery smooth muscle cells. Role in tissue factor expression. *Thromb Haemost*. 2005;93:1168-75.
85. Chung SW, Park JW, Lee SA, Eo SK and Kim K. Thrombin promotes proinflammatory phenotype in human vascular smooth muscle cell. *Biochem Biophys Res Commun*. 2010;396:748-54.

86. Jeong JY, Son Y, Kim BY, Eo SK, Rhim BY and Kim K. Multiple Signaling Pathways Contribute to the Thrombin-induced Secretory Phenotype in Vascular Smooth Muscle Cells. *Korean J Physiol Pharmacol*. 2015;19:549-55.
87. Djordjevic T, Hess J, Herkert O, Gorlach A and BelAiba RS. Rac regulates thrombin-induced tissue factor expression in pulmonary artery smooth muscle cells involving the nuclear factor-kappaB pathway. *Antioxidants & redox signaling*. 2004;6:713-20.
88. Yasumoto H, Kim S, Zhan Y, Miyazaki H, Hoshiga M, Kaneda Y, Morishita R and Iwao H. Dominant negative c-jun gene transfer inhibits vascular smooth muscle cell proliferation and neointimal hyperplasia in rats. *Gene Ther*. 2001;8:1682-9.
89. Schoenwaelder SM and Jackson SP. Ferric chloride thrombosis model: unraveling the vascular effects of a highly corrosive oxidant. *Blood*. 2015;126:2652-3.
90. Barr JD, Chauhan AK, Schaeffer GV, Hansen JK and Motto DG. Red blood cells mediate the onset of thrombosis in the ferric chloride murine model. *Blood*. 2013;121:3733-41.
91. Eckly A, Hechler B, Freund M, Zerr M, Cazenave JP, Lanza F, Mangin PH and Gachet C. Mechanisms underlying FeCl3-induced arterial thrombosis. *J Thromb Haemost*. 2011;9:779-89.
92. Drake TA, Morrissey JH and Edgington TS. Selective cellular expression of tissue factor in human tissues. Implications for disorders of hemostasis and thrombosis. *Am J Pathol*. 1989;134:1087-97.
93. Mackman N. The role of tissue factor and factor VIIa in hemostasis. *Anesthesia and analgesia*. 2009;108:1447-1452.
94. Butenas S, Bouchard BA, Brummel-Ziedins KE, Parhami-Seren B and Mann KG. Tissue factor activity in whole blood. *Blood*. 2005;105:2764-70.
95. Bode M and Mackman N. Regulation of tissue factor gene expression in monocytes and endothelial cells: Thromboxane A2 as a new player. *Vascular pharmacology*. 2014;62:57-62.
96. Raskob GE, Angchaisuksiri P, Blanco AN, Buller H, Gallus A, Hunt BJ, Hylek EM, Kakkar A, Konstantinides SV, McCumber M, Ozaki Y, Wendelboe A and Weitz JI. Thrombosis: a major contributor to global disease burden. *Arterioscler Thromb Vasc Biol*. 2014;34:2363-71.
97. Di Nisio M, van Es N and Buller HR. Deep vein thrombosis and pulmonary embolism. *Lancet*. 2016;388:3060-3073.
98. Virani SS, Alonso A, Benjamin EJ, Bittencourt MS, Callaway CW, Carson AP, Chamberlain AM, Chang AR, Cheng S, Delling FN, Djousse L, Elkind MSV, Ferguson JF, Fornage M, Khan SS, Kissela BM, Knutson KL, Kwan TW, Lackland DT, Lewis TT, Lichtman JH, Longenecker CT, Loop MS, Lutsey PL, Martin SS, Matsushita K, Moran AE, Mussolino ME, Perak AM, Rosamond WD, Roth GA, Sampson UKA, Satou GM, Schroeder EB, Shah SH, Shay CM, Spartano NL, Stokes A, Tirschwell DL, VanWagner LB and Tsao CW. Heart Disease and Stroke Statistics—2020 Update: A Report From the American Heart Association. *Circulation*. 2020;141:e139-e596.
99. Zhang X, Tang X, Ma F, Fan Y, Sun P, Zhu T, Zhang J, Hamblin MH, Chen YE and Yin KJ. Endothelium-targeted overexpression of Krüppel-like factor 11 protects the blood-brain barrier function after ischemic brain injury. *Brain Pathol*. 2020.
100. Glineur C, Gross B, Neve B, Rommens C, Chew GT, Martin-Nizard F, Rodríguez-Pascual F, Lamas S, Watts GF and Staels B. Fenofibrate inhibits endothelin-1 expression by peroxisome proliferator-activated receptor α-dependent and independent mechanisms in human endothelial cells. *Arterioscler Thromb Vasc Biol*. 2013;33:621-8.

101. Liang W, Fan Y, Lu H, Chang Z, Hu W, Sun J, Wang H, Zhu T, Wang J, Adili R, Garcia-Barrio MT, Holinstat M, Eitzman D, Zhang J and Chen YE. KLF11 (Kruppel-Like Factor 11) Inhibits Arterial Thrombosis via Suppression of Tissue Factor in the Vascular Wall. *Arteriosclerosis, Thrombosis, and Vascular Biology*. 2019;39:402-412.
102. Fan Y, Guo Y, Zhang J, Subramaniam M, Song C-Z, Urrutia R and Chen YE. Krüppel-Like Factor-11, a Transcription Factor Involved in Diabetes Mellitus, Suppresses Endothelial Cell Activation via the Nuclear Factor-κB Signaling Pathway. *Arteriosclerosis, Thrombosis, and Vascular Biology*. 2012;32:2981-2988.
103. Song CZ, Gavriilidis G, Asano H and Stamatoyannopoulos G. Functional study of transcription factor KLF11 by targeted gene inactivation. *Blood Cells Mol Dis*. 2005;34:53-9.
104. Wrobleski SK, Farris DM, Diaz JA, Myers DD, Jr. and Wakefield TW. Mouse complete stasis model of inferior vena cava thrombosis. *J Vis Exp*. 2011.
105. Chang Z, Zhao G, Zhao Y, Lu H, Xiong W, Liang W, Sun J, Wang H, Zhu T, Rom O, Guo Y, Fan Y, Chang L, Yang B, Garcia-Barrio MT, Lin JD, Chen YE and Zhang J. BAF60a Deficiency in Vascular Smooth Muscle Cells Prevents Abdominal Aortic Aneurysm by Reducing Inflammation and Extracellular Matrix Degradation. *Arteriosclerosis, Thrombosis, and Vascular Biology*. 2020;40:2494-2507.
106. Rom O, Xu G, Guo Y, Zhu Y, Wang H, Zhang J, Fan Y, Liang W, Lu H, Liu Y, Aviram M, Liu Z, Kim S, Liu W, Wang X, Chen YE and Villacorta L. Nitro-fatty acids protect against steatosis and fibrosis during development of nonalcoholic fatty liver disease in mice. *EBioMedicine*. 2019;41:62-72.
107. Hu W, Lu H, Zhang J, Fan Y, Chang Z, Liang W, Wang H, Zhu T, Garcia-Barrio MT, Peng D, Chen YE and Guo Y. Krüppel-like factor 14, a coronary artery disease associated transcription factor, inhibits endothelial inflammation via NF-κB signaling pathway. *Atherosclerosis*. 2018;278:39-48.
108. Kobayashi M, Inoue K, Warabi E, Minami T and Kodama T. A Simple Method of Isolating Mouse Aortic Endothelial Cells. *Journal of Atherosclerosis and Thrombosis*. 2005;12:138-142.
109. Day SM, Reeve JL, Pedersen B, Farris DM, Myers DD, Im M, Wakefield TW, Mackman N and Fay WP. Macrovascular thrombosis is driven by tissue factor derived primarily from the blood vessel wall. *Blood*. 2005;105:192-198.
110. Yau JW, Teoh H and Verma S. Endothelial cell control of thrombosis. *BMC Cardiovasc Disord*. 2015;15:130.
111. Wang M, Hao H, Leeper Nicholas J and Zhu L. Thrombotic Regulation From the Endothelial Cell Perspectives. *Arteriosclerosis, Thrombosis, and Vascular Biology*. 2018;38:e90-e95.
112. Moll T, Czyz M, Holzmüller H, Hofer-Warbinek R, Wagner E, Winkler H, Bach FH and Hofer E. Regulation of the tissue factor promoter in endothelial cells. Binding of NF kappa B-, AP-1-, and Sp1-like transcription factors. *J Biol Chem*. 1995;270:3849-57.
113. Mackman N. Regulation of the tissue factor gene. *Thrombosis and haemostasis*. 1997;78:747-54.
114. Shin IS, Kim JM, Kim KL, Jang SY, Jeon ES, Choi SH, Kim DK, Suh W and Kim YW. Early growth response factor-1 is associated with intraluminal thrombus formation in human abdominal aortic aneurysm. *J Am Coll Cardiol*. 2009;53:792-9.

115. Houston P, Campbell CJ, Svaren J, Milbrandt J and Braddock M. The Transcriptional Corepressor NAB2 Blocks Egr-1-Mediated Growth Factor Activation and Angiogenesis. *Biochemical and Biophysical Research Communications*. 2001;283:480-486.
116. Mechtcheriakova D, Wlachos A, Holzmüller H, Binder BR and Hofer E. Vascular Endothelial Cell Growth Factor–Induced Tissue Factor Expression in Endothelial Cells Is Mediated by EGR-1. *Blood*. 1999;93:3811-3823.
117. Bode M and Mackman N. Regulation of tissue factor gene expression in monocytes and endothelial cells: Thromboxane A2 as a new player. *Vascul Pharmacol*. 2014;62:57-62.
118. Swystun LL and Liaw PC. The role of leukocytes in thrombosis. *Blood*. 2016;128:753-762.
119. Everett BM, MacFadyen JG, Thuren T, Libby P, Glynn RJ and Ridker PM. Inhibition of Interleukin-1b and Reduction in Atherothrombotic Cardiovascular Events in the CANTOS Trial. *Journal of the American College of Cardiology*. 2020;76:1660-1670.
120. Khedkar SA, Sun X, Rigby AC and Feinberg MW. Discovery of small molecule inhibitors to Krüppel-like factor 10 (KLF10): implications for modulation of T regulatory cell differentiation. *J Med Chem*. 2015;58:1466-78.
121. Shen B, Smith RS, Jr., Hsu YT, Chao L and Chao J. Kruppel-like factor 4 is a novel mediator of Kallistatin in inhibiting endothelial inflammation via increased endothelial nitric-oxide synthase expression. *The Journal of biological chemistry*. 2009;284:35471-8.